Universidad de Huelva

Departamento de Química "Profesor José Carlos Vílchez Martín"

Funcionalización catalítica de metano y alcanos ligeros con complejos metálicos del grupo 11

Memoria para optar al grado de doctor
presentada por:

Riccardo Gava

Fecha de lectura: 23 de noviembre de 2017

Bajo la dirección de los doctores:

Pedro José Pérez Romero

Ana Caballero Bevia

Huelva, 2017

Universidad de Huelva

FUNCIONALIZACIÓN CATALÍTICA DE METANO Y ALCANOS LIGEROS CON COMPLEJOS METÁLICOS DEL GRUPO 11

Programa de Doctorado Ciencia y Tecnología Industrial y Ambiental

Riccardo Gava

Huelva, Noviembre 2017

FUNCIONALIZACIÓN CATALÍTICA DE METANO Y ALCANOS LIGEROS CON COMPLEJOS METÁLICOS DEL GRUPO 11

por

Riccardo Gava

Trabajo presentado para aspirar al

Título de Doctorado Internacional en Química

Huelva, Noviembre de 2017

Fdo: Riccardo Gava

Los Directores:

Fdo: Dr. Pedro J. Pérez Romero

Fdo: Dra. Ana Caballero Bevia

ÍNDICE

List of abbreviations

Å	Ångström
acac	Acetylacetonate anion
Ar	Aromatic
$BAr^{F'}{}_4$	Tetrakis-(3,5-bis-trifluoromethylphenil)borate
BINAP	2,2- Bis(diphenylphosphino)-1,1′-binaphthalene
br	Broad singlet
Bu	Butyl group
d	Doblet
DEF	Diethyl fumarate
DEM	Diethyl maleate
EDA	Ethyl diazoacetate
eq	Equation
Et	Ethyl group
EWG	Electron-withdrawing groups
FTIR	Fourier Transform Infrared Spectroscopy
GC	Gas cromatography
GC-MS	Gas-Masa cromatography
g-COSY	Gradient Correlation Spectroscopy
g-HSQC	Gradient Heteronuclear Single Quantum Coherence
g-HMBC	Gradient Heteronuclear Multiple Bond Correlation
h	Hours
Hz	Herz
IR	Infrared
J	Coupling constant measured in Hz
L	Ligand
m	Multiplet
M	Metal
Me	Methyl group
mg	Miligrams

MHz	Megaherz
min	Minutes
mL	Milliliters
mmoles	Millimoles
Ms	Mesytil group
NCMe	Acetonitrile (CH_3CN)
NMR	Nuclear Magnetic Resonance
OAc	Acetate group
ORTEP	Oak Ridge Thermal Ellipsoid Plot
OTf	Triflate group
PDI	Polydispersity index
Ph	Phenyl group
PPh_3	Ligand triphenylphosphine
ppm	Parts per million
q	Quartet
R_f	Perfluorinated alkyl group
r.t.	Room temperature
Rto	Rendimiento
s	Singlet
sc	Supercritic conditions
t	Triplet
THF	Tetrahydrofurane
TOF	Turnover frequency
TON	Turnover number
Tp^x	Tris(pirazolil)borato
$Tp^{(CF3)2Br}$	Tris(3,5-ditrifluoromethyl-4-bromo pirazolyl)borate
Tp^{Br3}	Tris(3,4,5-tribromo-pirazolyl)borate
Ts	Tosyl Group
μL	Microlitres
δ	Chemical shift (in ppm)
η	Hapticity indicator of a ligand

ν	Infrared Vibration Frequency
^{o}C	Celsius degree
ΔG	Activation free energy

RESUMEN

Los trabajos desarrollados en esta Tesis Doctoral se centran en el desarrollo de sistemas catalíticos capaces de funcionalizar moléculas que presentan una gran inercia química, como es el caso de los alcanos gaseosos (C_nH_{2n+2}, n = 1-4). La reacción empleada para conseguir tal fin es la de transferencia catalítica del grupo $CHCO_2Et$ a partir de diazoacetato de etilo (N_2=$CHCO_2Et$, EDA):

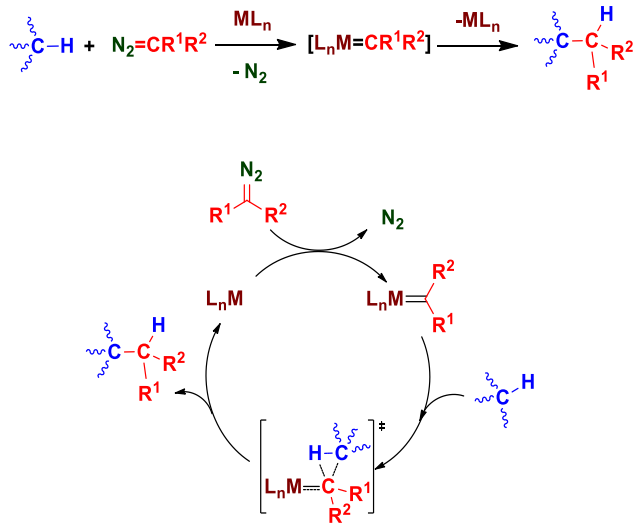

Funcionalización catalítica de enlaces carbono-hidrógeno de alcanos mediante inserción de carbenos proveniente de un diazocompuesto.

Los resultados se han agrupado en tres partes en las que se describen nuevos sistemas catalíticos para metano, etano, propano y butano (secciones 1 y 3), así como un estudio de la reactividad relativa de un conjunto de alcanos, tomando como referencia al metano (sección 2).

Sección 1: Nuevos catalizadores para la funcionalización catalítica de alcanos ligeros

Como punto de partida se ha sintetizado un nuevo ligando de la familia de los hidrotrispirazolilboratos (Tp^x), el hidrotris((3,5-bis(trifluorometil)-4-bromo)-pirazolil)borato ($Tp^{(CF3)2,Br}$), del que se han obtenido sus complejos de talio, cobre y plata: $TlTp^{(CF3)2,Br}$ (**1**) $Tp^{(CF3)2,Br}Cu(NCMe)$ (**2**) y $Tp^{(CF3)2,Br}Ag(thf)$

(**3**). Estos nuevos compuestos se han caracterizado espectroscópicamente, y sus estructuras en el estado sólido se han determinado mediante difracción de rayos X.

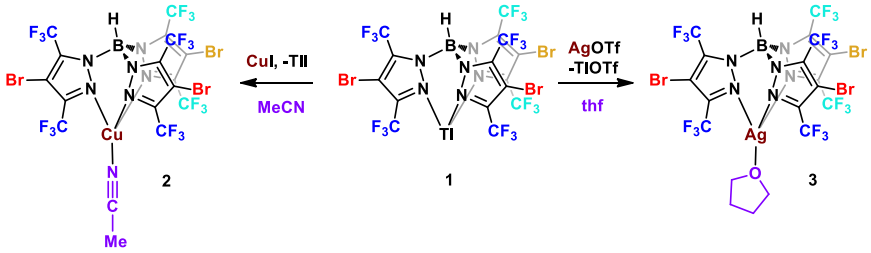

*Síntesis de los complejos **2** y **3** a partir de **1**.*

Los complejos **2** y **3** presentan actividad catalítica para la reacción de funcionalización de metano y otros alcanos ligeros empleando diazoacetato de etilo como fuente de carbenos y dióxido de carbono supercrítico como medio de reacción. Este es el primer ejemplo basado en cobre capaz de funcionalizar metano en condiciones homogéneas.

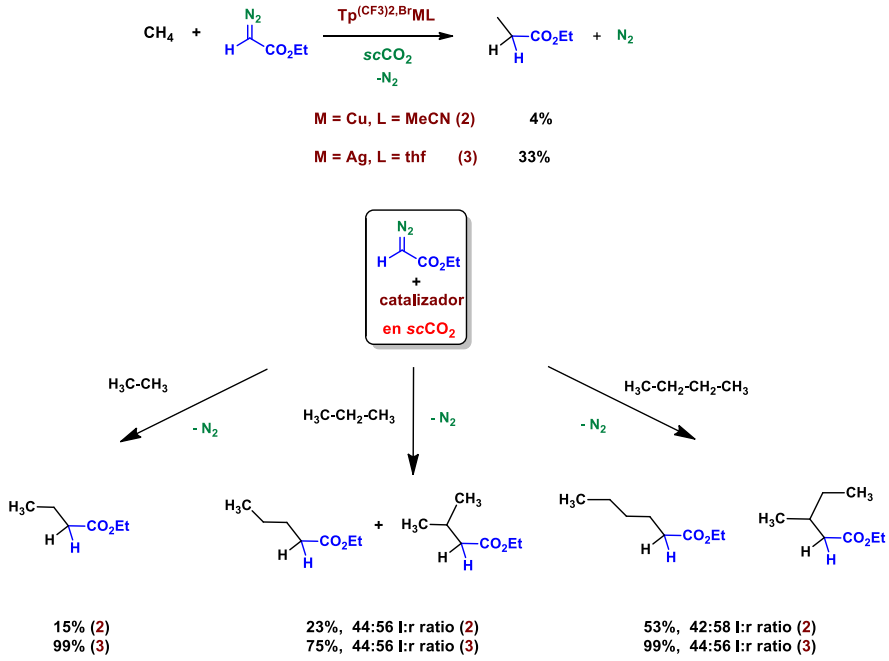

*Funcionalización catalítica de alcanos ligeros empleando los complejos **2** y **3** como catalizadores.*

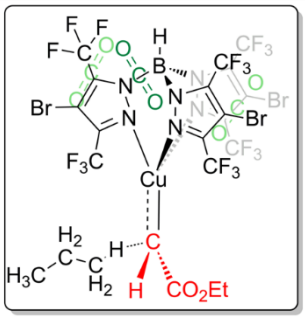

En las reacciones llevadas a cabo con el complejo **2** como catalizador se ha observado un efecto del medio de reacción que hace que en *sc*CO_2 aumente la regioselectividad hacia los sitios primarios de los alcanos líquidos, comparada con la observada empleando el alcano puro como medio de reacción. Este *efecto supercrítico* parece deberse a una interacción entre el medio supercrítico y el catalizador a través de sus átomos de fluor, que disminuye la densidad electrónica en el centro metálico.

Sección 2: Estudio de la reactividad relativa de alcanos hacia metalocarbenos

Mediante reacciones de competición de pares de alcanos con EDA, tanto en medio *sc*CO_2 como en alcano puro como disolventes, se ha determinado la reactividad relativa (R_r) de un total de 29 enlaces C-H de catorce alcanos (C_nH_{2n+2}, n = 1-8) distintos, usando diversos complejos de plata como precursores de los intermedios metalacarbénicos, y tomando el metano como referencia.

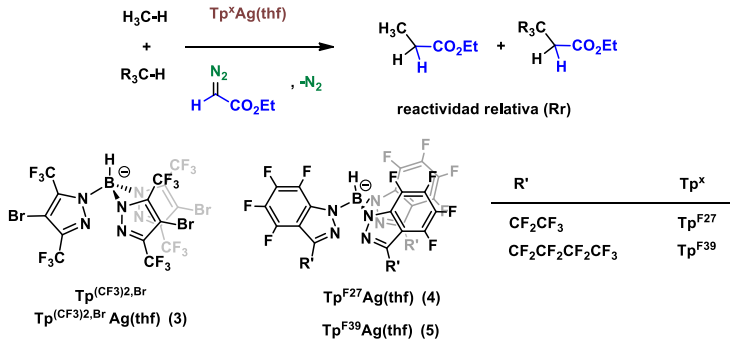

Experimentos de competición para determinar la reactividad relativa.

Los datos experimentales obtenidos han sido analizados de manera estadística, lo que ha permitido generar un modelo que ajusta dichos datos a una serie de descriptores topológicos de los enlaces C-H. De esta manera, una serie muy simple de reglas ha permitido modelar la reactividad relativa de alcanos no solo frente a los catalizadores de plata sino también a otros de rodio y cobre.

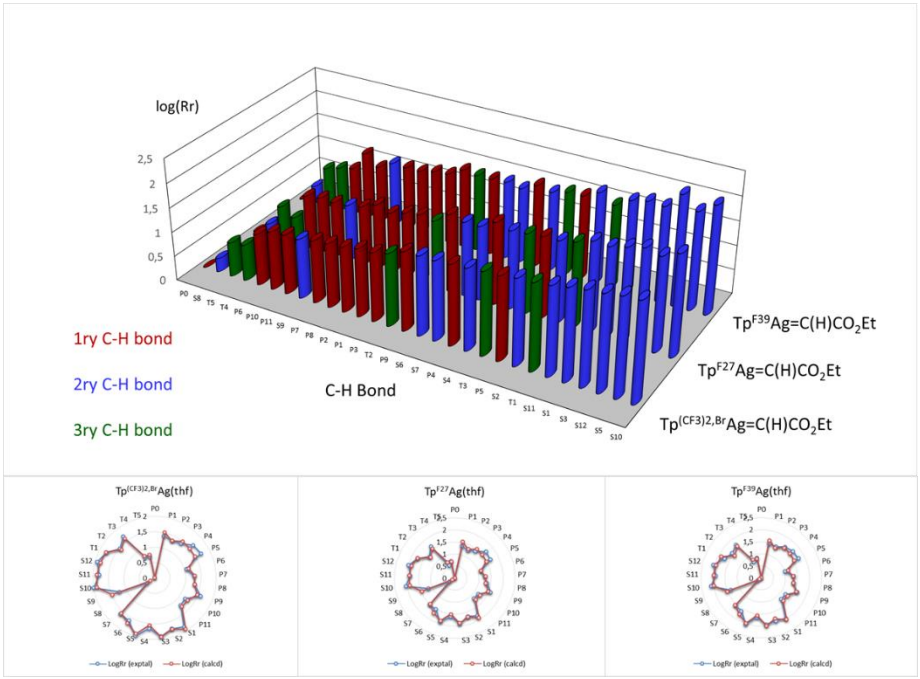

Variación de la reactividad relativa de los enlaces C-H tomando el del metano como referencia (arriba). Comparación de los datos experimentales (azul) con los del modelo (rojo) para los tres catalizadores de plata empleados (abajo).

Sección 3: Funcionalización catalítica de metano en agua a temperatura ambiente

Se ha desarrollado un sistema catalítico en el que la reacción de metano (o de otros alcanos gaseosos) con EDA en presencia del complejo **3** como catalizador se ha llevado a cabo en agua como disolvente. Para ello se hace necesario el concurso de un surfactante, como es el SDS (dodecilsulfato sódico), que proporciona la generación de micelas en cuyo interior apolar se acumulan los reactivos y el catalizador.

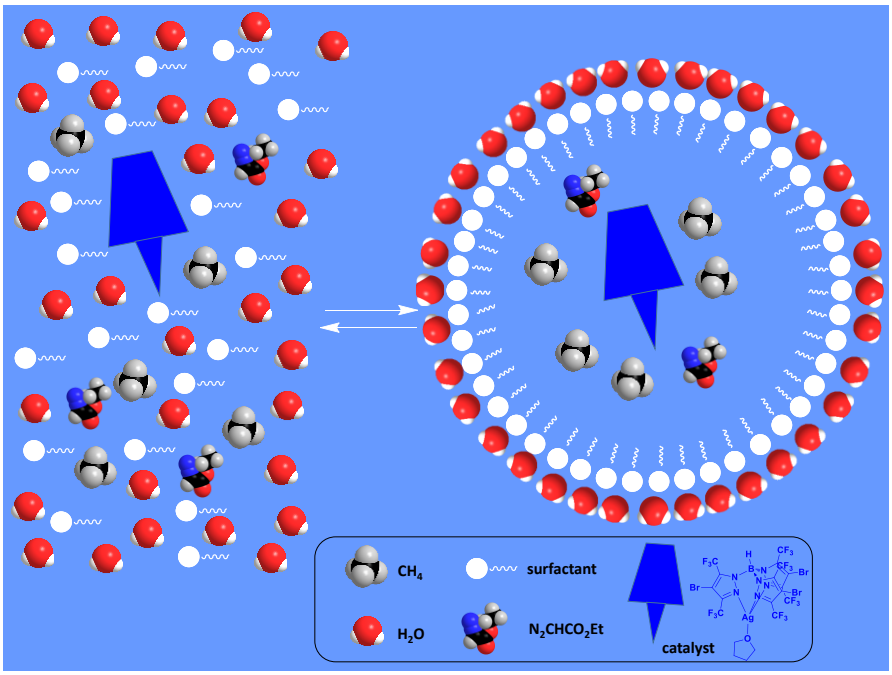

Esquema del sistema catalítico empleado para funcionalizar metano en agua mediante la formación de micelas.

Mediante esta estrategia se ha podido funcionalizar metano con un 8% de rendimiento respecto al EDA inicial empleado, habiéndose detectado que la mayoría del EDA restante se incorpora a las cadenas hidrofóbicas del surfactante.

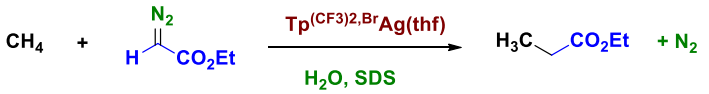

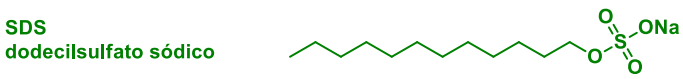

SUMMARY

The main objectives in this Ph. D. Thesis are focused in the development of catalytic systems toward the functionalization of highly inert molecules such as gaseous alkanes (C_nH_{2n+2}, n = 1-4). The reaction employed toward that end is the metal-catalyzed carbene ($CHCO_2Et$) transfer reaction from ethyl diazoacetate (N_2=$CHCO_2Et$, EDA):

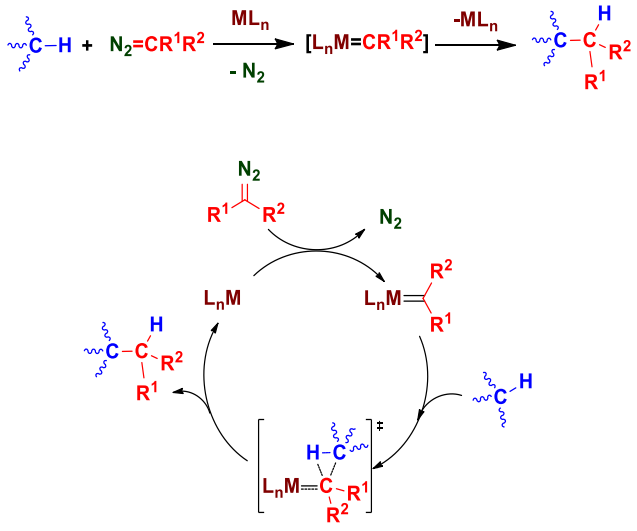

Carbon-hydrogen bond catalytic functionalization by means of metal-catalyzed carbene transfer reaction from diazocompounds.

The results have been classified in three Sections, describing novel catalytic systems for methane and light alkanes (ethane, propane, butane) catalytic functionalization (Sections 1 and 3) as well as a study for the quantification of the relative reactivity of a number of gaseous and liquid alkanes, with methane as the reference (Section 2).

Section 1: New catalysts for methane and light alkane functionalization

A new ligand of the hydrotris(pyrazolyl)borate (Tp^x) family has been synthetized, the hydrotris((3,5-bis(trifluoromethyl)-4-bromo)-pyrazolyl)borate ($Tp^{(CF3)2,Br}$). Its thalium, copper and silver complexes $TlTp^{(CF3)2,Br}$ (**1**) $Tp^{(CF3)2,Br}Cu(NCMe)$ (**2**) and $Tp^{(CF3)2,Br}Ag(thf)$ (**3**) have been prepared and fully characterized, including X-ray studies for their solid state structure.

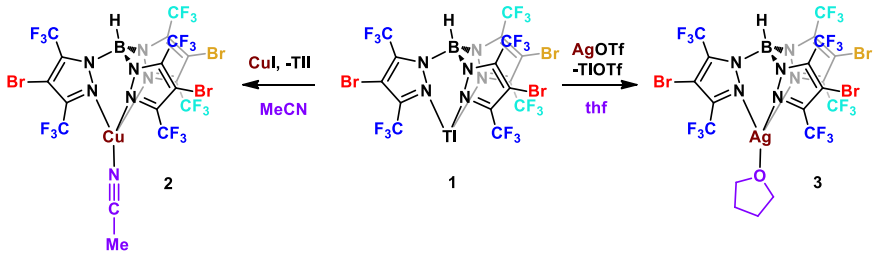

*Synthesis of complexes **2** and **3** from **1**.*

Complexes **2** and **3** display catalytic activity for the reaction of EDA and methane or other gaseous alkanes in supercritical carbon dioxide as the reaction medium. This is the first example of a soluble copper-based methane functionalization reaction.

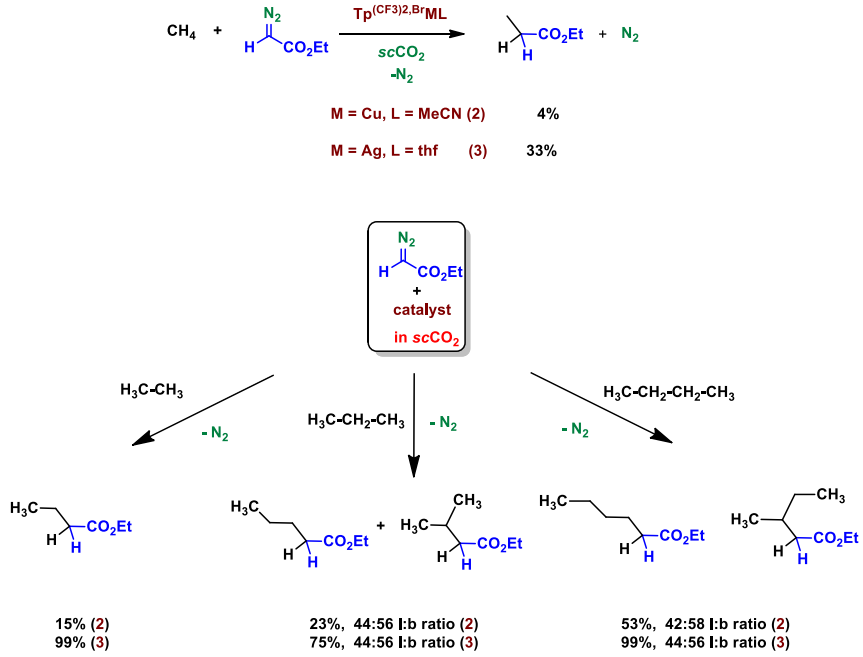

*Catalytic functionalization of light alkanes, including methane, with complexes **2** and **3** as catalysts.*

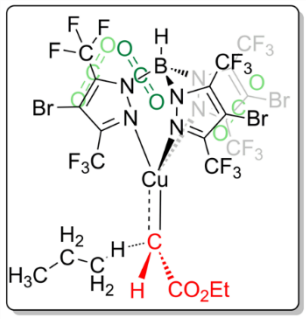

In the reactions carried out employing complex **2** as catalyst, an increase of the regioselectivity toward the primary sites has been observed when *sc*CO_2 is used as the reaction medium, comparing the results with those experiments performed in neat (liquid) alkanes. This "supercritical effect" seems to be related to an interaction of the supercritical medium with the catalyst through the fluorine atoms, which decrease the electron density at the metal center.

Section 2: Studies of the relative reactivity of alkanes toward metallocarbenes

The relative reactivity (R_r) of a series of fourteen alkanes (C_nH_{2n+2}, n = 1-8) and twenty-nine different carbon-hydrogen bonds has been determined upon performing competition experiments both in *sc*CO_2 and/or neat alkanes as the reaction media. Several silver-based catalysts have been used as the electrophile (metallocarbene) precursor, and the relative reactivity has been referenced to that of the methane carbon-hydrogen bond.

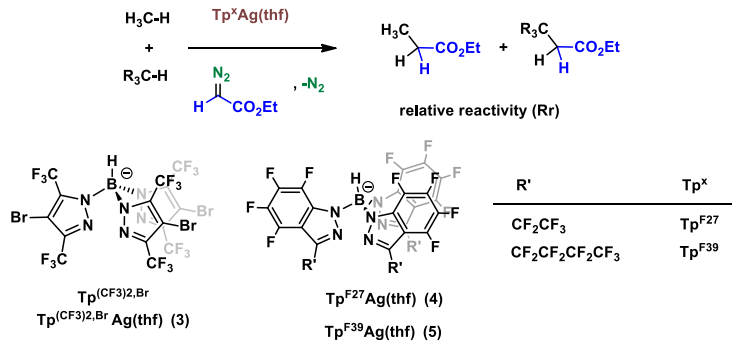

Competition experiments toward relative reactivity determination.

Experimental data have been analyzed from a statistic point of view, from which a simple model has been built. Such model consists of an equation an a series of very simple rules that, based on topological descriptors of each

C-H bond, leads to an estimated value of each relative reactivity that fits quite accurately with the experimental data. The model is not only applicable to the silver catalysts but also to others based on rhodium or copper.

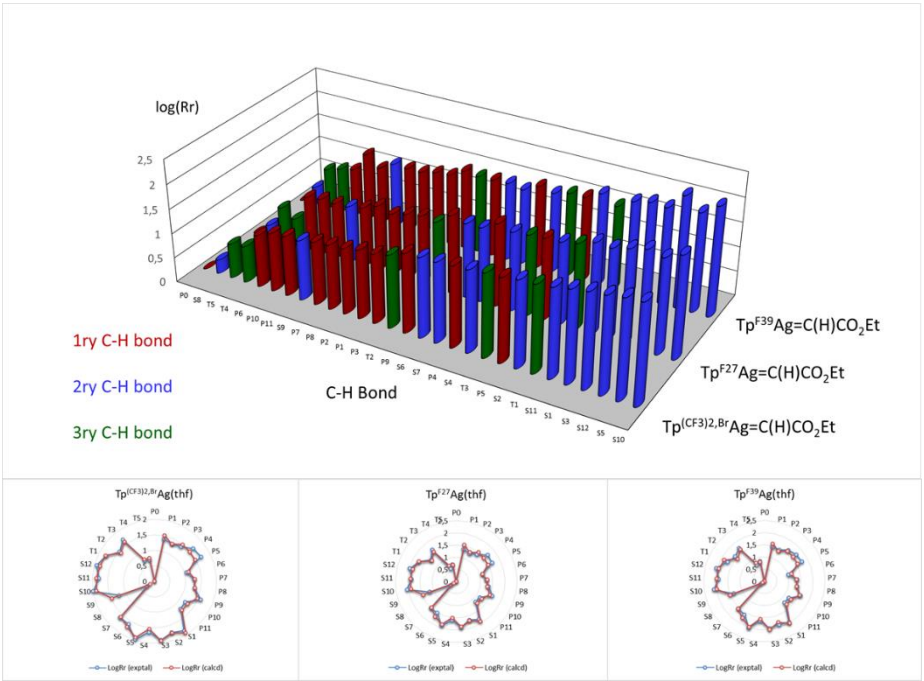

Variation of the relative reactivity of C-H bonds of the alkanes studied with methane as the reference (top). Comparison of experimental (blue) and estimated (red) values for the three silver-based catalysts (bottom).

Section 3: Methane catalytic functionalization in water at room temperature

A catalytic system for the reaction of methane (or other gaseous alkanes) with EDA in the presence of **3** as the catalysts that operates in water at room temperature has been developed. To achieve such outcome, a surfactant is required to generate micelles that concentrate catalyst and reactants in the inner hydrophobic cavity. Sodium docedyl sulphate has been found as the most appropriate surfactant for such purpose.

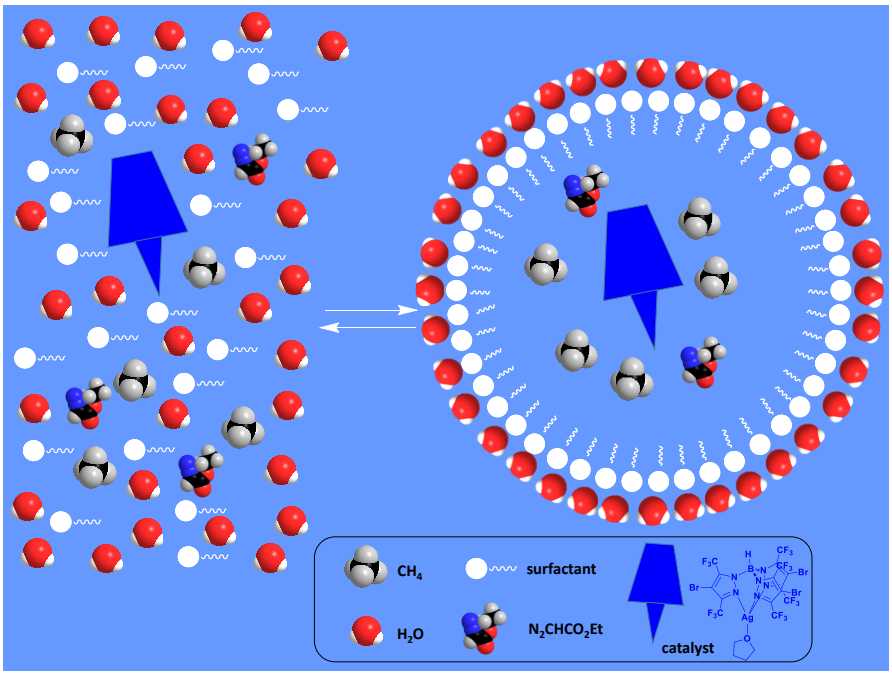

Catalytic system employed for methane functionalization in water through micellar catalysis.

With this strategy, methane has been converted into ethyl propionate with a 8% yield (EDA-based), whereas the remaining diazo reagent seems to be incorporated to the hydrophobic chains of the surfactant.

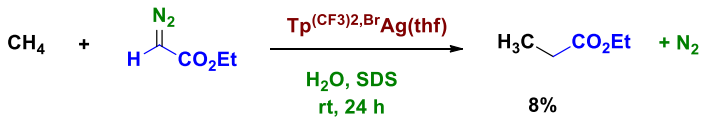

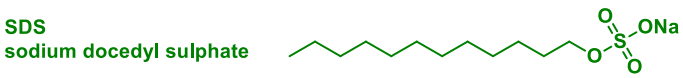

INTRODUCCIÓN

I. Activación y funcionalización de enlaces C-H de alcanos: generalidades.

La búsqueda de sistemas catalíticos capaces de transformar directamente los alcanos, C_nH_{2n+2}, moléculas simples y abundantes pero a su vez muy poco reactivas, en productos más complejos y con un cierto valor añadido constituye uno de los objetivos más importantes de la química moderna.[1,2] La enorme inercia química de estas moléculas, debido principalmente a su alta energía del enlace carbono-hidrógeno así como a la baja polaridad del mismo, hacen que los usos sintéticos de los alcanos a nivel industrial sean muy limitados.[3,4]

El campo de la activación de enlaces carbono-hidrógeno de alcanos, y en general de cualquier tipo de ellos, mediante complejos de los metales de transición puede considerarse como el eje principal de la química organometálica de las últimas décadas.[5] Mediante este proceso un enlace carbono-hidrógeno entra en un camino de reacción que lo convierte en uno o más enlaces de menor energía. La activación organometálica tiene lugar mediante distintos procesos sobradamente conocidos (metátesis de enlace sigma, adición oxidativa, adición 1,2) y por conocida[6] no merece más detalle en esta parte de la Introducción, que se enfoca principalmente a aplicaciones catalíticas desarrolladas sobre alcanos. La activación electrofilica,[2] conocida desde su descubrimiento por Shilov a finales de los años 60 del siglo pasado, es asimismo otra vía de activación de enlaces C-H de alcanos, con especial incidencia en determinados procesos catalíticos, como se expondrá más adelante.

De manera general, el proceso de activación de un enlace C-H suele suponer la interacción del mismo con un complejo metálico de tal suerte que se origine bien una interacción directa con el centro metálico y una subsiguiente rotura del enlace C-H o, de manera alternativa, una interacción del enlace C-H con un ligando que también conduzca a la rotura de aquel (Esquema I). Son numerosos los ejemplos descritos en la bibliografía en los que un complejo

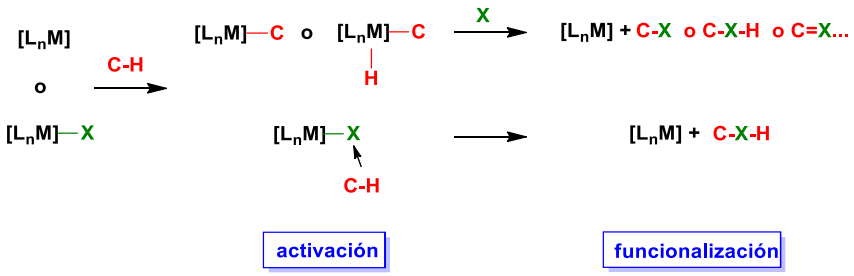

Esquema I. *Activación y funcionalización de enlaces carbono-hidrógeno.*

metálico induce la activación de un enlace carbono hidrógeno de un alcano.[3,6] Sin embargo, desde un punto de vista práctico en el que se desea la conversión del alcano en otro compuesto con mayor complejidad molecular, se hace preciso un segundo paso posterior (o simultáneo) a la activación: la funcionalización. En este paso tiene lugar la reacción del alcano, o de los fragmentos derivados de su activación, con otra entidad X así como la salida de la esfera de coordinación del metal del nuevo producto originado de dicha interacción. Son muy pocos los ejemplos donde una vez conseguida la activación de un alcano se puede alcanzar la correspondiente funcionalización. Ello es debido a que los compuestos metálicos obtenidos de la activación, que suelen contener enlaces metal-carbono, presentan una estabilidad considerable. Por ello, en los casos en los que se ha conseguido la deseada funcionalización de alcanos, se requieren condiciones de reacción drásticas.

La segunda ruta de activación se basa en la interacción del enlace C-H con un ligando X (Esquema I) y presenta como principal característica la ausencia de especies organometálicas derivadas de fragmentos del alcano y la consiguiente estabilidad antes mencionada. Por ello, esta segunda estrategia en la que la funcionalización tiene lugar mediante un mecanismo de esfera externa puede proporcionar sistemas catalíticos que no requieran condiciones tan extremas como las basadas en la activación por el centro metálico.

En el apartado siguiente se describen de manera general los principales sistemas catalíticos descritos para la funcionalización de alcanos, con especial énfasis al uso del metano como reactivo. Conviene recordar que el metano

presenta la mayor energía de disociación del enlace C-H (105 kcal mol^{-1}),[7] lo que le confiere una estabilidad excepcionalmente alta en comparación con el resto de los miembros de la serie homóloga de alcanos.

II. Funcionalización catalítica de alcanos.

Como ya se ha mencionado, no son muchos los sistemas descritos capaces de funcionalizar o transformar alcanos en otras moléculas más complejas.[1] De manera general, el Esquema II muestra los principales ejemplos, que pueden clasificarse en tres tipos según la naturaleza de la activación. La activación electrofílica, descubierta por Shilov,[2] requiere de condiciones

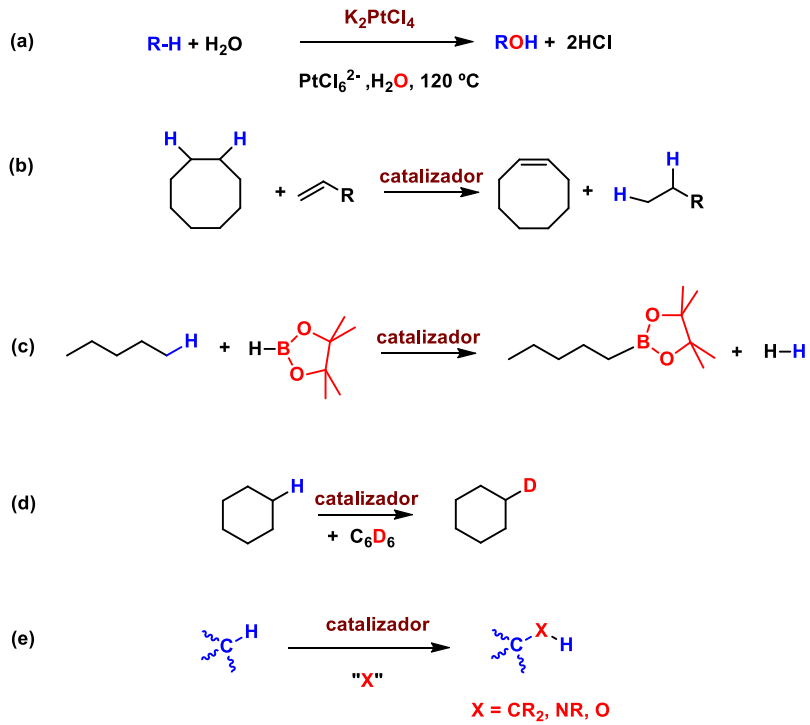

Esquema II. *Ejemplos representativos de reacciones de funcionalización catalítica de alcanos.*

drásticas y electrófilos de extraordinaria fuerza. En muchos casos estas reacciones tienen lugar en medio fuertemente ácido como el óleum. Un segundo tipo de reacciones supone la activación organometálica, que incluye procesos

de adiciones oxidativa-eliminación reductiva y/o metátesis de enlaces sigma.[6] En este tipo se engloban las reacciones de deshidrogenación de alcanos, de borilación catalítica de alcanos y de intercambio de H por D. Todas estas transformaciones requieren altas temperaturas para eliminar el producto deseado de la esfera de coordinación del metal. El tercer tipo de sistemas descritos corresponde al de activación por ligando, y entre ellas pueden destacarse la inserción de unidades carbenos, nitrenos u oxo en los enlaces C-H.[1] La inexistencia de interacción directa del enlace C-H del alcano con el centro metálico evita la formación de enlaces M-C y/o M-H robustos, por lo que la liberación del producto tiene lugar con mayor facilidad y las condiciones de reacción suelen ser suaves.

III. Funcionalización catalítica de metano.

La activación de metano constituye uno de los objetivos primordiales de la química actual,[8] para lo que se ha volcado numerosos esfuerzos desde los puntos de vista estequiométrico y catalítico, en este último caso tanto en fase homogénea[9] como heterogénea.[10] En un número especial de la revista *Chemical Reviews*[11] en este año 2017 dedicado a la activación de enlaces carbono-hidrógeno aparecen excelentes artículos de revisión de estos tópicos. A continuación se resumen los avances más destacados en la funcionalización catalítica de metano mediante catalizadores solubles. Se excluyen en este apartado aquellos procesos que tienen lugar de manera radicalaria[12] o en los que el metal no participa en el proceso de activación/funcionalización, sino en la generación de especies activas tales como radicales.

III. 1 Sistemas catalíticos basados en la activación electrofílica del enlace C-H.

Hace medio siglo, Shilov y colaboradores descubrieron que ciertos complejos de platino eran capaces de activar metano bajo determinadas condiciones de reacción. Así, el intercambio H/D de metano en un medio compuesto de ácido acético y agua deuterados fue posible gracias a la presencia de $PtCl_4^{2-}$ (Esquema IIIa).[13a] Como continuación de esos estudios, el mismo grupo consiguió la conversión catalítica de metano en metanol o cloruro de metilo empleando una sal de Pt(IV) como oxidante estequiométrico (Esquema IIIb).[13b]

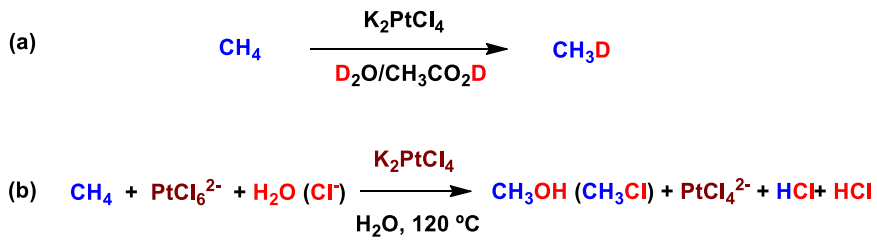

Esquema III. *Activación electrofílica de metano descrita por Shilov.*

Sobre la base de estos trabajos, el grupo de Periana desarrolló los sistemas de activación electrofílica de metano más activos conocidos hasta el momento. Los primeros resultados se publicaron en 1993 y se basan en el empleo de un sistema catalítico de mercurio[14] para la oxidación de metano a bisulfito de metilo, utilizando ácido sulfúrico concentrado como medio de reacción a 180 ºC, con unos valores de TOF de 10^{-3} s^{-1} (Esquema IV). En este proceso el metano se activa al interaccionar con el bisulfato de mercurio generando el correspondiente derivado de metilo que reacciona con ácido sulfúrico para producir bisulfato de metilo. El papel del ácido sulfúrico es el de la oxidación del complejo de mercurio para regenerar la especie inicial y poder reiniciar el ciclo catalítico, produciendo SO_2 como subproducto.

Posteriormente a estos resultados, Sen y colaboradores describieron[15] sistemas similares, generalmente estequiométricos, en los que se empleaban como oxidantes complejos de Ce(IV), Pd(II) o Hg(II) (catalítico) o $S_2O_8^{2-}$ en ácido sulfúrico concentrado.

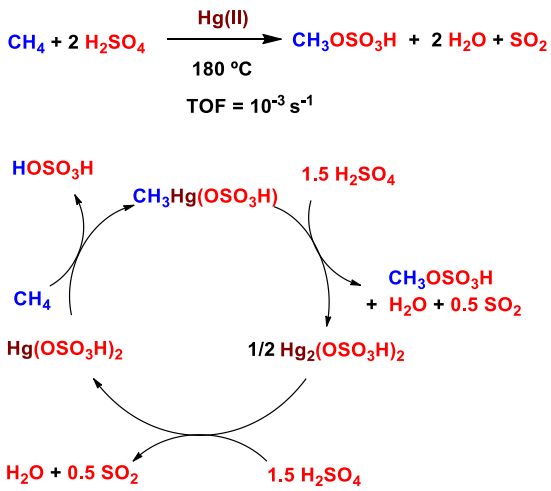

Esquema IV. *Ciclo catalítico propuesto para la reacción de funcionalización electrofílica de metano con un complejo de mercurio.*

En 1998, de nuevo Periana y colaboradores describieron un sistema basado en el anterior de mercurio pero esta vez con un catalizador de platino (II).[16] Este nuevo sistema toma el nombre de *Sistema Catalytica* y es, hasta el momento, el sistema más activo (Esquema V) en términos de selectividad (80% en bisulfato de metilo), conversión (90% del metano) y rendimiento (72%) conocido hasta la fecha. Está basado en el sistema de Shilov, si bien en este caso el complejo de Pt contiene ligandos bipiridina que aportan estabilidad al complejo y hacen que la actividad y selectividad de esta reacción sean altas en un medio de ácido sulfúrico concentrado a 220 ºC.

El mecanismo propuesto para el Sistema Catalytica se muestra en el Esquema V y es parecido al formulado anteriormente por Shilov donde se sugiere la formación de un intermedio de metil-platino. La oxidación del centro

metálico de Pt(II) a Pt(IV) es debida al óleum, una mezcla SO_3/H_2SO_4, que da como producto SO_2 tras actuar como oxidante. En el último paso del ciclo se libera el bisulfito de metilo y se regenera la especie catalíticamente activa. Estudios mecanísticos han demostrado que la activación del enlace C-H de metano ocurre en el centro de platino (II) mientras que la funcionalización del mismo es debida al centro de platino (IV).

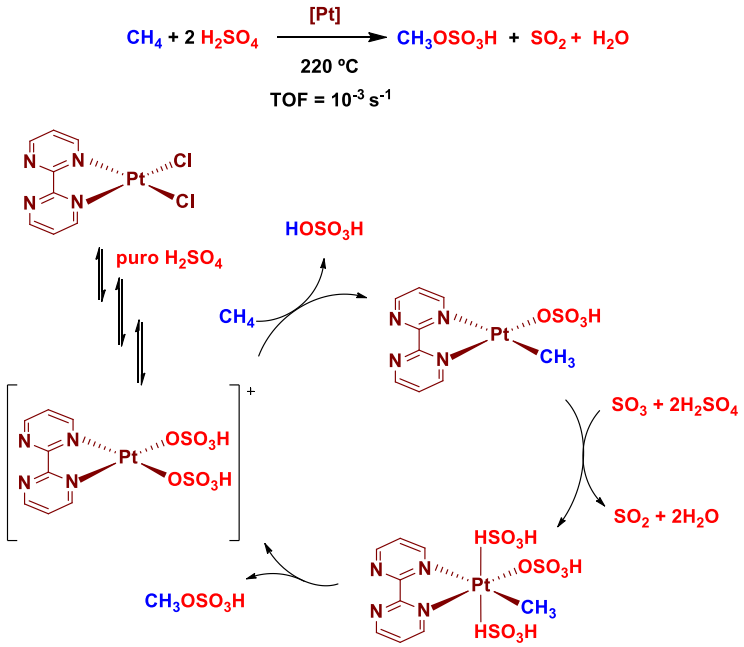

***Esquema V**. Sistema Catalytica de funcionalización electrofílica de metano con platino.*

Desde un punto de vista práctico, el Esquema VI muestra una hipotética aplicación de este proceso, en la que bisulfato de metilo podría convertirse en metanol por hidrólisis y el dióxido de azufre generado en este proceso convertirse en ácido sulfúrico por reacción con oxígeno y el catalizador apropiado.[1] Sin embargo el valor de TOF del proceso Catalytica es tan bajo (se encuentra mil veces por debajo de lo requerido desde un punto de vista industrial) que esta aplicación dista mucho de ser posible aún.

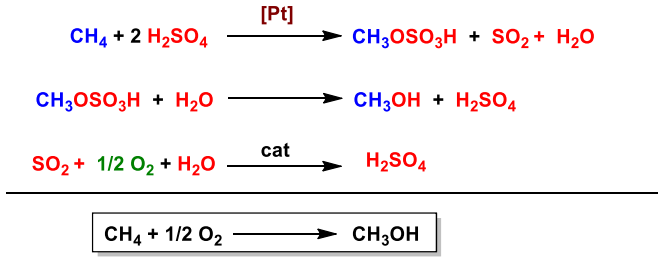

Esquema VI. *Hipótesis para la producción de metanol basado en el sistema Catalytica.*

Con posterioridad, el grupo de Periana describió[17] un proceso de oxidación de metano con haluros de oro para formar compuestos de tipo CH_3-OR (R = hidrogensulfito). Los grupos de Sen[18] y Strassner[19] habían ya preparado con anterioridad a estos resultados compuestos similares derivados del ácido trifluoroacético empleando catalizadores de paladio (Esquema VII).

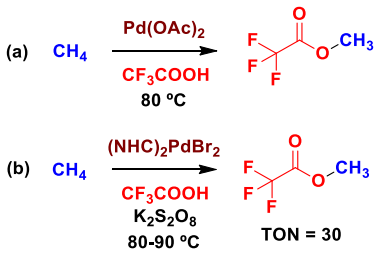

Esquema VII. *Otros ejemplos de funcionalización de CH_4 que originan enlaces C-O.*

Los ejemplos anteriores conducen a la formación de enlaces C-O a partir del metano. Un segundo tipo de funcionalización electrofílica de metano es el que proporciona nuevos enlaces C-C. De nuevo el grupo de Periana fue pionero en transformar metano en ácido acético con un sistema parecido al *Catalytica* pero con una sal de paladio (II) como catalizador.[20] En esta reacción se obtenía una mezcla de bisulfito de metilo y ácido acético con un TON de 4 respecto a este último. Estudios mecanísticos realizados con metano isotópicamente enriquecido en ^{13}C demostraron que el ácido acético provenía

de la reacción de dos moléculas de metano. El mecanismo propuesto implica la activación electrofílica de metano así como su oxidación hacia CO, que se

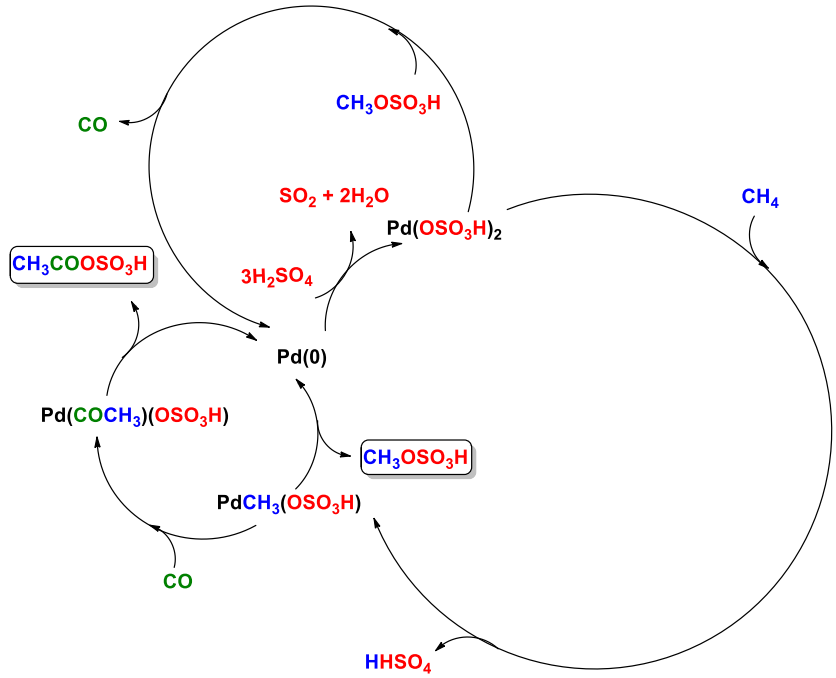

Esquema VIII. *Conversión de metano en ácido acético en condiciones similares al proceso Catalytica.*

activa más tarde a través de un intermedio acilo para finalmente producir el derivado de ácido acético (Esquema VIII).

Sucesivamente, Pombeiro y colaboradores[21] describieron un segundo ejemplo para la síntesis de ácido acético, empleando complejos de vanadio como catalizador [ec. (I)], en medio ácido trifluoroacético y con peroxodisulfato como oxidante. Los mejores rendimientos alcanzaron el 50%. Esta reacción presenta intermedios radicalarios, donde el metano proporciona el grupo metilo mientras que el ácido trifluoroacético es la fuente del grupo carbonilo. Además de ácido acético se detectaron también trifluoroacetato de metilo y sulfato de metilo como productos minoritarios.

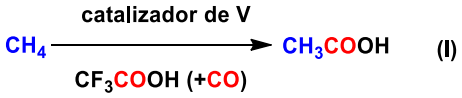

Más recientemente, Emsley, Caps, Basset y colaboradores han descrito la conversión subestequiométrica de metano en ácido acético utilizando heteropoliácidos quimioabsorbidos sobre sílice obteniendo bajos rendimientos [eq. (II)], [22] en un ejemplo de catálisis heterogénea.[12]

III. 2 Sistemas catalíticos basados en la activación organometálica del enlace C-H.

Sen y colaboradores describieron la conversión directa de metano en ácido acético[23] en presencia de D_2O, CO y O_2 y utilizando $RhCl_3$ como precursor catalítico [(ec. III)]. La reacción tiene lugar, según estudios experimentales[23] y teóricos,[24] mediante la adición oxidativa del enlace C-H del metano al centro de rodio, con un mecanismo distinto al del proceso Monsanto de conversión de metanol en ácido acético. La formación de metanol o derivados está influida por la presencia de ácidos fuertes en el medio de reacción.

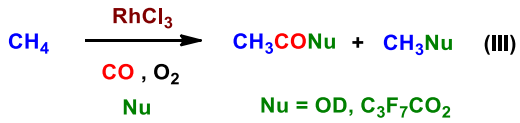

Tilley y colaboradores utilizaron compuestos de escandio para conseguir la activación de metano mediante metátesis de enlaces sigma desarrollando dos sistemas catalíticos. En el primero de ellos se describe la deshidrosililación de metano[25a] a través de una reacción donde Ph_2SiH_2 se convierte en Ph_2MeSiH bajo presión de metano con la mediación de Cp^*_2ScMe como catalizador (Esquema IXa) y la liberación de un equivalente de H_2 por

cada molécula de metano funcionalizada. El complejo Cp*$_2$ScMe transfiere el grupo metilo al silano a través de una metátesis de enlace sigma, dando lugar a la formación del producto.[25b]

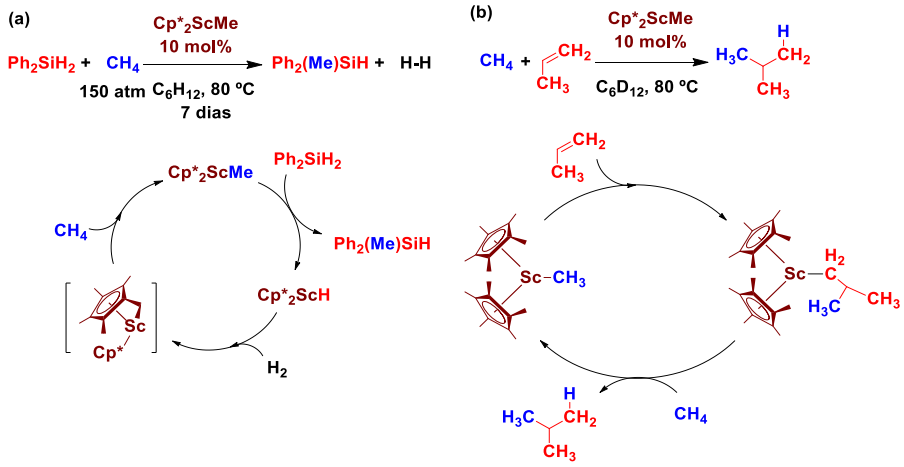

Esquema IX. *Sistemas catalíticos descritos por el grupo de Tilley para la funcionalización de metano.*

En el segundo sistema, el grupo de Tilley encontró que el complejo Cp*$_2$ScMe catalizaba la adición del enlace C-H del metano al doble enlace de propeno, con formación de isobutano (Esquema IXb).[26]

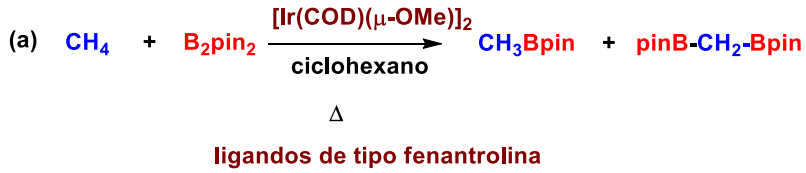

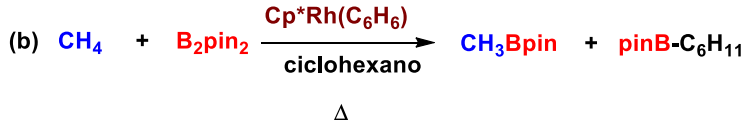

Esquema X. *Sistemas catalíticos descritos por Mindiola y Sanford para la borilación catalítica de metano.*

Más recientemente, en 2016, los grupos de Mindiola[27] y Sanford,[28] de manera independiente, describieron la reacción de conversión de un enlace C-H del metano en un enlace C-B. En el primer caso, el complejo comercial $[Ir(COD)(\mu\text{-}OMe)]_2$ en presencia de un derivado de la fenantrolina (Esquema Xa) presenta actividad catalítica para la reacción de metano y $B_2(pin)_2$, para dar CH_3Bpin (pin = pinacolato) con un rendimiento del 2% basado en el $B_2(pin)_2$. El grupo de Sanford empleó varios complejos de Rh, Ru e Ir (Esquema Xb), siendo el de rodio el más activo.

III. 3 Sistemas catalíticos basados en la inserción de un ligando carbeno en el enlace C-H del metano.

Una estrategia completamente distinta a las anteriormente descritas para funcionalizar metano consiste en la inserción de unidades carbénicas, procedentes de un diazo compuesto, en los enlaces C-H de este hidrocarburo. Si bien este procedimiento era conocido para alcanos líquidos a temperatura ambiente desde hace varias décadas,[29] su aplicación a metano y alcanos gaseosos no ha sido descrita hasta hace pocos años.

El mecanismo generalmente propuesto para este tipo de transformaciones se muestra en el Esquema XI.[30] El primer paso es la formación del intermedio metalocarbeno por reacción de un complejo metálico y un diazocompuesto. Este intermedio carbénico interacciona de manera concertada con el enlace C-H, que en el caso de alcanos es un nucleófilo muy débil. Ello explica la necesidad de un intermedio metalacarbeno altamente electrofílico. La reacción tiene lugar en un único paso que conduce al producto, liberando el centro metálico para un siguiente ciclo catalítico.

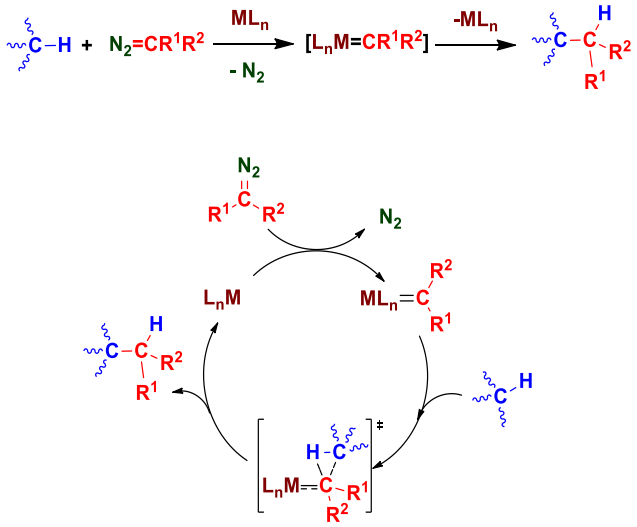

Esquema XI. *Funcionalización catalítica de enlaces carbono-hidrógeno de alcanos mediante inserción de carbenos proveniente de un diazocompuesto.*

A diferencia de las anteriores estrategias, en este caso no hay interacción del enlace C-H con el centro metálico, y no se forman por tanto nuevos enlaces M-C y/o M-H estables que dificulten la liberación del producto de la especie metálica. Es por ello por lo que este tipo de reacciones ocurren en condiciones suaves, a temperatura ambiente la mayoría de las veces, favoreciendo el establecimiento de un ciclo catalítico más eficiente que los basados en la activación organometálica o electrofílica. Sin embargo, este sistema tiene como inconveniente la existencia de una reacción secundaria que es la formación de las olefinas provenientes del acoplamiento de dos moléculas de diazocompuesto. Esta reacción puede ser controlada y minimizada manteniendo una concentración baja de diazocompuesto en el medio de reacción. Conviene asimismo señalar que la regioselectividad observada en este tipo de transformaciones sigue el orden de reactividad C-H terciario > C-H secundario > C-H primario > metano, paralelo al de las energías de disociación de tales enlaces[7] y opuesta a la descrita en la activación organometálica.[31]

En el caso particular del metano, a la dificultad que supone la presencia de un enlace muy poco reactivo hay que unir la naturaleza gaseosa del

hidrocarburo, que implica la necesidad de un disolvente para el catalizador y el diazocompuesto. Comoquiera que cualquier otro enlace C-H o C-X va a ser más reactivo que el metano, la elección de dicho disolvente no es trivial. Para solucionar este inconveniente se precisa de un medio de reacción que sea inerte hacia la reacción de transferencia de grupos carbeno. Nuestro grupo de investigación, en colaboración con el grupo de Gregorio Asensio de la Universidad de Valencia y con el de Michel Etienne del CNRS de Toulouse (Francia), desarrolló esta metodología empleando CO_2 supercrítico ($scCO_2$) como medio de reacción. Los catalizadores utilizados están basados en plata y contienen ligandos trisindazolilborato perfluorados del tipo $Tp^{F21}AgL$ y $Tp^{F27}AgL$ con un alto contenido en flúor, para favorecer su solubilidad en $scCO_2$ (Esquema XII).[32,33]

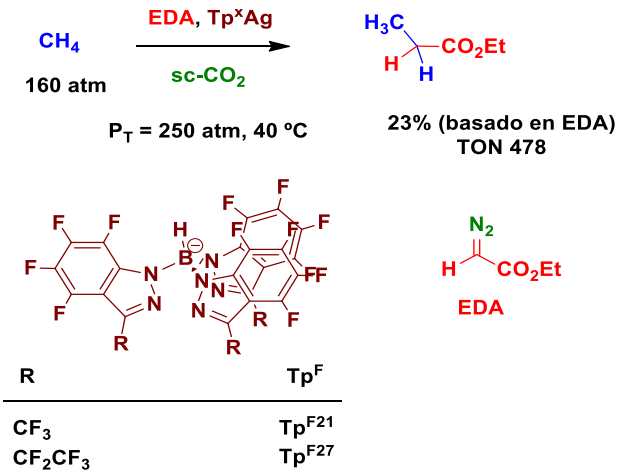

Esquema XII. *Funcionalización de metano mediante inserción de carbenos a partir de diazoacetato de etilo catalizada por plata y usando $scCO_2$ como medio de reacción.*

Los complejos de plata obtenidos son deficientes en densidad electrónica, como se deduce de los valores de ν(CO) de 2165, 2166 cm^{-1} para $Tp^{F21}Ag(CO)$ y $Tp^{F27}Ag(CO)$, respectivamente. Ello favorece la reacción del intermedio metalacarbeno con el enlace C-H del metano (Esquema XII). De esta forma, bajo una presión total de 250 atm y a una temperatura de 40 ºC se

pudo obtener un 23 % de propionato de etilo, basado en el diazoacetato de etilo inicial, con un valor de TON = 478.[34]

IV. Reactividad de alcanos frente a electrófilos.

La reacción anteriormente descrita se basa en un ataque de un electrófilo consistente en un complejo metalacarbénico al enlace C-H que ejerce de nucleófilo. Este tipo de reacciones, empleando electrófilos más fuertes y simples como el H^+, fueron desarrolladas por Olah y colaboradores en las décadas de los 60 y 70 del pasado siglo.[35] En su caso, la reacción de un electrófilo fuerte, como H^+, R^+, X^+ o NO_2^+, con alcanos provocaba la sustitución de un hidrógeno o de un grupo CR_3 del alcano por uno de estos grupos. Estos trabajos condujeron a la determinación de diferentes patrones de reactividad de los alcanos, no sólo de los enlaces carbono-hidrógeno, sino también de los enlaces carbono-carbono, que eran susceptibles al ataque del electrófilo (Esquema XIII).[36] Entre los mayores avances que proporcionaron estos estudios

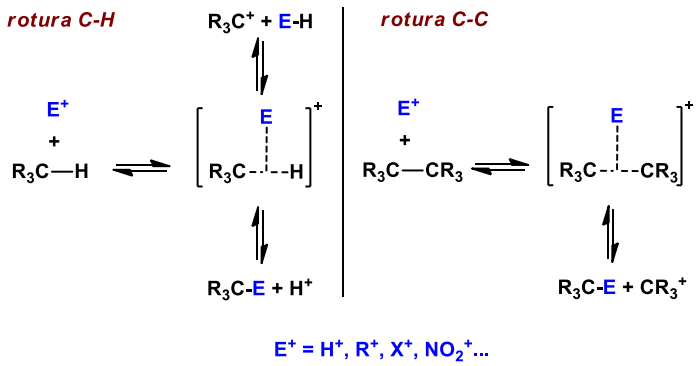

Esquema XIII. *Ataque electrofílico a un enlace C-H o C-C de alcanos.*

cabe destacar la propuesta de iones carbonio como intermedios así como de estados de transición de tres centros y dos electrones, debido al ataque del electrófilo sobre la nube sigma del enlace C-H o C-C.

Consecuencia de los trabajos anteriores es la conocida escala de basicidad de enlaces sigma,[36] que proporciona un orden cualitativo para la nucleofilia de los enlaces C-H y C-C frente a los electrófilos empleados. Dicha escala sigue el orden metano < C-H primario < C-H secundario < carbono-carbono < C-H terciario. Siguiendo esta tendencia general, la reactividad de un enlace C-H específico depende de factores electrónicos y estéricos asociados tanto a la estructura de hidrocarburos como a la naturaleza del electrófilo. Curiosamente este orden suele emplearse de manera generalizada a cualquier tipo de reacciones, a pesar de las reservas descritas por Olah al afirmar que tanto la naturaleza del enlace C-H/C-C en cuestión como la del electrófilo pueden alterar el orden de reactividad. De hecho, en algunos casos la comparación directa de reactividades relativas entre enlaces de distintos sustratos resultaba difícil de establecer. El Esquema XIV muestra la reacción

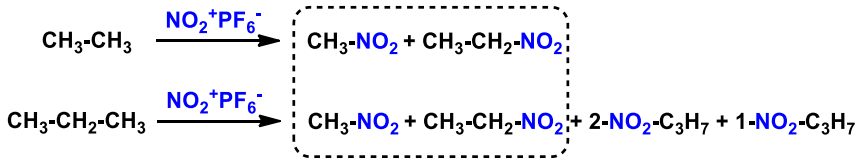

Esquema XIV. *Reacción de nitración de etano y propano.*

de nitración del etano y del propano llevadas a cabo por el grupo de Olah. La formación de los mismos productos en ambas reacciones impide que puedan obtenerse valores de reactividad relativa. Esta circunstancia, unida a la dificultad intrínseca derivada de la naturaleza de los alcanos más ligeros, que son gaseosos o líquidos dependiendo del número de carbonos en la cadena, han impedido el desarrollo de estudios amplios que permitan proponer un orden de reactividad para una serie de enlaces C-H de los alcanos.

V. Sistemas catalíticos en dióxido de carbono supercrítico.

El dióxido de carbono supercrítico (*sc*CO_2) se ha revelado en las últimas décadas como un medio de reacción atractivo, primero para procesos de extracción/separación[37] y posteriormente para fines sintéticos.[38] Un fluido supercrítico es aquella sustancia que se encuentra en condiciones de presión y temperatura por encima de su punto crítico. En tales condiciones presenta propiedades que se asemejan a las de un gas y un líquido. El *sc*CO_2 es uno de los fluidos comprimidos más empleados ya que presenta un punto crítico bastante accesible (31.1 ° C y 73 bar) (Figura I)[39] en comparación con otras sustancias (por ejemplo 374.2 ° C y 220.5 bar para el H_2O o 240.6 ° C y 79.9 bar para el CH_3OH). Asimismo, esta sustancia en estas condiciones tiene un gran poder de solvatación que puede ser modificado con la temperatura y la

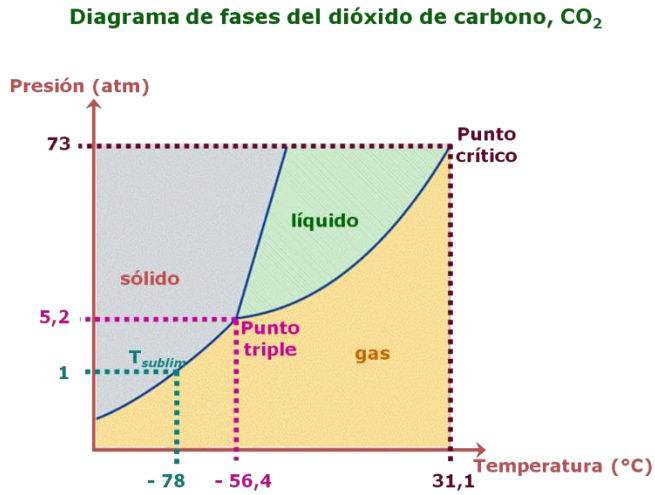

Figura I. *Diagrama de fases (presión vs temperatura) para el dióxido de carbono.*

presión, a la vez que su coste es asequible. Estas y otras propiedades han convertido al *sc*CO_2 en el disolvente de elección para procesos industriales importantes como la extracción de cafeína,[40] en transformaciones farmacéuticas[41] o en el procesamiento de polímeros.[42]

El empleo de *sc*CO_2 como medio de reacción en síntesis orgánica comenzó a finales de los años ochenta y actualmente constituye un campo de investigación muy activo. Hay abundantes ejemplos de sistemas catalíticos tanto homogéneos[43] como heterogéneos[44] que emplean este fluido como medio de reacción. El principal inconveniente que surge en estos sistemas es la baja solubilidad de los catalizadores metálicos en *sc*CO_2. Este problema se puede solventar con el diseño inteligente de ligandos que contengan los sustituyentes apropiados para la interacción con las moléculas de dióxido de carbono del fluido y consigan la solubilización del catalizador. La estrategia usual consiste en la introducción de grupos CO_2-fílicos como grupos fluorados, silanos, siloxanos y poliacetatos, entre otros.[45]

VI. Sistemas catalíticos en agua.

Cada vez es mayor la preocupación de la sociedad por el medio ambiente y en esta área la Química juega un papel importante. La Química Sostenible o Química verde tiene como premisa fundamental el diseño de productos y procesos que empleen y produzcan la menor cantidad de sustancias tóxicas posibles y con el menor consumo energético, y así afectar al medio ambiente lo menos posible. Estos objetivos quedan plasmados en los denominados Doce Principios de la Química Sostenible,[46] en donde uno de ellos es el empleo de catalizadores y de disolventes que sean lo más respetuosos posible con la naturaleza.[47] Teniendo en cuenta que en una reacción química normalmente el 80% en masa es disolvente,[47b] la búsqueda de disolventes alternativos con bajo impacto medioambiental es fundamental para cumplir los estándares de la química verde.

Entre todos los disolventes que se puedan emplear en una reacción química, el agua es sin duda el disolvente más sostenible que pueda usarse. Además, es un disolvente muy barato, no es tóxico ni inflamable, no contribuye a las emisiones de efecto invernadero, no requiere de síntesis, la energía necesaria para su aislamiento en forma pura es baja y su factor E[48] es igual a

cero, lo que significa que no se considera un residuo en las transformaciones químicas. Además tiene una acidez regulable, una gran capacidad calorífica y un calor de evaporación que permite un fácil control de las reacciones exotérmicas. A pesar de todas estas propiedades, el agua es uno de los disolventes menos empleado en catálisis debido a su alta polaridad y a que forma puentes de hidrógeno que aumentan el efecto hidrófobo, no ayudando a la solvatación de moléculas apolares y dificultando las reacciones químicas. Generalmente, los complejos metálicos que se emplean como catalizadores no son solubles en este medio, pero este problema se puede solventar introduciendo ciertos grupos en su estructura que ayudan a su solubilidad. Así pues, cada vez es mayor el número de trabajos que emplean este disolvente en reacciones catalíticas. Uno de los primeros trabajos en donde se empleó agua como medio de reacción tuvo lugar a principios de los años 80 con un proceso para convertir propeno en 1-buteno usando un catalizador de Rh con ligandos fosfina.[47a] Desde entonces, la comunidad científica ha dedicado grandes esfuerzos para la utilización de agua como medio de reacción.[49] Además presenta como ventaja adicional el posible reciclado del catalizador en estos sistemas, ya que los productos se pueden extraer con un disolvente orgánico inmiscible en agua, separándose de esta forma del catalizador, que quedaría disuelto en agua.

Además del uso de catalizadores que sean ya, por diseño, solubles en agua (Figura IIa), existen varias estrategias para solubilizar catalizadores que, en principio, son insolubles en dicho medio. En el caso de catalizadores que son solubles en medio orgánico, la modificación parcial de su estructura con grupos que le proporcionen dicha solubilidad es la estrategia más común (Figura IIb). A nivel supramolecular existen otras dos aproximaciones. La primera de ellas (Figura IIc) consiste en la adición de moléculas de surfactantes que forman micelas, concentrando en su interior hidrófobo al catalizador y los reactivos, facilitando así la reacción catalítica. La segunda estrategia también hace uso de la formación de micelas, si bien en este caso el surfactante ya lleva

unido el catalizador que queda en la parte externa (o interna) de la denominada metalomicela ((Figura IId). En el siguiente apartado se realiza un breve resumen del estado del arte de la catálisis micelar.

VI. 1 Catálisis micelar. Generalidades.

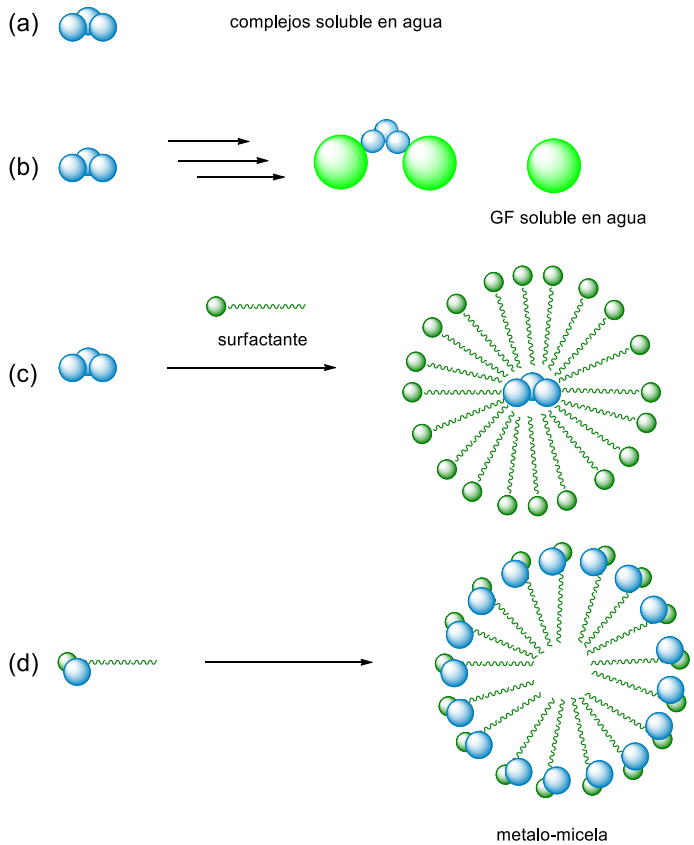

Figura II. *Catálisis metálica en agua: (a) catalizador intrínsecamente soluble en agua; (b) modificación covalente de ligandos con grupo funcionales solubles en agua; (c) catalizadores solubles en micelas. (d) aductos covalentes metal-surfactante formando metalomicelas.*

Los tensioactivos o surfactantes (denominación abreviada de agentes activos en la superficie) son moléculas ambifílicas: poseen una cabeza hidrofílica altamente polar y una cadena carbonada hidrofóbica que puede contener grupos aromáticos o alifáticos. Cuando estas sustancias se añaden al agua y superan un valor determinado de concentración, denominado

concentración micelar crítica, forman estructuras supramoleculares llamadas micelas, ya que las cabezas hidrofílicas quedan expuestas al medio acuoso mientras que las cadenas hidrofóbicas se dirigen hacia el interior de la región formada por la micela sin estar en contacto con el agua (Figura III). El Esquema XV muestra los surfactantes más empleados en la generación de micelas en medio acuoso.

El uso de tensioactivos en condiciones micelares representa uno de los métodos más sencillos para inducir procesos catalíticos en agua con catalizadores no solubles, ya que muchos tensioactivos se emplean en la fabricación de detergentes.[50] En estos sistemas, los reactivos y productos orgánicos además del catalizador quedan disueltos dentro de la micela, separados de la fase acuosa. Una vez terminada la reacción, los productos orgánicos se separan de la mezcla de reacción mediante extracción con el disolvente orgánico adecuado, reteniéndose en la fase acuosa el surfactante y el catalizador. Desde un punto de vista conceptual, las micelas se pueden considerar como nanorreactores donde en su interior hay una alta concentración de reactivos.

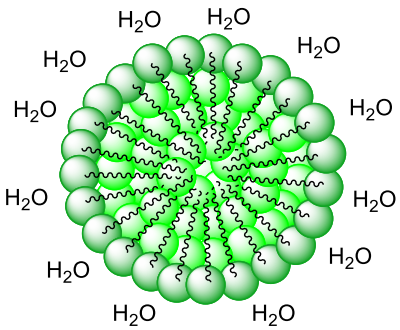

Figura III. *Estructura general de una micela.*

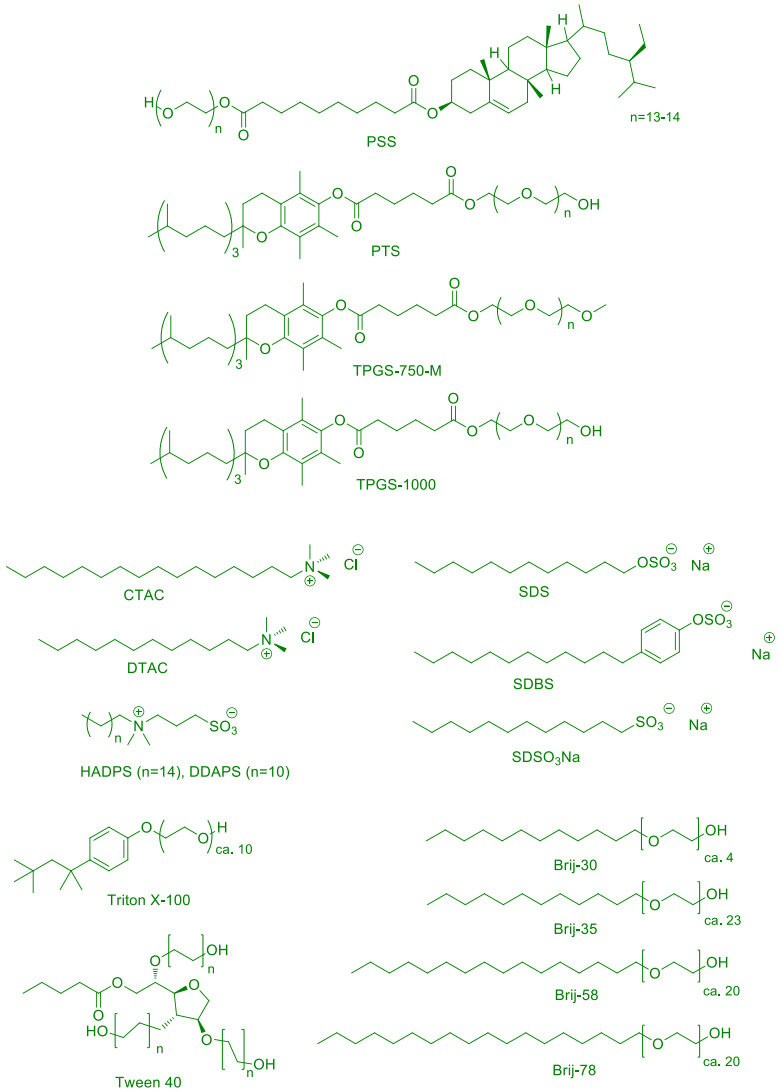

Esquema XV. *Estructuras de los surfactantes comerciales más comunes.*

VI. 2 Catálisis micelar. Ejemplos.

Las aziridinas son intermedios químicos muy importantes ya que forman parte de muchos productos farmacéuticos útiles. Su síntesis no es trivial y a menudo requiere del empleo de fuentes de N complejas. Existen algunos ejemplos en la bibliografía en donde se han conseguido aziridinar olefinas en

agua, empleando diversos surfactantes. Unos de estos trabajos, descrito por De Vos y colaboradores,[51] permitió la incorporación directa de amoníaco a olefinas utilizando surfantantes no iónicos, tales como alcoholes grasos etoxilados o ésteres de sorbitán, con yodo molecular como catalizador en presencia de un agente blanqueante (Esquema XVI). En estas condiciones el resultado de la reacción catalítica mejoró con respecto a lo descrito en disolventes orgánicos

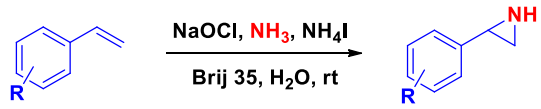

Esquema XVI. *Síntesis de aziridina a partir de alquenos con hipoclorito, amoníaco y yoduro de amonio en agua.*

La oxidación de sustratos bencílicos a los correspondientes compuestos carbonílicos es una reacción altamente deseable que a menudo hace uso de catalizadores de metales de transición. Novák y colaboradores propusieron[52] el uso de hidroperóxido de *t*-butilo como oxidante en presencia de catalizadores de Fe(III) tales como $FeCl_3$ o $Fe_2(SO_4)_3$, y del tensioactivo aniónico SDS (dodecilsulfato sódico), para promover la reacción en medio acuoso (Esquema XVII).

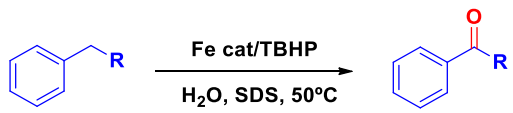

Esquema XVII. *Oxidación bencílica en agua catalizada por Fe en presencia de un surfactante.*

También se ha conseguido mediante esta estrategia la síntesis de fenol a partir del correspondiente ácido borónico con oxígeno molecular en agua empleando compuestos de Cu(II) y el tensioactivo Brij S-100.[53] De esta forma no se precisan ni bases ni ligandos auxiliares, consiguiéndose altos rendimientos en los productos bajo condiciones experimentales suaves (Esquema XVIII).

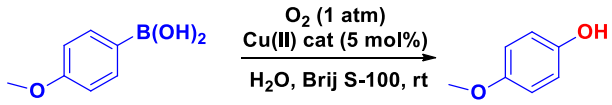

Esquema XVIII. *Síntesis de derivados de fenol en agua catalizada por un catalizador de cobre (II).*

Otro tipo de transformaciones desarrolladas con esta metodología es la de formación de enlaces carbono-carbono. Por ejemplo, en las reacciones de alquilación de Friedel-Crafts de indoles en agua se ha empleado dodecilsulfato sódico (SDS) como tensioactivo y compuestos de Cu(II) como catalizador. La velocidad de esta reacción en estas condiciones es sustancialmente mayor a la de la reacción sin surfactante debido a la combinación sinérgica del compuesto metálico y los agregados micelares (Esquema XIX).[54]

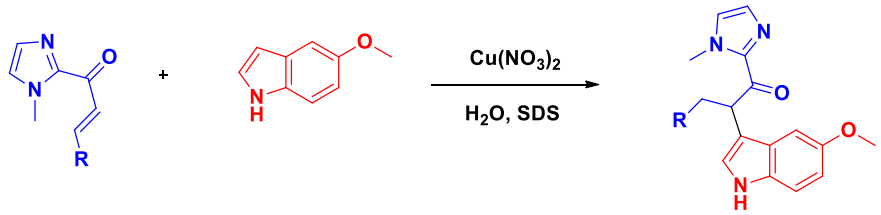

Esquema XIX. *Alquilación vinílica de Friedel-Crafts catalizada por Cu(II) en agua.*

La reacción de acoplamiento cruzado de Suzuki-Miyaura es otro proceso catalítico de formación de nuevos enlaces C-C que se ha podido realizar en condiciones de catálisis micelar, empleando agua como disolvente. A pesar de los grandes avances conseguidos en esta reacción, el acoplamiento de cloruros de arilo, fácilmente disponibles y de bajo coste, con cloruros de heteroarilo sigue siendo difícil de lograr. Recientemente, Yu y Liu propusieron[55] un sistema catalítico consistente en el uso de cloruro de metil-trioctil-amonio como aditivo para la reacción entre cloruros de arilo y ácidos arilborónicos a 100 °C usando una carga muy baja de $Pd(OAc)_2$/(2-mesitilindenil)diciclohexilfosfina como precursor catalítico (Esquema XX).

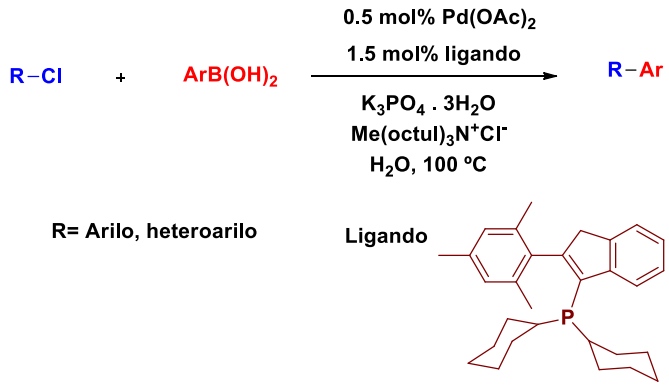

Esquema XX. *Reacción de acoplamiento cruzado de cloruros de arilo y heteroarilo en medios micelares.*

OBJETIVOS

Sobre la base de los precedentes bibliográficos expuestos en la Introducción, se han fijado los siguientes objetivos para esta Tesis Doctoral:

1) Desarrollo de nuevos catalizadores basados en metales del grupo 11 capaces de promover la funcionalización de los enlaces C-H del metano y alcanos ligeros mediante inserción de grupos carbeno a partir de diazo compuestos en *sc*CO_2.

2) Estudio de la reactividad relativa de una serie de alcanos gaseosos y líquidos, tomando el metano como referencia, que proporcionen información adicional a la conocida escala de basicidad sigma de Olah.

3) Estudio del agua como medio de reacción para la reacción de metano y alcanos gaseosos empleando los catalizadores que operan en medio *sc*CO_2 y la formación de micelas con surfactantes.

OBJECTIVES

Based on the literature precedents briefly presented in the Introduction, the following objectives have been targeted for this Ph. D. Thesis:

1) Development of new catalysts based on coinage metals with activity toward the functionalization of methane and light alkanes upon carbene insertion reactions, using diazo compounds as the carbene source and *sc*CO_2 as the reaction medium.

2) Study of the relative reactivity of a series of alkanes, gaseous and liquids, using methane as the reference, aiming to provide additional information to the sigma basicity scale proposed by Olah.

3) Use of water as the reaction medium for the catalytic functionalization of methane and gaseous alkanes, using the same catalysts developed for *sc*CO_2 and in the presence of surfactants that may generate micelles.

RESULTS AND DISCUSSION

Section 1

New catalysts for methane and light alkanes functionalization

1. Synthesis of the novel fluorinated trispyrazolylborate ligand $Tp^{(CF3)2,Br}$.

As described in the Introduction, our group has previously described the use of highly fluorinated Tp^xAgL complexes as catalysts for the functionalization of gaseous alkanes, including methane, by means of the carbene transfer reaction using ethyl diazoacetate (EDA) as the carbene source and *sc*CO_2 as reaction medium.[34,56] The design of these fluorine-containing Tp^x ligands obeys two requirements to achieve such alkane functionalization. On one side, the presence fluorinated groups in the pyrazol rings decreases the donor capabilities of the ligand to the metal center, thus increasing its electrophilicity and that of the metal-carbene intermediate,[29] to react with the poor nucleophile alkane C-H bond. On the other, the need of *sc*CO_2 as the reaction medium also impulses the use of fluorinated ligand, in view the well-known capabilities of fluorine-containing complexes to dissolve in such medium.[45b] In spite of that, the complexes prepared with the series of fully fluorinated trisindazolylborates[56] mentioned in the Introduction were only soluble to a certain extent, the solubility being even lower for the copper complexes when compared to the silver analogues.

On the basis of the above, the design of a new trispyrazolylborate ligand containing trisubstituted pyrazolyl rings, each one bearing two -CF_3 and one –Br substituents was targeted. Previous work carried out in our group demonstrated[57] that the $Tp^{Br3}Cu(NCMe)$ complex partially dissolved in a fluorous phase, therefore it was expected that the combination of fluorine and bromine substituents in the same ligand could improve the solubility of its copper and silver complexes in *sc*CO_2.

With this idea in mind, the new thalium complex $TlTp^{(CF3)2,Br}$ (**1**) was synthetized upon direct reaction of the 3,5-bis(trifluoromethyl)-4-bromo-pyrazole (obtained by the multi-step protocol shown in Scheme 1)[58] and $TlBH_4$ (prepared using TlAcO and KBH_4 in water). This method avoids the isolation

of the potassium salt and the subsequent low-yielding transmetallation step with thalium nitrate, that is the common strategy described for other $TlTp^x$ ligands.[59]

Complex **1** was characterized on the basis of spectroscopic and analytic data, as well as by X-ray single-crystal studies (Scheme 1). NMR spectra (^{19}F or ^{13}C) showed one set of resonances for the pyrazolyl rings, such equivalency assessing the C_{3v} symmetry expected for a compound bearing three N-Tl bonds. Figure 1 displays the ^{19}F NMR spectrum, where the CF_3 groups resonate as a singlet at -57.1 and a doublet centered at -60.1 ppm, as a consequence of the existence of two series of non-equivalent CF_3 groups, corresponding to those

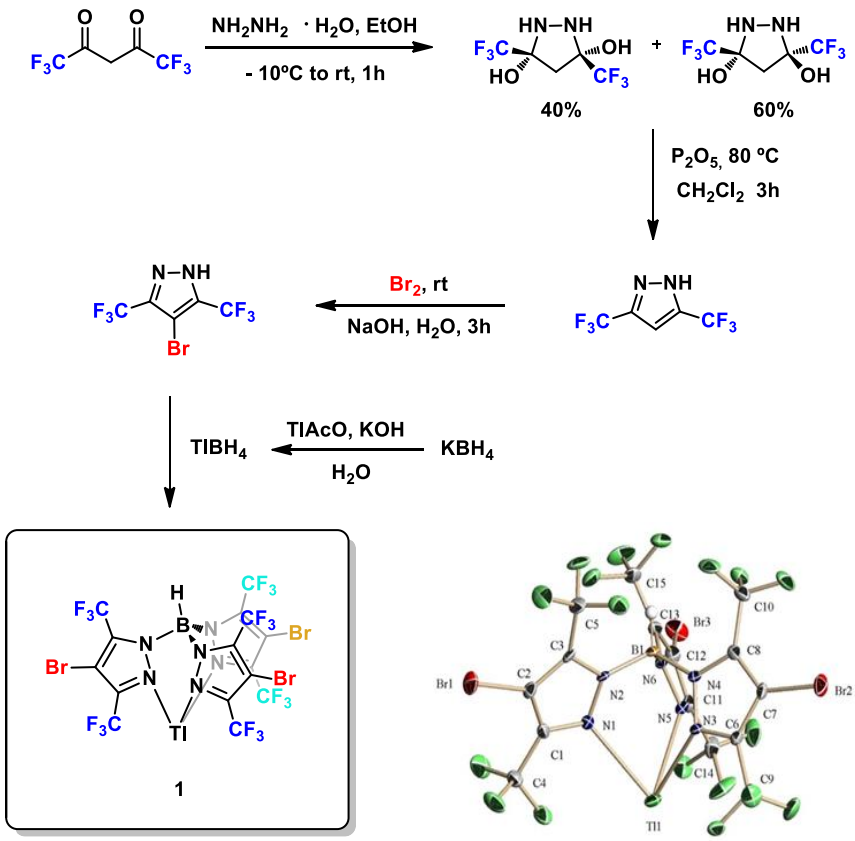

Scheme 1. Syntheses of the 3,5-bis(trifluoromethyl)-4-bromo-pyrazole and the corresponding thalium hydrotris(3,5-bis(trifluoromethyl)-4-bromo-pyrazolyl)-borate complex (**1**). Its X-ray structure (ORTEP view) shows thermal ellipsoids at the 50% level probability.

near the boron and close to the thalium, respectively. The coupling constant observed serves to assign that resonance to the latter, since the Tl nucleus is active in NMR ($J_{F\text{-}Tl}$ = 972 Hz).

Slow crystallization of $CHCl_3$ solutions of **1** gave colorless crystals, some of them suitable for X-ray diffraction studies. The solid state structure

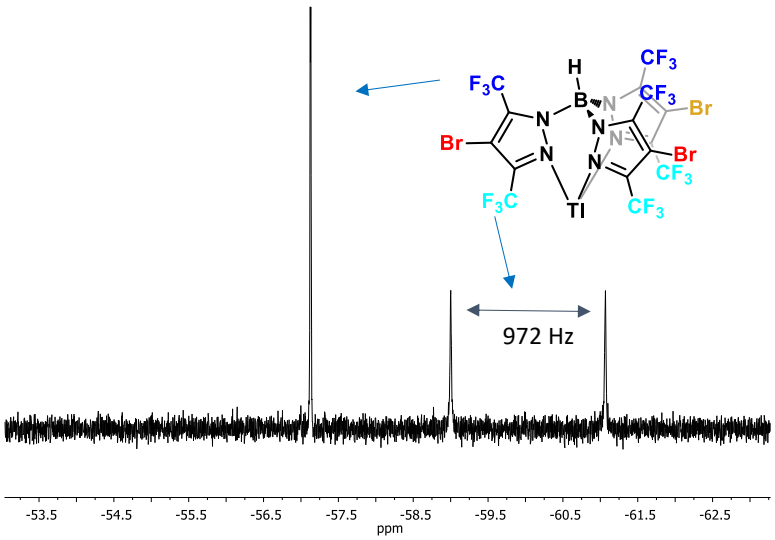

Figure 1. ^{19}F-NMR (470 MHz, $CDCl_3$, 20 ºC) spectrum of complex **1**.

(Scheme 1) was in agreement with the geometry proposed from NMR data in solution, the three pyrazolyl rings being equivalents and the $Tp^{(CF3)2,Br}$ ligand displaying a κ^3 coordination mode. Two of the three N-Tl distances are identical (Table 1), the third being slightly longer.

Table 1. Selection of distances [Å] and angles [º] in complex **1**

Distances		Angles	
Tl(1)-N(1)	2.727(5)	N(1)-Tl(1)-N(5)	71.39(15)
Tl(1)-N(5)	2.738(5)	N(1)-Tl(1)-N(3)	71.35(15)
Tl(1)-N(3)	2.761(5)	N(5)-Tl(1)-N(3)	66.68(15)

2. Synthesis and characterization of copper and silver complexes containing the ligand $Tp^{(CF3)2,Br}$.

Once the new ligand $Tp^{(CF3)2,Br}$ was available, the copper and silver derivatives were prepared by transmetallation reactions with CuI or AgOTf in acetonitrile or tetrahydrofuran as solvents, at room temperature, respectively (Scheme 2). Following this procedure, the complexes $Tp^{(CF3)2,Br}$Cu(NCMe) (**2**) and $Tp^{(CF3)2,Br}$Ag(thf) (**3**) were isolated in good yields (70-75%).

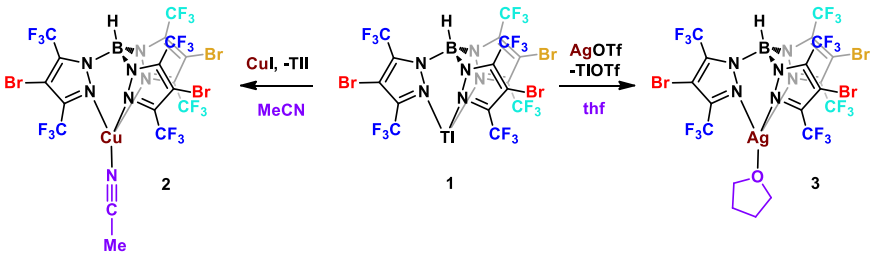

Scheme 2. Synthesis of complexes **2** and **3**.

The ^{19}F NMR spectra of complexes **2** and **3** are shown in Figure 2. As expected, only two resonances appear for the six CF_3 groups in both complexes, each accounting for three of them, corresponding to those close to the boron and near the metal center, respectively. Also, the three pyrazolyl rings are equivalent, allowing the proposal of the trispyrazolylborate ligand in a tricoordinated, κ^3-fashion (Scheme 2). The ^1H and ^{13}C NMR spectra, as well as

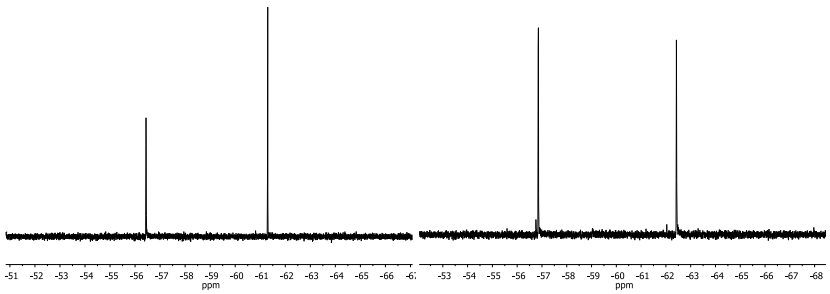

Figure 2. ^{19}F-NMR (470 MHz, $CDCl_3$, 20 ^oC) spectra of complexes **2** (left) and **3** (right).

the elemental analyses, demonstrated the presence of a fourth ligand coordinated to the metal center: acetonitrile in **2** and tetrahydrofuran in **3**, i. e., the solvents employed in the synthetic procedure.

The X-ray studies carried out with complexes **2** and **3** (Figure 3) showed that the $Tp^{(CF3)2,Br}$ ligand is bonded to the metal center in a tricoordinated fashion. The geometry around the metal center consists of a distorted tetrahedron, formed by the three donor atoms of the scorpionate ligand and a fourth atom from the solvent molecule. Bond distances and angles are similar to those found for other related complexes of these metals with trispyrazolylborate ligands.[32,60] The most relevant crystallographic data are shown in Tables 2 and 3. In both complexes, the M-N_{pyr} distances display the same pattern: two of them are nearly identical whereas the third is shorter, a feature commonly observed for $Tp^{x}ML$ complexes (M = Cu, Ag).[32,60] In the copper case, the acetonitrile ligand is slightly bend with respect to the B-Cu axis, albeit such deviation is also well known for such class of compounds.[32]

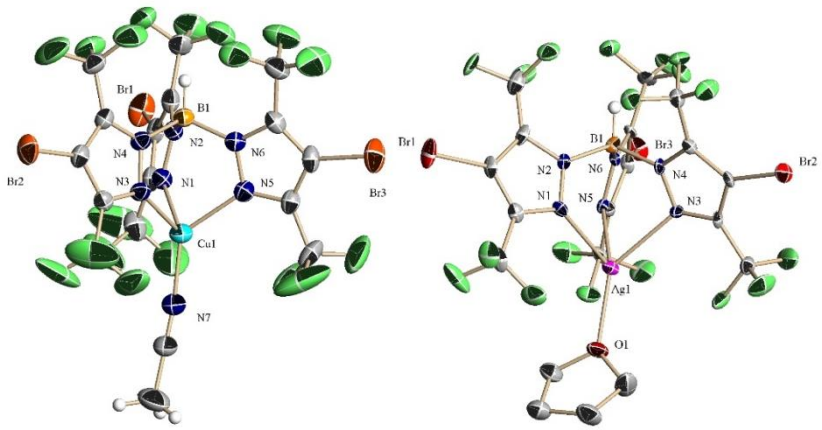

Figure 3. ORTEP view of the molecules of complexes **2** and **3** (hydrogen atoms are excluded for clarity). Thermal ellipsoids are set to 50% level probability.

Table 2. Selection of distances [Å] and angles [º] of complex **2**

Distances		Angles	
Cu(1)-N(7)	1.891(7)	N(7)-Cu(1)-N(5)	129.3(3)
Cu(1)-N(5)	2.080(6)	N(7)-Cu(1)-N(1)	126.4(3)
Cu(1)-N(1)	2.100(5)	N(5)-Cu(1)-N(1)	90.1(2)
Cu(1)-N(3)	2.116(5)	N(7)-Cu(1)-N(3)	121.8(2)
		N(5)-Cu(1)-N(3)	87.6(2)
		N(1)-Cu(1)-N(3)	89.6(2)

Table 3. Selection of distances [Å] and angles [º] of complex **3**

Distances		Angles	
		O(1)-Ag(1)-N(5)	135.2(5)
Ag(1)-O(1)	2.230(13)	O(1)-Ag(1)-N(3)	136.8(5)
Ag(1)-N(5)	2.380(13)	N(5)-Ag(1)-N(3)	77.1(4)
Ag(1)-N(3)	2.387(13)	O(1)-Ag(1)-N(1)	122.0(5)
Ag(1)-N(1)	2.439(14)	N(5)-Ag(1)-N(1)	82.6(4)
		N(3)-Ag(1)-N(1)	83.5(4)

2.1 Evaluation of the electronic density of the metal center in complexes 2 and 3.

A very useful tool for estimating the electronic density of the metal in a complex consists of measuring the frequency of the ν(CO) band in the carbonyl derivatives using infrared spectroscopy. Therefore, the carbonyl adduct of the corresponding compound needs to be formed. In the case of complexes **2** and **3**, this is simply achieved by bubbling CO through their dichloromethane solutions (Scheme 3), which are further investigated by solution.

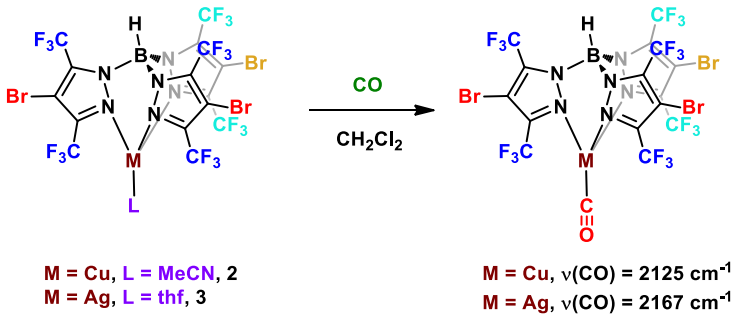

Scheme 3. In situ generation of carbonyl adducts of the $Tp^{(CF3)2,Br}M$ core.

The solution ν(CO) values of the carbonyl adducts $Tp^{(CF3)2,Br}M(CO)$ of 2125 cm^{-1} (M = Cu) and 2167 cm^{-1} (M = Ag) indicate a poor electron density at the metal center. The latter value is nearly identical to those obtained for an array of five complexes of silver with fluorinated tris(indazolyl)borate ligands bearing fluorine atoms,[32,33] or to that of the related $Tp^{(CF3)2}Ag(CO)$ (2162 cm^{-1} in solution, 2178 cm^{-1} in the solid state),[61] and constitutes another example of a non-classical silver-carbonyl complex.[62] Such low electron density constitutes one of the targeted requirements for this new ligand toward its subsequent use as catalyst for the functionalization of alkane C-H bonds.

3. Study of the catalytic activity of complexes 2 and 3 in the functionalization of gaseous alkane C-H bonds.

The goal of the design of the new ligand **1** and their copper and silver derivatives **2** and **3** was the development of more soluble catalysts for the functionalization of methane in *sc*CO_2 with EDA. The reaction is performed in a high pressure reactor, where the catalyst precursor and EDA are placed along with carbon dioxide (90 atm) and methane (160 atm) at 40 ºC. These values of pressure and temperature ensured that supercritical conditions were reached. For the sake of clarity, a description of the experimental device and procedure employed is provided below.

3.1 Description of the experimental device.

The performance of reactions in *sc*CO_2 requires experimental devices designed to work at high pressures and allowing a delicate control of pressure and temperature conditions. Our group started to work in this area nearly ten years ago, in collaboration with the group of Prof. Gregorio Asensio (Universidad de Valencia), with a long experience in the use of this reaction medium. Since then, our group has developed a high pressure lab where the work described in this Thesis has been carried out.

Figure 4 shows the available systems at the Homogeneous Catalysis Laboratory – Universidad de Huelva. It consists of a supercritical fluid plant, initially design for extraction, which contains a high pressure reactor, equipped with two sapphire windows and a piston pump to introduce carbon dioxide into the reactor. The plant is computer-controlled in terms of temperature and pressure, and the maximum working pressure is 300 atm. The reactor is employed as the reservoir for the mixture of *sc*CO_2 and the gaseous alkane to feed other three reactors where the catalytic reaction takes place.

Figure 4. Supercritical fluid plant (left) with the gas chromatograph and the three high pressure reactors (right).

The system contains a GC where the reaction mixtures can be analyzed on line, just by opening a valve from each reactor. A special reduction valve allows the decrease of the reactor pressure of 250 atm to the 2 atm required for automatic injection in the GC.

The procedure for the catalytic experiment is the following. The catalyst is placed in a cylindrical polypropylene vessel with both ends covered with a permeable membrane (Figure 5). In another polypropylene conical vessel EDA is placed, and both containers are attached to the stir bar of the reactor. The reactor is closed and pressurized with the gaseous alkane and subsequently with carbon dioxide at a temperature of 40 ° C.

Figure 5. Initial setup of reactants in the reactor.

It is worth recalling that above 31 ºC and 72 atm, the critical point of CO_2 is exceeded, so the experiments must be carried out above those limits to ensure the maintenance of supercritical conditions. Once the desired reaction time was reached, the reaction mixture was analyzed by GC from which, on the basis of previously recorded calibration lines (see Experimental Section), the exact amount of the products was obtained.

3.2 Catalytic activity of complexes 2 and 3 toward methane functionalization and other gaseous alkanes.

Notably, the combination of CF_3 and Br substituents in the pyrazol rings proved to be effective in dissolving complexes **2** and **3** in all cases in the mixtures of methane and *sc*CO_2, at variance with the previously employed

fluorinated derivatives that showed only partial solubility.[56] After 8 h, the reaction mixture was analyzed with GC directly connected to the pressure vessel, showing the formation of ethyl propionate, the product resulting from the insertion of the $CHCO_2Et$ moiety into the methane C-H bond (eq. 1). Albeit in low yield (4% with respect to initial EDA), the results observed with the copper-based catalyst **2** represent the first example of the catalytic modification of methane with this metal under homogeneous conditions. Moreover, the remaining 96% of initial EDA was converted into a mixture of diethyl fumarate and maleate,[63] products derived from the metal-catalyzed carbene coupling. It is well-known that the formation of these products can be minimized maintaining a low concentration of EDA in the reaction mixture, using slow addition devices. At the present stage such experiment has not been achieved, due to the use of high pressure conditions. However, with the appropriate engineering design, the enhancement of the yields into the methane derivative would be achievable. Increasing the relative amount of catalyst with respect to EDA is not a solution, since it was demonstrated that such strategy favors the formation of the formal carbene-coupling products, diethyl fumarate and maleate.[64]

The silver catalyst **3** was more efficient with methane in terms of yields,

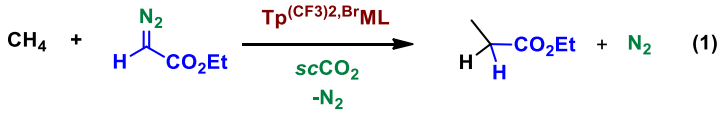

M = Cu, L = MeCN (2) 4%

M = Ag, L = thf (3) 33%

and similar to those reported with the aforementioned fluorinated trisindazolylborate silver catalysts.[34,56] The difference between both metals stands on the relative barriers of C-H insertion and carbene coupling (Scheme 4). Previous work provided a computational model[30b,63b] showing that this reaction occurs through the intermediacy of a metallocarbene intermediate, that

very recently has been detected with this family of catalysts.[65] The relative barriers of the steps involving the interaction of such intermediate with a second molecule of diazo reagent or with the alkane govern the reaction outcome. For copper-based catalysts, that difference is higher (Scheme 4) than those calculated for the silver counterpart. This is in agreement with the observation that, under the same experimental conditions, larger amounts of the alkane functionalized product with the silver catalyst are obtained.

The diazo reagent N_2=$CHCO_2Et$ and the complexes **2** and **3** have been also employed for the conversion of alkanes C2-C4 (ethane, propane and n-butane) into esters upon chain carbene insertion (Scheme 5). As with methane, the reaction must be carried out in supercritical carbon dioxide ($scCO_2$) as the

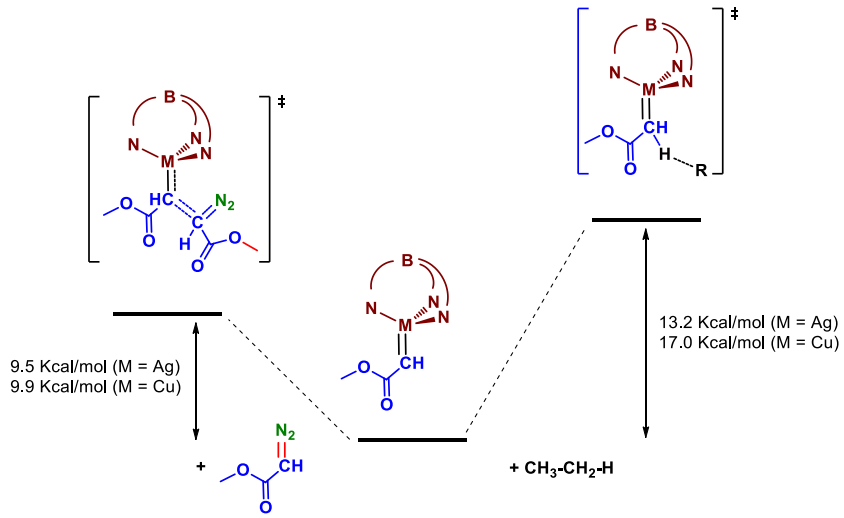

Scheme 4. Comparison of the relative barriers of the interaction of the metallocarbene intermediate with a second molecule of diazo compound (left) or ethane (right). Data taken from reference 61b.

reaction medium due to the low reactivity of these substrates (any other C-H bond would react more readily than that of the alkane) and its gaseous nature. Scheme 5 displays the catalytic results obtained for these reactions. To the best of our knowledge, there is no previous report on the use of copper catalysts for the functionalization of these light alkanes by carbene insertion, the already

described catalytic systems being limited to alkanes ranging from pentane to polyolefins.[29]

Complex **2** catalyzes the functionalization of those C2-C4 alkanes at a larger extent than that of methane: 15% with ethane, 23% with propane and 53% with butane (EDA-based yields). Complex **3** induces a larger degree of

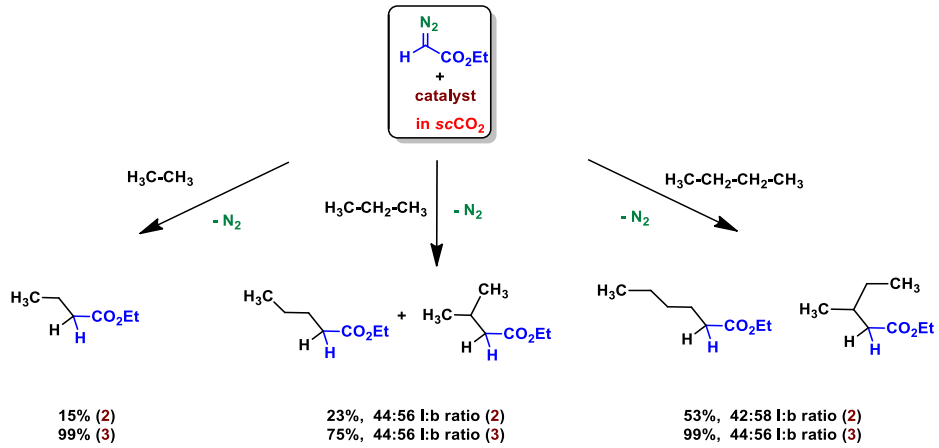

Scheme 5. Catalytic functionalization of alkanes C2−C4 with ethyl diazoacetate and complexes **2** and **3** as catalysts (l:b = linear:branched).

functionalization (Scheme 5), in line with previous work from our laboratory with other silver-based catalysts.[34,56] As expected, the silver catalyst **3** is more active than the copper analog, due to the already mentioned tendency of the latter to favor carbene coupling, a reaction that is disfavored with the former. The groups of Caulton and Mindiola[66] have also described related transformations with a silver-based catalyst, for ethane and propane as substrates.

The existence of two different C-H bonds in the molecules of propane and butane originates a mixture of compounds derived from the metal-catalyzed insertion of the carbene moiety into both sites. Previous catalytic systems based on Tp^xM (M = Cu, Ag) cores have shown that the copper derivative provides

none or very low functionalization of the primary sites, whereas the silver analogue does effectively promote it.[32,67,68] Thus, the regioselectivity observed with the C3-C4 alkanes and **2** as the catalyst can be considered as unexpected, since it has now been found that under the reaction conditions, i. e. the reaction of the alkane and EDA in *sc*CO_2, both metal catalysts behave in a very similar manner in terms of regioselectivity. This effect could be of interest from the point of view of exerting a certain control of the nature of the metal in the regioselectivity of the reaction, and will be discussed in detail in the following section.

3.3 The supercritical effect in the regioselectivity of alkane functionalization.

To shed light about the surprising behavior of the copper catalyst in supercritical carbon dioxide, regarding the regioselectivity of the reaction, the functionalization of other liquid alkanes as hexane, pentane or 2-methylbutane using either the neat alkane or *sc*CO_2 as the reaction medium and complexes **2** and **3** as the catalyst has been studied. The results were as surprising as those commented above: a noticeable change in the regioselectivity was induced just by changing the reaction medium from liquid alkane to *sc*CO_2. Figure 6 displays two GC traces of the reactions of hexane and EDA in the presence of **2** as the catalyst, from which the difference in regioselectivity is clearly visible. The ratio of the product derived from the functionalization of the primary sites increased from 7% in neat hexane to 30 % in *sc*CO_2, in experiments in which all variables were maintained. Interestingly, the regioselectivity of the reaction remained unaltered when using the silver catalyst **3** either in neat hexane or *sc*CO_2.

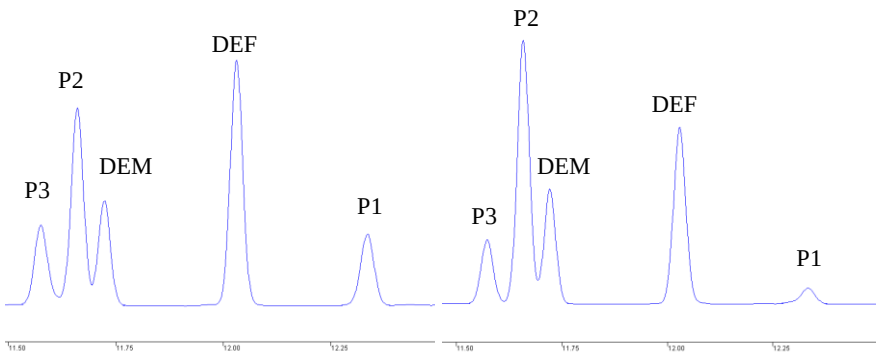

Figure 6. GC traces of the reaction of hexane and EDA in *sc*CO_2 (left) or neat hexane (right), using copper complex **2** as the catalyst. P1, P2 and P3 corresponds to the products derived from carbene insertion into C1, C2 and C3 and DEM and DEF corresponds to diethyl maleate and diethyl fumarate derived from coupling between two molecules of EDA.

Further experiments were carried out with pentane and 2-methylbutane, with the same pattern of reactivity being found: the copper-based catalyst exerts the enhancement of the functionalization of the primary sites when employing *sc*CO_2 as the reaction medium: a five-fold increase was observed for the three alkanes employed (Scheme 6). All experiments were carried out at 40 ºC, including those in neat alkanes, therefore the observed behavior cannot be related to temperature.

At this stage, several questions may be raised about this unprecedented performance. First, it could be thought that the mere presence of a high pressure of carbon dioxide could be responsible of the change in regioselectivity. However, upon performing the reaction in neat hexane under an atmosphere of carbon dioxide (100 atm) but at room temperature (therefore out of the supercritical conditions region), the regioselectivity observed was similar to that in the absence of carbon dioxide (Scheme 6). This experiment suggests that the dramatic change observed in the product distribution by increasing the amount of carbene insertion into the primary sites should be attributed to an effect of the supercritical phase conditions.

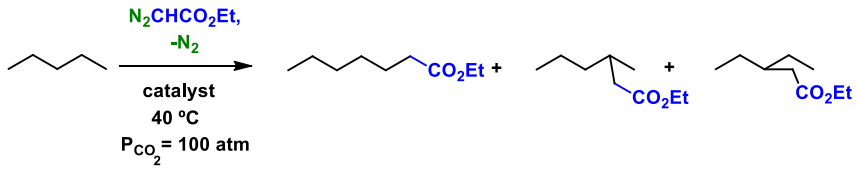

neat pentane	6	77	17	**Catalyst 2**
pentane in $scCO_2$	31	56	13	
neat pentane	38	44	18	**Catalyst 3**
pentane in $scCO_2$	40	48	12	

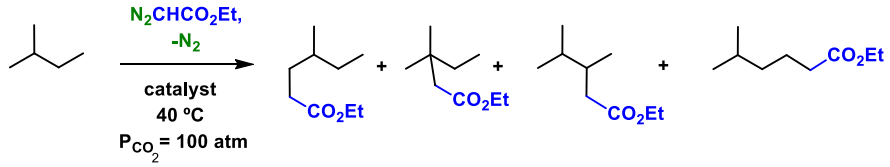

neat 2-methylbutane	5	76	14	5	**Catalyst 2**
2-methylbutane in $scCO_2$	32	15	21	32	
neat 2-methylbutane	33	13	21	33	**Catalyst 3**
2-methylbutane in $scCO_2$	31	16	21	32	

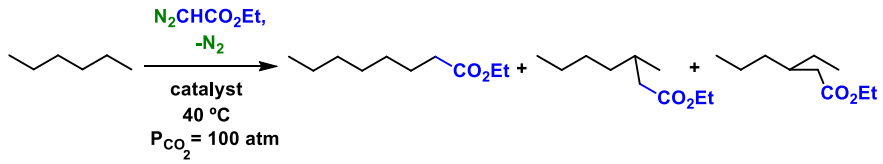

neat hexane	7	74	19	**Catalyst 2**
hexane in $scCO_2$	30	48	22	
neat hexane	37	43	20	**Catalyst 3**
hexane in $scCO_2$	33	46	21	
neat hexane, 100 atm CO_2, 22 ºC	8	69	23	**Catalyst 2**

Scheme 6. Influence of the reaction medium in the regioselectivity of the functionalization of alkanes with complexes **2** and **3** (values correspond to distribution of products).

The influence of the catalyst concentration in the regioselectivity, using pentane as the substrate, has also been investigated. Upon utilizing different catalyst loadings both in neat alkane and in the supercritical fluid, we have not found evidences of any effect in the regioselectivities observed (Scheme 7), just a slight decrease of the functionalization in the primary sites when using a 1:33 catalyst-to-EDA ratio in *sc*CO_2.

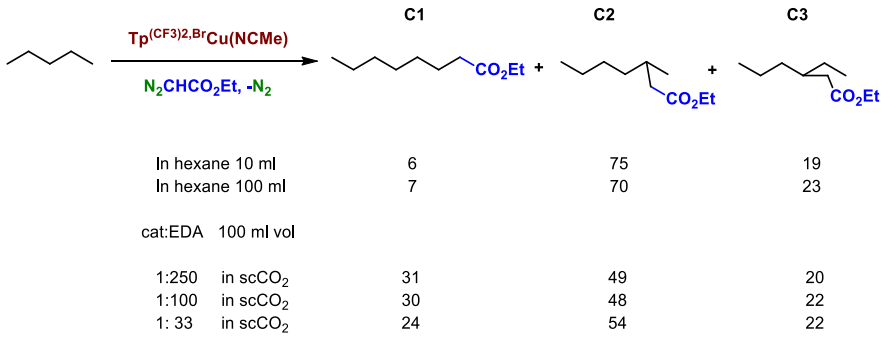

	C1	C2	C3
In hexane 10 ml	6	75	19
In hexane 100 ml	7	70	23
cat:EDA 100 ml vol			
1:250 in $scCO_2$	31	49	20
1:100 in $scCO_2$	30	48	22
1: 33 in $scCO_2$	24	54	22

Scheme 7. Study of the influence of the catalyst concentration in the regioselectivity of the functionalization of pentane in neat alkane and *sc*CO_2.

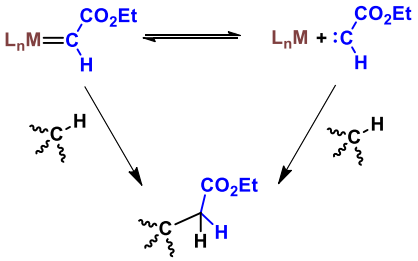

Scheme 8. C-H functionalization from metal-carbene or free carbenes.

A second issue deals with the plausible involvement of free carbenes in this case. The mechanism of this metal-based carbene transfer from diazo compounds is well established to occur through the intermediacy of metallocarbene intermediates that in some cases have been detected and/or isolated.[65] However, it can be thought that the observed reactivity could be related to the dissociation of the carbene ligand and that the reaction takes place through free carbenes, a rare but already proposed route in some cases (Scheme 8).[69]

Previous work from our laboratory showed that the regioselectivity of hexane functionalization depends on the catalyst structure,[33,70] excluding the involvement of free carbenes. To reinforce this, a series of experiments in *sc*CO_2 has been carried out with hexane to compare the effect of catalysts **2** and

3 with the regioselectivity of the reaction carried out in the absence of catalyst under irradiation conditions, thus generating the free carbene. The results are shown in Scheme 9: the observance of a completely different distribution of products can be interpreted as the consequence of the non-involvement of free carbenes in this transformation.

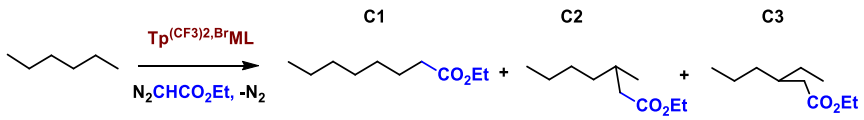

	C1	C2	C3
$Tp^{(CF3)2,Br}Cu(NCMe)$	1	2.4	1.1
$Tp^{(CF3)2,Br}Ag(thf)$	1	2.1	0.95
hν 365 nm	1	3.2	2.2

Scheme 9. Functionalization of n-hexane under catalytic or photochemical conditions.

3.3.1 The catalyst-scCO_2 interaction.

The results presented above indicate that the supercritical phase induces a change in the regioselectivity of the alkane functionalization reaction with the copper-based catalyst but not with its silver analogue. Previous studies showed that increasing the electrophilicity at the metal center (and subsequently at the carbene ligand) correlates well with a certain enhancement in the functionalization at the primary sites with this methodology.[70] Diminishing electron density at the carbene carbon atom must be related to the lowering of π-backdonation from the metal center to the carbene ligand, as a result of a decrease in the donation capabilities of the trispyrazolylborate ligand (Figure 7).

A plausible explanation for that picture would be based on the already described,[71] so-called "CO_2-philicity" of fluorocarbons, which, in this case, would consist of the interaction of the CF_3 groups with carbon dioxide

molecules (at very high concentrations in the supercritical phase). In *sc*CO_2, donation of electron density from the fluorine atoms to the carbon atom of CO_2 would decrease the electron-donating capabilities of the Tp^x ligand and would subsequently enhance the electrophilicity of the carbene ligand. The lack of this effect in the silver system could be attributed to the already decreased π-backdonation in this complex, which eventually reaches the limit of electrophilicity.

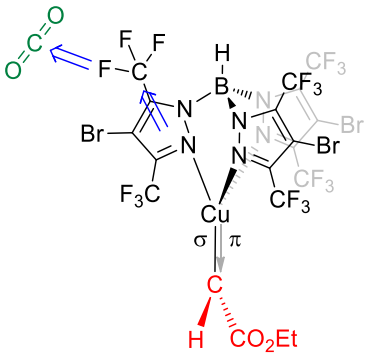

Figure 7. The flux of electron density in complex **2** when dissolved in *sc*CO_2.

Does the observance of this effect depend of the presence of electronegative, electron withdrawing nature of the substituents in the Tp^x ligand? In one of the first examples of the potential of these Tp^xCu complexes to catalyze this transformation, alkanes were functionalized upon treating them with ethyl diazoacetate by using the $Tp^{Br3}Cu(NCMe)$ complex as the catalyst.[72] Insertion of the carbene group took place exclusively into secondary and/or tertiary sites and no reactivity was observed at the primary C-H bonds. Exploration of the catalytic capabilities of this complex in *sc*CO_2 in the reaction with ethyl diazoacetate and n-hexane has provided some light to this issue. Although the complex is not very soluble, a certain degree of hexane functionalization was observed (yield <5%). Interestingly, the product derived from functionalization of the primary sites was not observed. This finding proved that the enhancement in the selectivity toward primary sites with complex **2** as the catalyst is due to the presence of the fluorine atoms.

3.3.2 Computational study.

A computational study with the B3LYP-D3 functional was subsequently performed to validate the above proposal of electronic flux that might occur at the copper center when catalyst **2** is dissolved in *sc*CO_2. This study has been performed by the group of Prof. Feliu Maseras at the Institute of Chemical Research of Catalonia (ICIQ). As modeling of the supercritical carbon dioxide environment is not common in DFT calculations of transition-metal compounds, a computational procedure had to be devised. From the point of view of dielectric constant, the medium is very similar to hexane, as dielectric constants between 1.1 and 1.5 have been reported. The experimental data, however, point to a potential involvement of carbon dioxide molecules in the inner coordination sphere of the carbene complex. This is represented by including three explicit carbon dioxide molecules. The number of molecules was selected from the optimized structure in preliminary calculations with a single carbon dioxide molecule, which suggests the placement of three molecules because of the C3 symmetry of the ligand. Preliminary calculations confirmed that the observed variations do not depend critically on the number of solvent molecules.

The reaction of the $Tp^{(CF3)2,Br}Cu(CHCO_2Et)(CO_2)_3$ and $Tp^{(CF3)2,Br}Ag(CHCO_2Et)(CO_2)_3$ complexes derived from catalysts **2** and **3**, respectively, with the primary and secondary C-H bonds of propane was modeled, with the results shown in Figure 8 and Table 4. The barriers reported in Table 4 are very low, which is consistent with a very fast reaction between the carbene complex and the alkane and is in agreement with previous computational studies.[30b] The fact that one of the barriers was negative in terms of free energy is a simple consequence of the fact that the geometries were optimized in potential energy, and the chemical meaning is that the barrier, if it exists, is very low for this process. In the presence of such low barriers, the diffusion of reactants for the bimolecular process has to be taken into account.

It is in particular relevant that the self-diffusion activation energy of hexane was reported experimentally to be 2.18 kcal·mol^{-1}.[73] Only two of the eight barriers reported in Table 4 are above the diffusion limit, and both of them correspond to primary C-H activation by the $Tp^{(CF3)2,Br}Cu$ complex with values of 3.8 and 2.7 kcal·mol^{-1} in alkane medium and *sc*CO_2 medium, respectively. This fits well with our experimental observation that the secondary/primary ratio for systems with a silver catalyst is independent from the medium. The regioselectivity for these silver systems does not depend on the electronic nature of the metal but on the physical phenomena (e.g., diffusion, transport) that are more likely independent of the complex. If the process is controlled by diffusion, the competition between the different C-H bonds is no longer ruled by the very low C-H activation barriers. Instead, it depends on the orientation of the approaching molecules. As a first approach, the probability of competing C-H activations is associated to statistical considerations, and the more abundant C-H bonds are thus more likely to be activated. This agrees with the experimental results.

Table 4. Computed activation energies (kcal/mol) and C_{carb}-H bond length (Å) in TS for Cu and Ag catalysts under both reaction conditions (neat hexane and *sc*CO_2). (Tp^x = $Tp^{(CF3)2,Br}$)

Metal complex	$\Delta G_{act\ prim}$	C_{carb}-H	$\Delta G_{act\ sec}$	C_{carb}-H
Tp^xCu	3.8	1.657	0.1	1.212
$Tp^xCu(CO_2)_3$	2.7		- [a]	
Tp^xAg	0.8	1.878	- [b]	.- [b]
$Tp^x Ag(CO_2)_3$	0.2		- [b]	- [b]

[a] The barrier for this process disappears due to free energy correction. The computed free energy of the transition state is 0.4 kcal/mol below the reactants. [b] Structure could not be optimized, barrierless process.

Regardless of what diffusion limits allow to observe experimentally, it is clear from Table 4 that the presence of CO_2 reduces the activation barrier in all cases. The C_{carb}-H distances in the transition states are also presented in the Table. There is some electronic control in the case of the primary carbon atoms, and the C-H distance is longer (1.878 vs. 1.657 Å) in the case of the silver complex with a lower barrier. For the case of the secondary carbon atom, the distance is shorter because the process is controlled by steric effects rather than electronic effects.

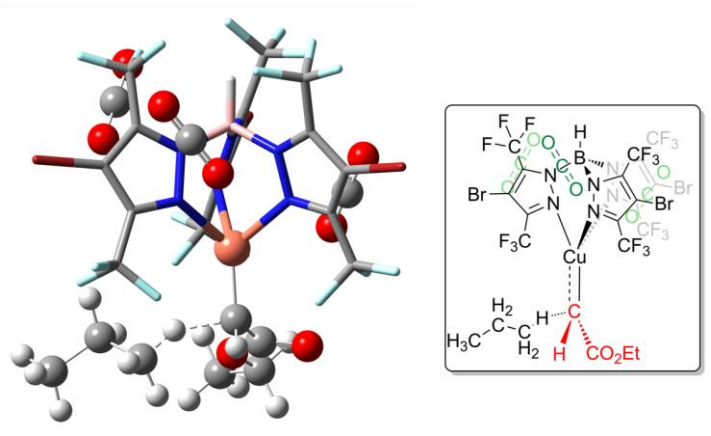

Figure 8. Optimized structure of the transition state of the primary C-H activation of propane by $Tp^{(CF3)2,Br}Cu(CHCO_2Et)(CO_2)_3$.

The optimized structure of one of the transition states is represented in Figure 8. The carbon dioxide molecules do not favor the process by getting close to the reaction center but instead by interacting through rather long distances with the $Tp^{(CF3)2,Br}$ ligand. There is one C_{CO2}-F contact in the 2.75/2.95 Å range for each carbon dioxide, and the shortest contacts between the carbon dioxide and the pyrazolyl rings are in the 3.3 Å range. Although the distances are long, the effect on the energy is clear and reproduces well the experimental observation. It seems that electrophilic carbon dioxide is able to abstract some density from the $Tp^{(CF3)2,Br}$ ligand, which ultimately leads to diminished electron density at the carbene carbon atom, and this renders the C-H bond more reactive. We hypothesize that the low barriers involved in these processes make

them especially sensitive to these seemingly subtle interactions. This acceleration phenomenon is not observed in reactions below the critical temperature, even if there were some solubility of carbon dioxide in the alkane reaction media, because the low availability of carbon dioxide makes the concentration of the "activated" catalyst much lower, which thus results in a negligible effect on the reaction rate. The non-observance of the same effect in the experiments on the silver system is due to the fact that the barriers are already below the diffusion limit for these complexes, which are no longer sensitive to electronic enhancements.

Conclusions of Section 1

The new hydrotris((3,5-bis(trifluoromethyl)-4-bromo)-pyrazolyl)borate ligand ($Tp^{(CF3)2,Br}$) has been prepared as well as its Tl, Cu and Ag complexes: $TlTp^{(CF3)2,Br}$ (**1**) $Tp^{(CF3)2,Br}Cu(NCMe)$ (**2)** and $Tp^{(CF3)2,Br}Ag(thf)$ (**3)**.

Complexes **2** and **3** catalyze the reaction of methane and gaseous alkanes with ethyl diazoacetate (N_2=$CHCO_2Et$) leading to carbene-insertion derivatives. In the case of **2**, this is the first example of an homogeneous copper-based catalyst for methane functionalization.

Also for **2** as the catalyst, it has been found anovel effect of the reaction medium in the regioselectivity of the above reactions. When *sc*CO_2 was employed as the reaction solvent, the selectivity toward the primary sites increased up to a five times compared to those experiments carried out in neat alkanes. This *supercritical effect* seems to be originated in a CO_2-fluorine interaction that abstract electronic density from the metal center.

Section 2

Studies of the relative reactivity of alkanes toward metallocarbenes

4. The Sigma-basicity scale for alkane electrophilic substitution reactions.

As we have previously mentioned, the functionalization of hydrocarbons C-H bonds with in situ generated metal-carbene species has been extensively studied in our research group since 2000 (Figure 9a).[29] Mechanistic studies have demonstrated the existence of such intermediates[65] whereas DFT studies have shown that the insertion reaction occurs in a single step in which the metallocarbene intermediate interacts with the C-H bond (Figure 9b).[30b]

Nearly have a century ago, Nobel Laureate G. A. Olah studied the

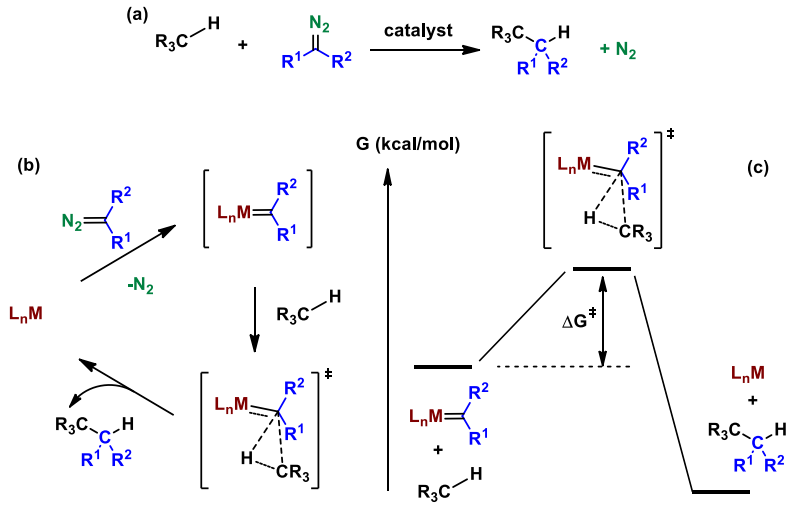

Figure 9. a) The catalytic insertion of a carbene group into a C-H bond. b) The reaction pathway associated to that transformation. c) The C-H functionalization takes place in one step from the metallocarbene and the alkane substrate.

reactivity of alkanes toward strong electrophiles such as superacids and other E^+ groups (E^+ = R^+, NO^{2+}, X^+; R = organic group, X = halogen).[35,36] This reaction induced the substitution of E^+ for H^+ in the parent alkane, in a process that was performed with methane and the lower members of the C_nH_{2n+2} series. Different reaction patterns were found not only for C-H but also for C-C bonds, demonstrating that carbonium ions are intermediate species in these transformations (see Scheme XIII in the Introduction).[35,36] Such three center, two-electron pentacoordinated species results when the electrophiles interact with σ C-H or C-C bonds (Figure 10).

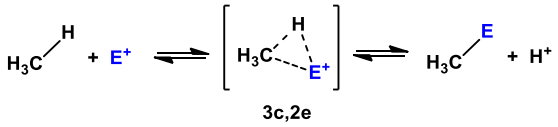

Figure 10. The 3-center, 2-electron intermediate in Olah's work, a pentacoordinated carbonium ion.

The direct comparison of the transition states shown in Figures 9 and 10 reveals the existence of similarities between these two processes, where the C-H bond of the alkane interacts with the electrophile, i. e., either a superacid (or related) or the metallocarbene. Therefore, the metal-catalyzed functionalization of C-H bonds of alkanes by means of carbene insertion from diazo compounds could be intended as a model of Olah's system to determine the relative reactivity of a series of carbon-hydrogen bonds in the C_nH_{2n+2} series. Despite the huge development in the field of nucleophilicity scales, mainly propelled by Mayr and co-workers,[74] the knowledge of the relative reactivity of C-H bonds belonging to different methyl, methylene or methine groups in homologate series of alkanes remains a challenge nowadays. Moreover, there are some advantages in the former transformation when compared with the latter:

- The reaction with diazo compounds does not undergo carbon-carbon cleavage, at variance with the reaction with strong electrophiles. Thus, each different C-H bond leads to a different product. In Olah's work, different alkanes gave mixture of products from C-H and C-C cleavage, and the existence of identical products in some cases precluded the determination of the relative reactivity of each C-H bond. It is the case, as an example, of the nitration of ethane or propane already mentioned in the Introduction.
- The relative reactivity of different C-H bonds (primary, secondary and tertiary sites) can be thus measured by conducting competition experiments with the diazo reagent and the appropriate catalyst. Since each type of bond of each alkane originates a single type of product in

the carbene insertion reaction, there are no ambiguities regarding the origin of the selectivity.

- The reactivity of both liquid and gaseous alkanes can be measured upon employing either the hydrocarbon itself or supercritical carbon dioxide as the reaction media. This advantage is the result of the development in our group of catalysts that are soluble in both media and that are capable of inducing methane functionalization, allowing the use of the lowest member of the C_nH_{2n+2} series as the reference for a scale of relative reactivity.

4.1 Study of the relative reactivity of C-H bonds in the functionalization of alkanes catalyzed by complexes Tp^xAg.

On these grounds, we have experimentally addressed the quantitative measurement of the reactivity as nucleophiles of the twenty-nine different C-H bonds of fourteen linear, cyclic or branched alkanes containing up to eight-carbon atoms shown in Figure 11b using methane as the reference. As the electrophile, we have employed three in situ generated highly electrophilic metal-carbene species (Figure 11a).

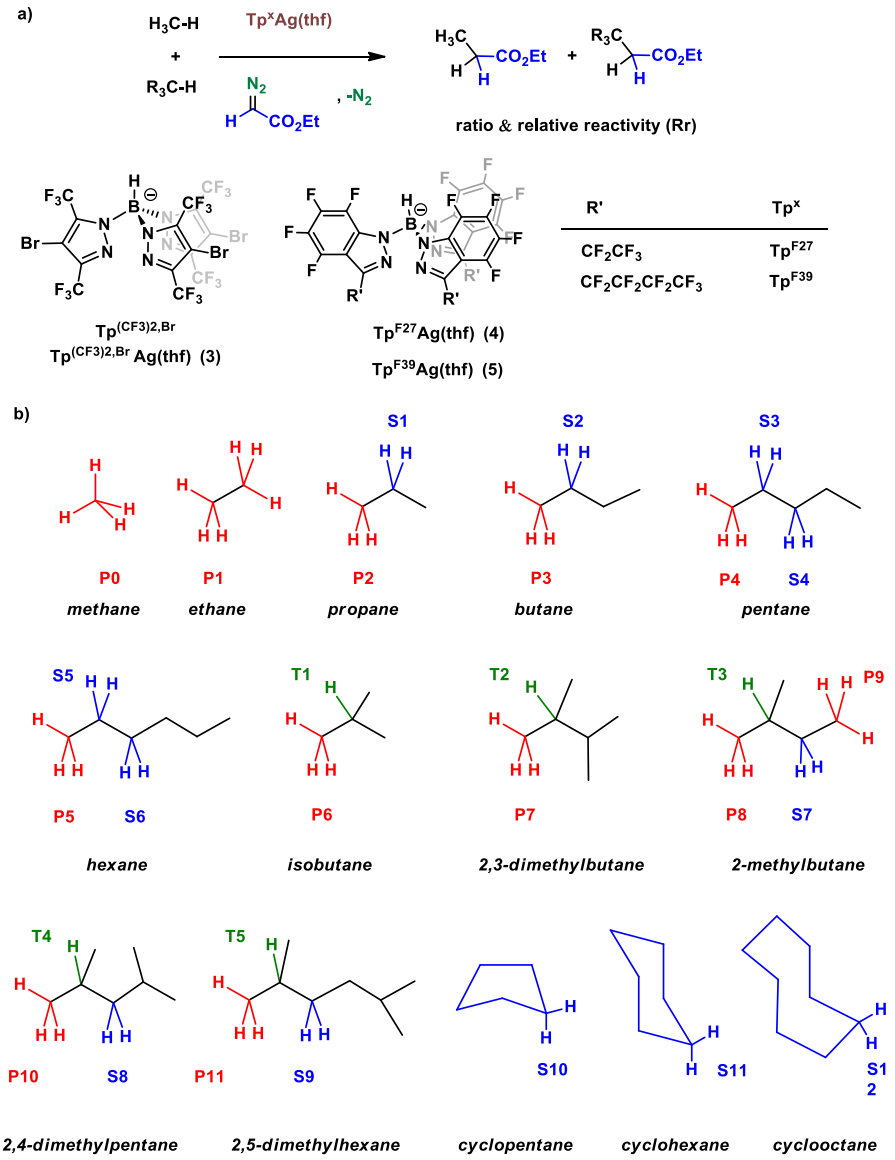

Figure 11. a) Mixtures of two alkanes are reacted with EDA in the presence of a silver complex to induce the catalytic insertion of the carbene $CHCO_2Et$ group into their C-H bonds. b) The fourteen linear, branched or cyclic alkanes bearing twenty-nine different C-H bonds that have been studied in this work.

Noteworthy, the studies discussed in Section 1 have shown that the site selectivity observed in the formal carbene insertion reaction into the C-H bonds of alkanes with the silver catalysts does not depend on the reaction medium,

unlike with the analogue copper-based catalysts. In this manner, the relative reactivity (R_r) of each C-H bond referred to that of methane has been accurately measured. The R_r values obtained for the twenty-nine C-H bonds, normalized by the number of identical C-H bonds in each molecule, in the $Tp^{(CF3)2,Br}Ag(thf)$-catalyzed carbene insertion reactions are collected in Figure 12. The scale ranges is from $R_r = 1$ for methane to $R_r = 100$ for cyclopentane. The corresponding $\log(R_r)$ values were taken for simplicity based on their direct relation with $\Delta G^{\ddagger}$ in the interaction step between the electrophile (silver carbene) and the nucleophile (alkane C-H bond). Such values correspond to kinetic selectivities, as they depend on the relative activation barriers for the transition states shown in Figure 13.

A bar graph of $\log(R_r)$ for the three silver-based electrophiles ($Tp^{(CF3)2,Br}Ag(thf)$, **3**; $Tp^{F27}Ag(thf)$, **4**; $Tp^{F39}Ag(thf)$, **5**; is shown in Figure 12b. The primary sites of linear alkanes (P2-P5) increase their relative reactivity when enlarging the chain, very likely as the result of the inductive effect. Also, within the same alkane, most of them (with few exceptions) verify the expected order proposed by Olah. However, the overall picture reveals the absence of a general reactivity pattern associated with each type (primary, secondary or tertiary) of C-H bond: secondary sites seems more reactive (blue bars) whereas some tertiary sites (green bar) are located among the less reactive C-H bonds.

These findings are in contrast with the general belief that the relative reactivity of alkanes when acting as nucleophiles follows the order tertiary >secondary >primary, with only a few exceptions. Since the molecules studied are exclusively formed by saturated C-H bonds, lacking of heteroatoms or multiple bonds that could serve as directing or activating groups, the nucleophilic character of each C-H bond (referred to a given electrophile) depends on the effect that the alkyl groups exert on this given reaction site.

a

Bond	Rr	log(Rr)	Bond	Rr	log(Rr)	Bond	Rr	log(Rr)
P0	1,0	0,00	S1	70,8	1,85	T1	56,2	1,75
P1	24,5	1,39	S2	55,0	1,74	T2	29,5	1,47
P2	21,4	1,33	S3	79,4	1,90	T3	47,9	1,68
P3	25,1	1,40	S4	44,7	1,65	T4	5,5	0,74
P4	42,7	1,63	S5	95,5	1,98	T5	5,0	0,52
P5	49,0	1,69	S6	40,7	1,63			
P6	11,5	1,06	S7	40,6	1,61			
P7	19,1	1,28	S8	1,9	0,28			
P8	20,4	1,31	S9	16,6	1,35			
P9	39,8	1,60	S10	100,0	2,00			
P10	15,5	1,19	S11	61,7	1,79			
P11	16,6	1,04	S12	85,1	1,93			

b

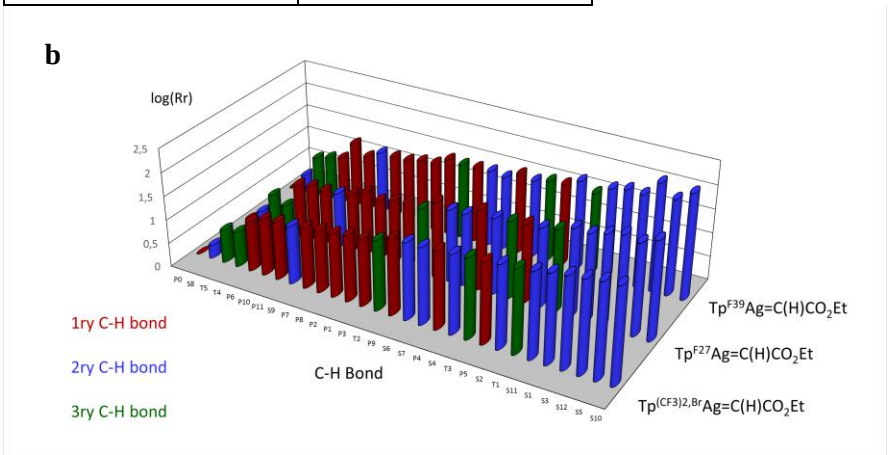

Figure 12. a) The values of R_r (and $\log(R_r)$) obtained with $Tp^{(CF3)2,Br}Ag(thf)$ as the electrophile precursor. b) Bar plot of values of $\log(R_r)$ for the three silver electrophiles employed.

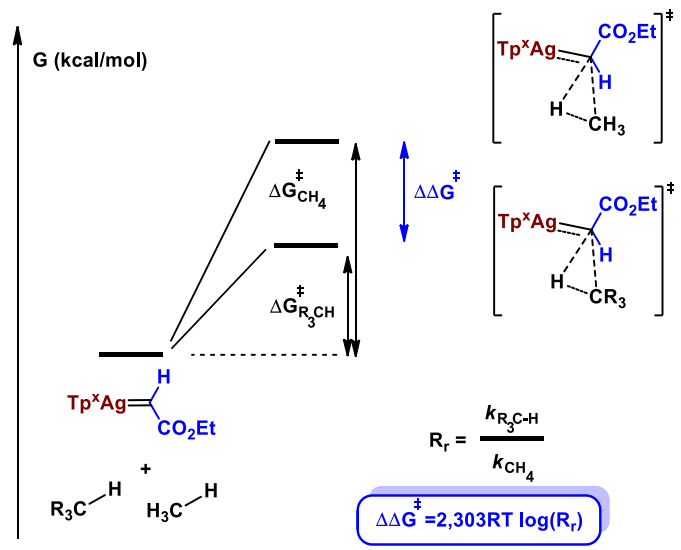

4.2 Description of the experimental device.

Competition experiments with mixtures of the fourteen C1-C8 alkanes and ethyl diazoacetate (EDA) in the presence of silver complexes of composition $Tp^xAg(thf)$ (**3-5**) as the catalyst (Figure 11a) have been performed in the homogeneous phase either in supercritical carbon dioxide or in neat alkane solution (see Experimental Section for more details). The competitions experiments between gaseous alkanes have been developed in HPLC columns (Figure 14) used as reactors due to their properties of withstanding a high pressure (more than 350 bars) and the possibility of quantifying the amount of gaseous alkanes introduced by weight measuring. Once charged the columns with EDA, catalyst and the mixtures of alkanes, were introduced into a sonication bath at 40 ºC during 4 h (Figure 14). In the case of methane and ethane, the gaseous mixture was directly injected in a modified gas chromatograph. In the case of other alkanes, once the reaction has finished, the reactor was cooled to -100ºC before depressurization through two traps consecutively connected and cooled with liquid nitrogen. Once depressurization was completed, the reactor was allowed to reach room temperature and the complete system was rinsed with dichloromethane. The competitions experiments between liquid alkanes have been developed using conventional Schlenk techniques. Products were analyzed by GC using calibration curves (see Experimental Section).

Figure 14. Left: HPLC column system. Right: Sonication bath with HPLC column inside.

An example of GC evaluation of a competition experiment between cyclohexane and pentane is shown in Figure 15. By means of the different of calibration curves with isolated or purchased products, the relative reactivity of the different C-H bonds has been obtained.

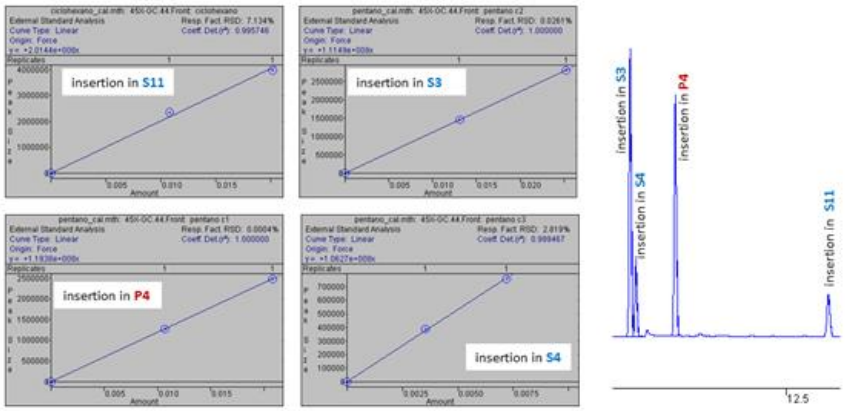

Figure 15. Chromatogram and calibration curves for the competition experiment between pentane and cyclohexane.

4.3. Modelling the experimental relative reactivity values.

Once all the results of the 29 C-H bonds and the three silver complexes were obtained, we wondered about the existence of any correlation between the structure of the hydrocarbon and the reactivity of the different C-H bonds. Accordingly, a multivariate data analysis was carried out by building a simple model in which each bond was described, in a first approach, by up to twenty elemental topological descriptors (Table 5). This work has been also carried out by the group of Feliu Maseras. A series of topological properties of the C-H bonds, such as the substitution of the ipso carbon (primary, secondary or tertiary), the number of primary, secondary or tertiary carbons in alpha, beta, gamma or delta positions, the length of the chains in the ipso carbon (shortest, medium and longest chain) and the eventual cyclic nature of the alkane were employed in this study. The development of such model is included in the Experimental Section, but will not be discussed here since it has been developed

in a parallel manner by Maseras' group. Only the comparison with the experimental data is presented in this section.

The systematic evaluation of the descriptors shown in Table 5 looking for sets of them that would provide a high correlation between the experimental

Table 5. Definition of the descriptors used in the multivariate data analysis.

	Descriptor
1	Is the ipso carbon primary? 1 if yes, 0 if no
2	Is the ipso carbon secondary? 1 if yes, 0 if no
3	Length of the shortest chain (number of carbons) on the ipso carbon (for the presented alkanes equals to: Is the ipso carbon tertiary? 1 if yes, 0 if no)
4	Number of CH_3 in alpha = Number of primary carbons in alpha.
5	Number of CH_2 in alpha = Number of secondary carbons in alpha
6	Number of CH in alpha = Number of tertiary carbons in alpha.
7	Number of CH_3 in beta = Number of primary carbons in beta.
8	Number of CH_2 in beta = Number of secondary carbons in beta.
9	Number of CH in beta = Number of tertiary carbons in beta.
10	Number of CH_3 in gamma = Number of primary carbons in gamma.
11	Number of CH_2 in gamma = Number of secondary carbons in gamma.
12	Number of CH in gamma = Number of tertiary carbons in gamma.
13	Number of CH_3 in delta = Number of primary carbons in delta.
14	Number of CH_2 in delta = Number of secondary carbons in delta.
15	Number of CH in delta = Number of tertiary carbons in delta.
16	Is it a cycloalkane? 1 if yes, 0 if no
17	Length of the medium chain (number of carbons) on the ipso carbon.
18	Length of the longer chain (number of carbons) on the ipso carbon.
19	Type of Ipso carbon: 1 for primary, 2 for secondary and 3 for tertiary.
20	"Steric parameter" 1 for S8, T4 and T5 0 for the rest.

and calculated values was performed. As a result of it, it was found that a set of 6 descriptors was good enough providing a correlation index r^2= 0.936 for $Tp^{(CF3)2,Br}Ag$. A similar treatment for the experimental results from the $Tp^{F27}Ag$ and $Tp^{F39}Ag$ systems yielded r^2 values of 0.920 and 0.942, respectively.

The results from the statistical analysis can be rearranged to produce an equation for the estimation of $\log(R_r)$ consisting of seven components, i. e. one independent term and six descriptors D_i each of them weighed by a coefficient

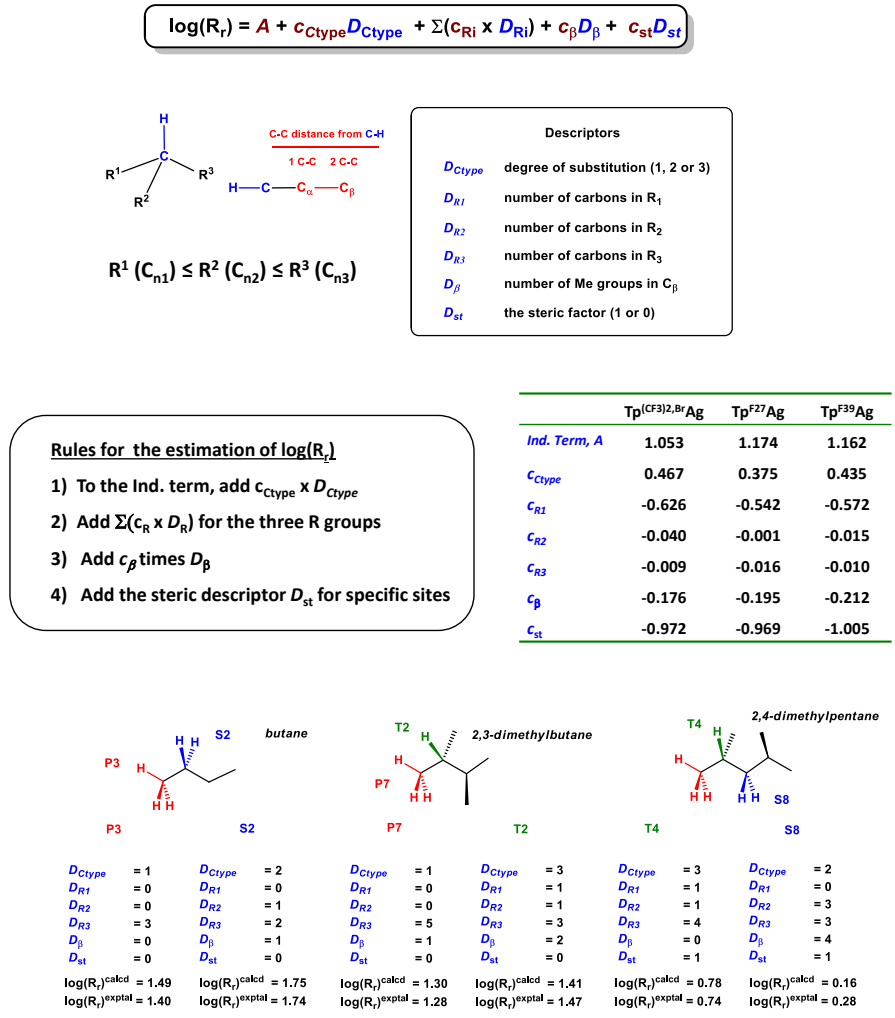

	$Tp^{(CF3)2,Br}Ag$	$Tp^{F27}Ag$	$Tp^{F39}Ag$
Ind. Term, A	1.053	1.174	1.162
c_{Ctype}	0.467	0.375	0.435
c_{R1}	-0.626	-0.542	-0.572
c_{R2}	-0.040	-0.001	-0.015
c_{R3}	-0.009	-0.016	-0.010
c_{β}	-0.176	-0.195	-0.212
c_{st}	-0.972	-0.969	-1.005

Figure 16. The equation provided by the model. The descriptors and coefficients, calculated for each electrophile.

c_i (Figure 16). The descriptors are the following: (i) the type of C-H bond relative to the number of non-hydrogen substituents (primary, secondary or tertiary, D_{Ctype}); (ii) three descriptors related to the number of carbon atoms in each of the R groups, from lowest to highest C_n ($R^1 \leq R^2 \leq R^3$, D_{R1}, D_{R2}, D_{R3}); (iii) the number of methyl groups (D_β) at the beta positions, and (iv) a steric

Table 6. Predicted reactivity and its comparison with the experimental value for each bond and catalyst.

	Predicted log(R_r)			Errors (Exp-Pred) log(R_r)		
	3	**4**	**5**	**3**	**4**	**5**
P1	1.51	1.53	1.59	-0.12	-0.18	-0.14
P2	1.33	1.32	1.36	0.00	-0.05	0.06
P3	1.49	1.50	1.57	-0.09	-0.10	0.04
P4	1.48	1.48	1.55	0.15	0.20	0.15
P5	1.48	1.47	1.54	0.21	0.19	0.19
P6	1.14	1.11	1.14	-0.08	0.01	-0.13
P7	1.30	1.27	1.33	-0.02	-0.04	0.02
P8	1.31	1.29	1.34	0.00	0.06	0.01
P9	1.48	1.48	1.55	0.12	0.10	0.04
P10	1.29	1.26	1.32	-0.10	-0.10	-0.11
P11	1.28	1.24	1.31	-0.06	-0.09	-0.11
S1	1.94	1.91	2.01	-0.09	-0.09	-0.05
S2	1.75	1.70	1.78	-0.01	-0.03	0.10
S3	1.92	1.87	1.99	-0.02	0.03	-0.05
S4	1.54	1.50	1.56	0.11	0.10	0.08
S5	1.91	1.86	1.98	0.07	0.05	0.03
S6	1.71	1.68	1.76	-0.10	-0.17	-0.16
S7	1.57	1.48	1.56	0.04	0.03	-0.01
S8	0.17	0.12	0.10	0.11	0.14	0.07
S9	1.48	1.47	1.52	-0.26	-0.30	-0.16
S10	1.89	1.89	1.98	0.11	0.16	0.12
S11	1.87	1.88	1.97	-0.08	-0.04	-0.08
S12	1.82	1.86	1.94	0.11	0.12	0.11
T1	1.78	1.74	1.87	-0.03	-0.01	-0.16
T2	1.41	1.32	1.43	0.06	0.04	0.15
T3	1.60	1.53	1.65	0.08	0.10	0.07
T4	0.78	0.72	0.83	-0.04	-0.15	-0.09
T5	0.77	0.70	0.82	-0.07	0.02	0.03

factor (D_{st}) for highly hindered sites. This model has been applied to the array of C-H bonds shown in Figure 11 allowing the modeling of their relative reactivity with respect to methane. Table 6 contains the calculated values for log(R_r) following a simple sum rule where each term is added sequentially as

displayed in Figure 16. For hindered secondary or tertiary sites, the steric descriptor D_{st} must be added, either when a secondary carbon is directly bonded to two tertiary carbons (S8) or, for tertiary carbons, when the C_β is substituted (T4 or T5, respectively), the resulting *cisoid* conformation affecting the steric pressure on the tertiary site. Remarkably, this descriptor contributes to the same extent on the reactivity of the three congested C-H bonds regardless of the origin of the steric hindrance.

The plot of the experimental and calculated values for $\log(R_r)$ for the three $Tp^xAg{=}C(H)CO_2Et$ electrophiles tested (Figure 17) shows in all cases a good correlation in spite of the simplicity of the model. To the best of our knowledge, this is the first approach to the quantitative modelling of the reactivity of non-activated C-H bonds of alkanes towards electrophiles. We must emphasize that a marginally better fit could be achieved by increasing the number of descriptors, albeit at this stage our aim is focused in proposing an accurate approach based on an easy to handle, chemically meaningful model.

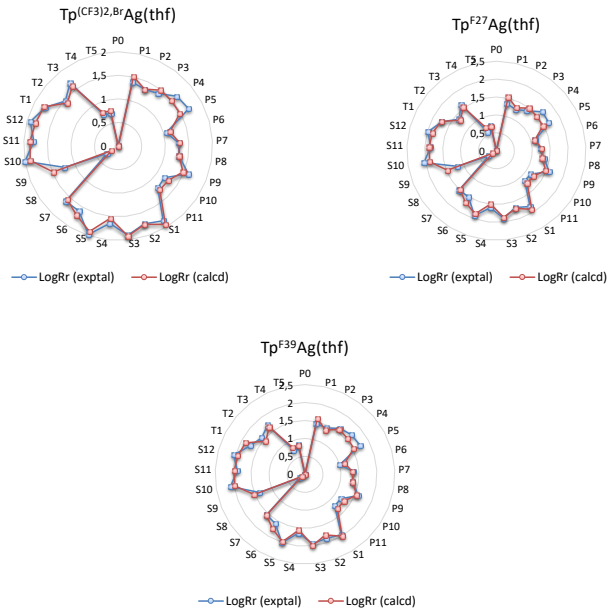

Figure 17. Correlations of experimental and calculated values of $\log(R_r)$ obtained for the three silver electrophiles employed in this work.

4.4. Extension of the modelling to other metals.

The previous log(R_r) scales cannot be determined for other metals due to their lack of reactivity towards methane and other gaseous alkanes. Thus, a new log(R_r) scale has been built using cyclohexane as the reference (Scheme 10), performing a series of competition experiments between cyclohexane and the eight liquid alkanes (C_{nH2n+2}, n > 4) shown in Figure 11. The insertion reaction was catalyzed by three silver complexes (**3-5**) employed in the

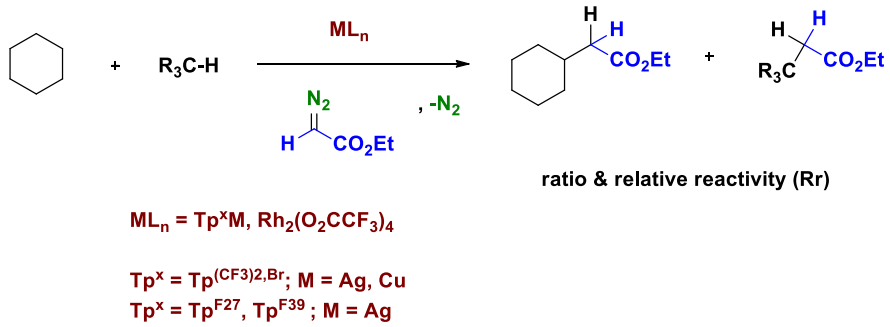

Scheme 10. The reaction of cyclohexane and an alkane partner in the presence of silver-, rhodium- or copper-based catalysts.

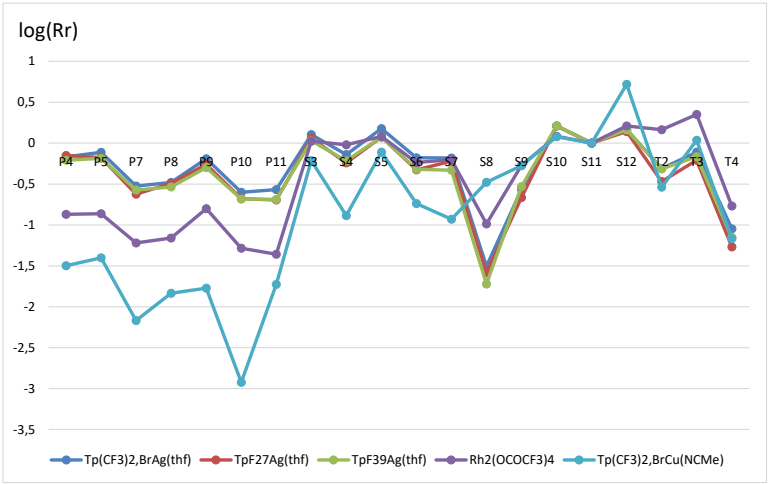

Figure 18. The relative reactivity, obtained with the five different catalysts, with cyclohexane as reference.

previous paragraphs as well as with the dirhodium complex $[Rh_2(OCOCF_3)_4]$ (**6**) and the copper complex $Tp^{(CF3)2,Br}Cu(NCMe)$ (**2**).

Figure 18 represents the values of $log(R_r)$ for the five different catalysts. The three silver-based electrophiles behave similarly, with slight or no difference in the relative reactivity of the C-H bonds. It is clearly observed that primary sites are less reactive with the rhodium- and, more drastically, with the copper-based catalysts compared to the silver electrophiles. It is also noteworthy that complexes **2** and **3** only differ in the metal center, the ligand being the same, thus it is the nature of the metal that is influencing the reaction outcome. For secondary sites, the $log(R_r)$ values are similar for the silver- and rhodium based catalysts, but slightly lower for that based in copper. In the region of the tertiary sites, copper- and silver-based catalysts show similar behavior, the rhodium catalyst providing the highest relative reactivities.

Does the behavior observed for these additional metals fit in the previous model? A similar multivariate analysis was performed by the group of Maseras with the set of data containing the relative reactivity for different alkanes with the three silver catalysts and two extra catalysts, $[Rh_2(OCOCF_3)_4]$ (**6**) and $Tp^{(CF3)2,Br}Cu(NCMe)$ (**2**). To our delight, it was found that the same descriptors, equation and rules shown in Figure 16 described faithfully this new set of data obtained independently of the metal. The graphical comparison between the experimental and calculated values for log(Rr) for catalysts **2**, **3** and that based on rhodium is depicted in Figure 19: only small deviations were observed between both series.

The radial plots shown in Figures 17 and 19 reveal the existence of a pattern that is clearly electrophile-dependent. The three silver-based systems (Figure 17) show a quite similar behavior in terms of relative reactivity, the effect of the electrophile being not significant. However, when comparing the three metals (Figure 19) the situation varies, the shapes being substantially

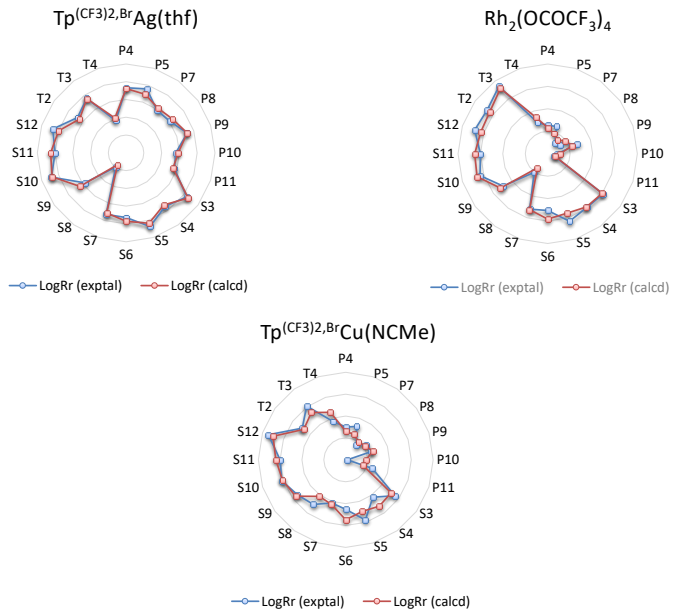

Figure 19. A comparison (radial plots) of the experimental and calculated values for log(R_r) for the extended set of catalysts and with cyclohexane as reference.

different. This is an interesting issue, since this study can also provide information about the influence that each electrophile may exert in the relative reactivity. We have found a correlation between the independent term (*A*) of our model and the ν(CO) values in $Tp^xM(CO)$ (M = Cu, Ag) as well as in $Rh_2(OCOCF_3)_4(CO)$[75] (Figure 20). Thus, this independent term that arises from our simple model can be considered as a measure of the electrophilicity of the metallocarbene species.

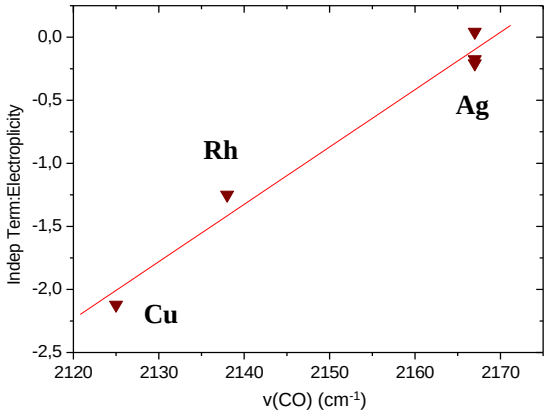

Figure 20. The correlation between the independent term *A* and the ν(CO) values of the carbonyl complexes $Tp^xM(CO)$ (M = Cu, Ag) as well as in $Rh_2(OCOCF_3)_4(CO)$.

Conclusions of Section 2

The relative reactivity (R_r), of a number (29) of carbon-hydrogen bonds of alkanes (14) acting as (weak) nucleophiles in their reaction with *in situ* generated silver-carbene complexes as the (strong) electrophile has been measured.

The experimental data of the relative reactivity have served as the basis for a model that, with a set of simple rules derived from a statistical analysis, has led to a highly accurate fitting of the calculated values with respect to the experimental data.

The above approach has been expanded to other metals such as rhodium and copper, revealing the validity of the model.

Section 3

Methane catalytic functionalization in water at room temperature

5. The need of methane as raw material.

In the last century, the development of the chemical science has progressed from the first atomic model proposed by Böhr (1913)[76] to the plethora of novel chemical transformations that have emerged since then, and that provide an exquisite control of the composition and properties of the targeted products. In an era in which natural macromolecules can be modified into artificial metalloenzymes, where catalytic systems afford a given product upon completely controlling the selectivity, or the production of ultrapure materials for photo- or electronic devices has become routine, it is quite surprising that one of the remaining challenges deals with one of the simplest molecules in Earth: methane. The existence of huge deposits of this gas available along with the need to replace oil as the main source for many chemicals and fuels has propelled a number of research programs toward the use of methane as the alternative toward that end. [8,9,10]

Why has Chemistry yet failed in providing an extensive use of methane as raw material? There are several reasons to explain this fact. First, methane is a quite inert molecule, this behavior being the result of a very high bond dissociation energy of the carbon-hydrogen bond (105 kcal mol^{-1}, the highest of the alkane series).[7] In addition, the polarity of this bond is quite low, due to the relatively similar values of the electronegativities of carbon and hydrogen ($\chi_C = 2.55$; $\chi_H = 2.20$).[77] On the other hand, it is this inertness that has allowed the existence of the aforementioned deposits in the Earth crust. Secondly, such inertness constitutes a drawback since in most cases, when methane is converted into a value added product, the latter is most reactive than the former and thus selectivity problems due to the formation of mixture of products, are common. Not less important is the gaseous nature of methane, which complicates the design of the chemical system, with issues due to the election of solvents or catalysts, among others.

In spite of the above, there is a need to develop synthetic procedures that employs methane as reactant. Since methane cannot be liquefied for transport, it is quite desirable its conversion into a liquid product that can be transported at a reasonable cost. This goal goes beyond Chemistry itself, since there are important environmental implications. When petroleum is extracted, there is an amount of natural gas also emerging that is just burned, without any use, contributing to the increment of CO_2 in the atmosphere and the well-known pernicious effect of it. Ten years ago, Millesi and co-workers estimated that this flared gas accounted for ca. 25% of the needs of natural gas for USA.[78]

In the last decades, as enumerated in the Introduction, there has been a number of systems described for the conversion of methane into valuable products, albeit their use at a practical scale is not possible, mainly due to two factors. First of all, most of them are not fast enough, in terms of chemical kinetics: usually a minimum of 1 s^{-1} of turnover frequency is required from an industrial perspective. Secondly, there is also a general need of harsh conditions, particularly in the oxidation reactions, using corrosive reaction media. Figure 21 displays the catalysts, solvents and temperatures employed in the representative examples described to date, including the formation of C-O, C-C and C-B bonds in a catalytic manner,[79] which have already been discussed in the Introduction. The lowest temperature is 40 ºC, in the system employing *sc*CO_2 as reaction medium. Interestingly, only one example takes place in aqueous medium, albeit at 90 ºC.

The reaction conditions shown in Figure 21 are in contrast with those that Nature uses for the oxidation of methane, by means of the enzymes named methane monooxygenases (MMOs).[80] There are two types of them, the soluble and particulate versions, sMMO and p-MMO, respectively. These enzymes, the only examples known for methane transformation at ambient conditions, are part of methanotrophic bacteria, and provides the conversion of methane into methanol using molecular O_2 as the oxidant, and obviously with water as the biological solvent.

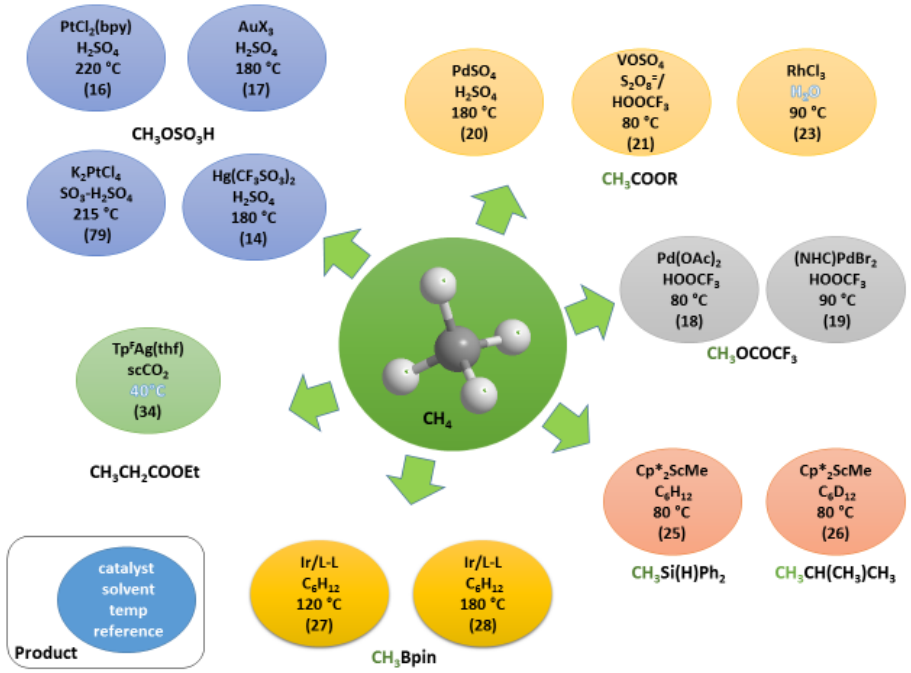

Figure 21. Representative examples of methane catalytic functionalization showing reaction conditions.

Figure 22 shows two examples of the above enzymes. As in any enzyme, the bulk is formed by peptides chains that constitute most of the structure. A minor fraction of the enzyme contains the so-called active site, where usually transition metal ions are bound to donor atoms of peptide residues, constituting the pocket where the catalytic reaction takes place. Such pocket has been demonstrated being hydrophobic in nature, thus favoring the concentration of the non-polar methane. The active site of sMMO is based on a diiron center whereas in the case of pMMO there are several variations with dicopper and monocopper environments.

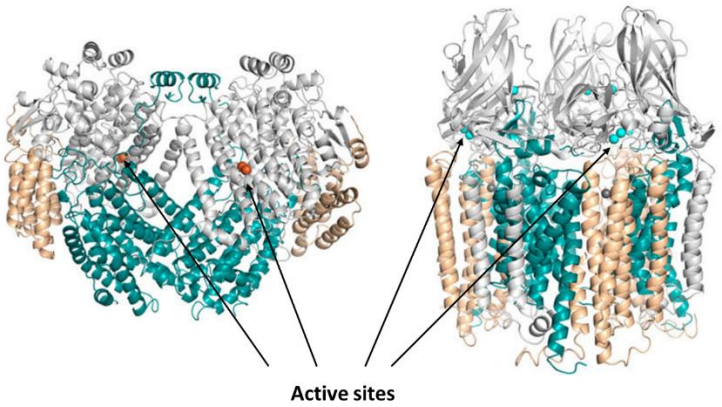

Figure 22. Examples of sMMO (left) and pMMO (right). Figure taken from reference 80.

5.1 Surfactants in water as promoters of hydrophobic pockets for gaseous alkanes.

Since bacteria takes advantage of the existence of hydrophobic pockets to concentrate methane in the active sites of the MMO enzymes, we envisaged a strategy to apply such effect to the reaction of gaseous alkanes and ethyl diazoacetate in the presence of the silver based catalysts employed in the previous Sections. As shown in Figure 21, and to the best of our knowledge, there is no report to date for the conversion of methane in water at room temperature leading to the isolation or detection of a unique product in a controlled manner. The strategy consists of the use of surfactants that originate micelles in water (Figure 23), in such a way that the inner vesicle of the micelles concentrate the hydrophobic reactants as well as the catalyst, that contains a considerably high percentage of fluorine. This concentration effect has been invoked by Lipshutz and co-workers to explain[81] the outstanding behavior observed for a number of reactions when carried out in a water-surfactant reaction medium. Interestingly, when liquid alkanes were reacted in water with EDA in the presence of these catalysts, an emulsion is formed and the reaction takes place in the organic phase,[82] with no activation of the OH bond of water.[83]

Obviously, gaseous alkanes do not form emulsion, a drawback that could be surpassed with the aid of the surfactants.

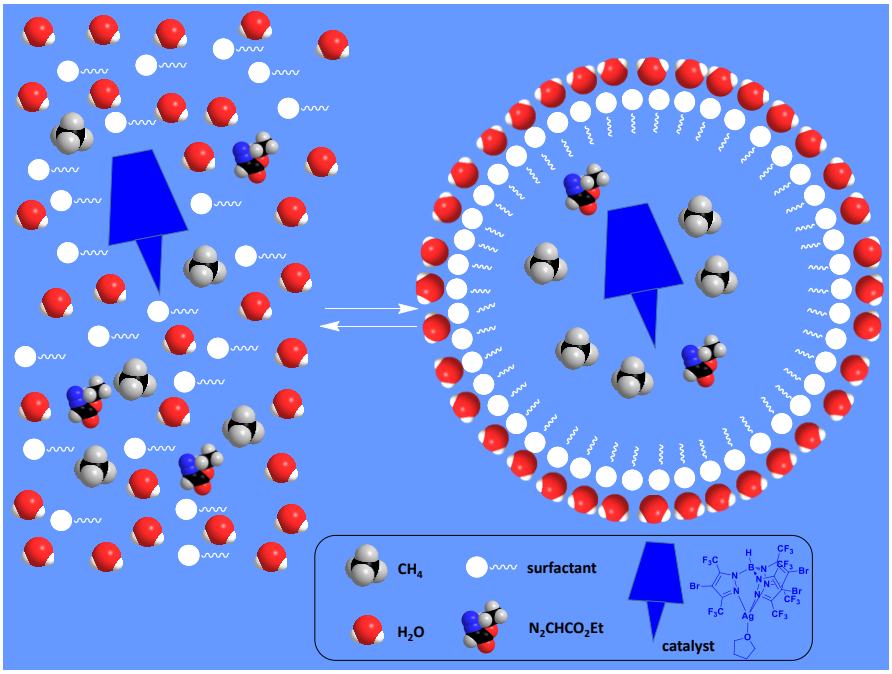

Figure 23. The micellar catalytic system designed for the gaseous alkane functionalization in water.

5.2 Methane and light alkane functionalization in water at room temperature.

In a first approach to this idea, ethane was chosen as the substrate, since previous studies demonstrated that is ca. 25 times more reactive than methane for the targeted reaction. Three surfactants were screened (Table 7), namely Triton X-100, TPGS-750-M and SDS (see Introduction for their corresponding composition). The catalyst (**3**, 0,01 mmol) and a water solution of the surfactant (10% w/w) were introduced into the reactor before ethyl diazoacetate (0.5 mmol) was added. Then the ethane pressurized tank was connected to the reactor until a 35 atm internal pressure was stabilized. After 14 h of stirring at room temperature, depressurization was carried out passing the gases through two consecutive cold traps to avoid any leaking of the products. The aqueous reaction mixture was treated with diethyl ether and the organic layer, containing

the products, was added to the traps. All the organic fractions were investigated by GC leading to conversion. Table 7 shows the results of this screening, showing that SDS (sodium dodecyl sulfate) was the most convenient surfactant, leading to a 53% yield of ethyl butyrate, based on initial EDA. It is worth

Table 7. Reaction of ethane and ethyl diazoacetate in water using surfactants and $Tp^{(CF3)2,Br}Ag(thf)$ (**3**) as catalyst.[a]

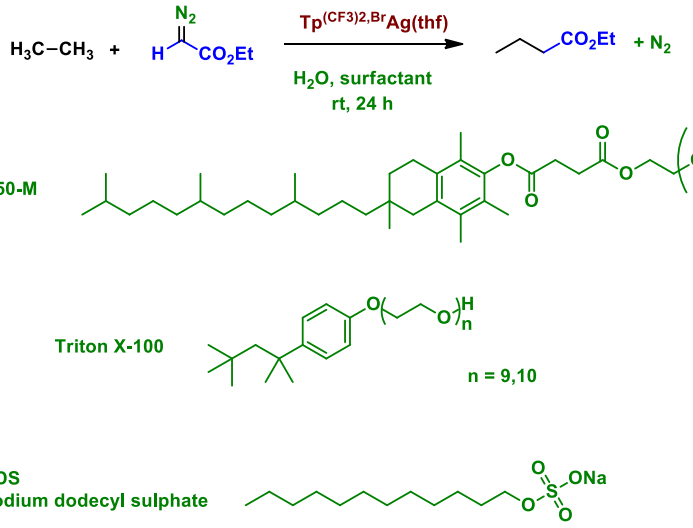

Entry	Surfactant	Amount surf. (mL or g)	V_{H2O} (mL)	Yield (%)
1	Triton™ X-100	6 mL	24	<2
2	Triton™ X-100	2 mL	22	<2
3	Triton™ X-100	1 mL	50	<2
4	TPGS-750-M[b]	25 mL		6
5	TPGS-750-M	2 g	20	nd[c]
6	SDS	20 g	40	nd[c]
7	SDS	10 g	40	24
8	**SDS**	**2.5 g**	**20**	**53**
9	--	--	20	nd[c]

[a.] General Conditions: 0.01 mmol of **3**; 0.5 mmol EDA; 35 atm ethane; X mL or g of surfactant and V mL of H_2O. [b] Solution in water 2 % wt [c] No product detected.

mentioning that in the absence of the silver catalyst, no consumption of the

diazocompound was observed. Moreover, the nature of the surfactant seems crucial in the reaction outcome, since with the same solvent (water), temperature (25 ºC), catalyst (**3**) and reactants (ethane and ethyl diazoacetate), the yield range varied dramatically from barely null (entries 1-3) to 53% (entry 8).

Once SDS was detected as a good promoter for micelles that efficiently concentrates reactants and catalyst, we wondered about the use of other catalysts that have shown activity toward C-H functionalization by carbene transfer from diazo compounds. Thus, we employed complexes **2**, **6** and the IPrAuCl/$NaBAr^F_4$ in the reaction shown in Table 7. However, none of them under the optimized conditions (Table 7, entry 8) gave detectable amounts of ethyl butyrate. Thus, it is complex **3** that seems to be the appropriate election for this transformation in water and room temperature.

Table 8. Methane catalytic functionalization in water at room temperature using SDS as surfactant and $Tp^{(CF3)2,Br}Ag(thf)$ (**3**) as catalyst.[a]

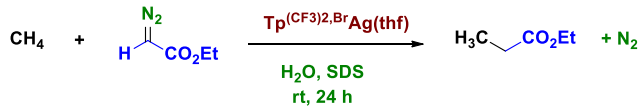

Entry	$P_{methane}$ (atm)	SDS (g)	Mmol EDA	Yield (%)
1	40	2.5	0.5	1
2	100	2.5	0.5	2
3	160	2.5	0.5	4
4	160	1	0.5	4
5	160	1	0.25	6
6	160	3	0.5	3
7	**160**	**1.5**	**0.25**	**8**

[a.] General Conditions: 0.01 mmol of catalyst, 20 mL of H_2O, 24 h at 25 ºC.

Having determined the best catalyst, surfactant and reaction conditions, methane was then investigated as the substrate. Table 8 displays the results of a series of experiments in which methane and ethyl diazoacetate were reacted in water in the presence of SDS. When total pressure of methane was varied from 40 to 160, the yield into ethyl propionate varied from 1 to 4% entries 1-

3). This is probably the expected effect of an increase of the solubility of methane in water due to the external pressure. The solubility of ethane and methane in water at room temperature and at 1 atm are 3.9 x 10^{-5} and 2.8 x 10^{-5} (fraction molar concentration).[84] This somewhat linear effect of $P_{methane}$ on the yields finds no parallelism with the concentration of surfactant. Thus, the use of 1, 2.5 or 3 g of SDS (entries 4, 3 and 6), maintaining the rest of variables unchanged, does not induce an increase in the functionalization of methane. The use of the higher catalyst-to-EDA ratio of 1:25 improved the yield (entries 4 and 5), an effect that has been previously observed and explained.[63b] The experiment shown in entry 7 using 1.5 g of SDS and such 1:25 ratio under 160 atm of methane led to a 8% yield into ethyl propionate (EDA-based), in the first example of a transformation of methane in water at room temperature leading to a unique product that do not undergo further functionalization.

Propane and butane have also been tested as substrates in this novel catalytic system. As shown in Figure 24, both alkanes were converted into mixtures of the two products derived from the insertion of the $CHCO_2Et$ unit

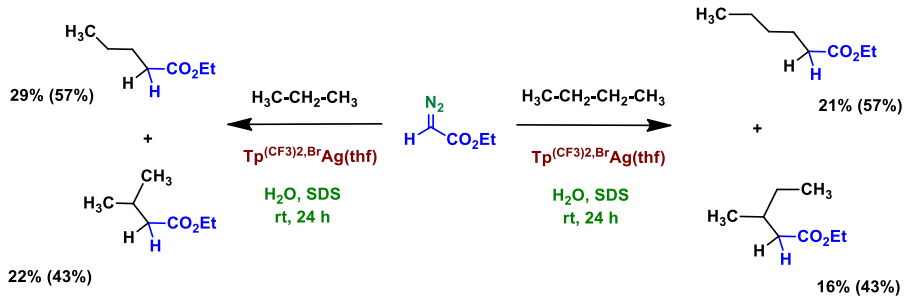

Figure 24. Propane and butane functionalization in water at room temperature. Numbers indicate EDA-based yields, distribution of products given in parentheses.

into the primary and secondary C-H bonds available in their molecules. The secondary sites were preferred, in line with the previous studies carried out in our laboratories. In fact, the regioselectivity observed, identical for both substrates (43:57), was also quite similar to that found in *sc*CO_2 (44:56, see

Scheme 5), indicating that the catalytic reaction *per se* is not affected neither by the micelle nor by the reaction medium.

The yields into the functionalized alkanes varied within the range 8-53%, and are EDA-based. Since EDA is consumed at the end of the 24 h reaction period, we wondered about the remaining up to the initial 100%. A common reaction is the catalytic coupling of two molecules of EDA to give mixtures of the olefins diethyl fumarate or maleate. However, the amounts of such olefins did not account, by far, for the required EDA to accomplish mass balance. Figure 25 shows the GC trace of the final reaction mixture with ethane as the alkane. It is clearly observable that marginal amounts of DEF/DEM are formed. A second explanation would involve the formation of ethyl glycolate, $HOCH_2CO_2Et$, from the catalytic functionalization of the O-H bond in water by $CHCO_2Et$ insertion. In spite of being water the solvent, we have not detected ethyl glycolate in significant amounts neither in the extracted organic phase (Figure 25) nor even in the crude in the aqueous reaction mixture after 24 h. This fact proves that when the carbene unit is transferred from the silver center,

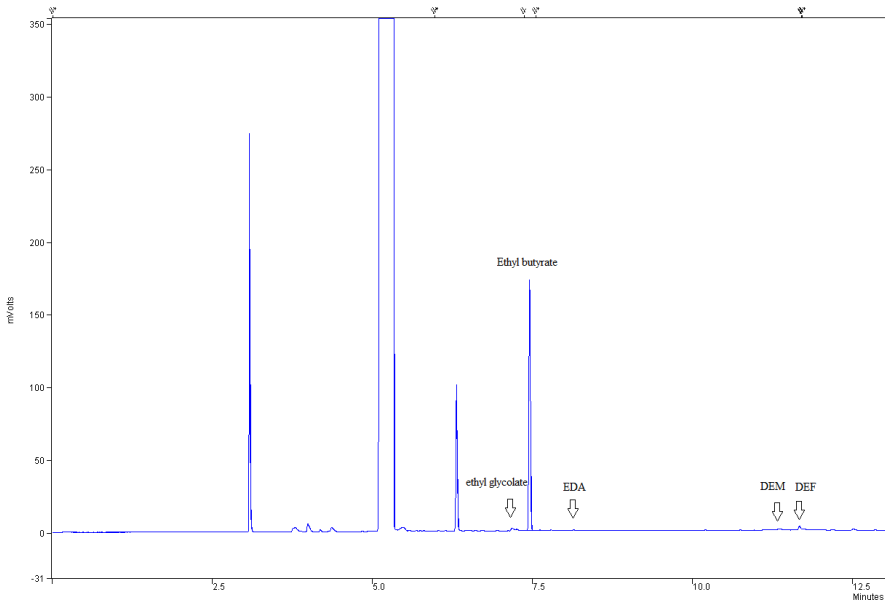

Figure 25. Chromatogram of reaction with ethane.

water molecules are not available at a significant concentration in the close vicinity, in line with the proposed hydrophobicity of the inner side of the micelle.

Having discarded the above two explanations, the third and last option is that the aliphatic chains of sodium dodecyl are modified by C-H functionalization. Given that the apolar side of the micelle is plenty of such chains, we investigated this possibility upon carrying out the ethane functionalization but using D_2O as the solvent, with SDS as the surfactant the catalyst **3** and ethyl diazoacetate. After 24 h of stirring at room temperature, the reaction mixture was investigated by NMR, showing the main incorporation of the $CHCO_2Et$ unit into the terminal methyl groups of the dodecyl fragments. Figure 26a shows the gHMBC- NMR spectrum where the triplet centered at 2.36 ppm in the proton axis is associated with the methylene group attached to the CO_2Et moiety (resonances in the ^{13}C axis) generated after the insertion of the carbene into such terminal methyl site. The triplet at 2.23 ppm corresponds to the product derived from ethane functionalization, i. e., ethyl butyrate. Interestingly, when the reaction in the absence of ethane, with just SDS, the catalyst and EDA in D_2O constituting the reaction mixture, two resonances appear in that region: in addition to the triplet at 2.36 ppm, a set of resonances within the range 2.19-2.26 ppm (Figure 26b) has been identified as derived from the insertion of the carbene groups in secondary sites, albeit at this stage we have not precisely determined the position of the incorporation. Thus, it seems that with ethane the main incorporation in the SDS chains take splace in the primary sites whereas in its absence, some secondary sites, that would become available, are also modified.

a

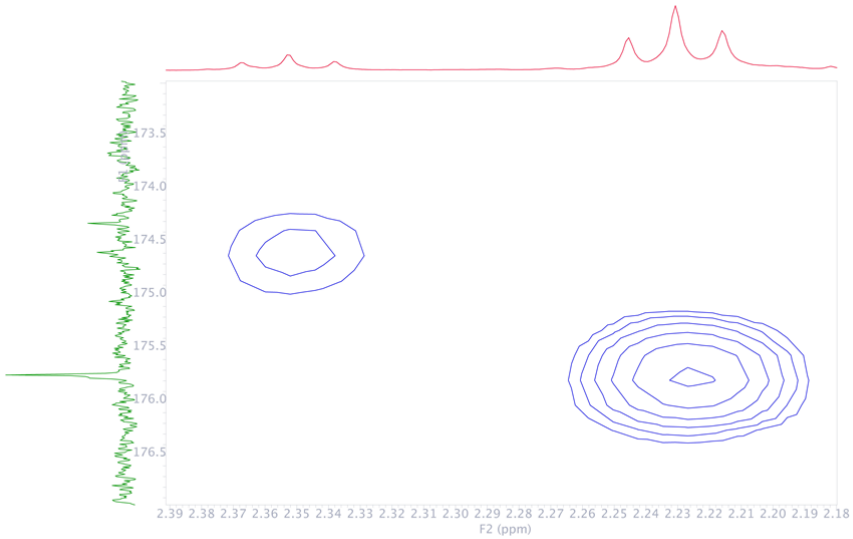

b

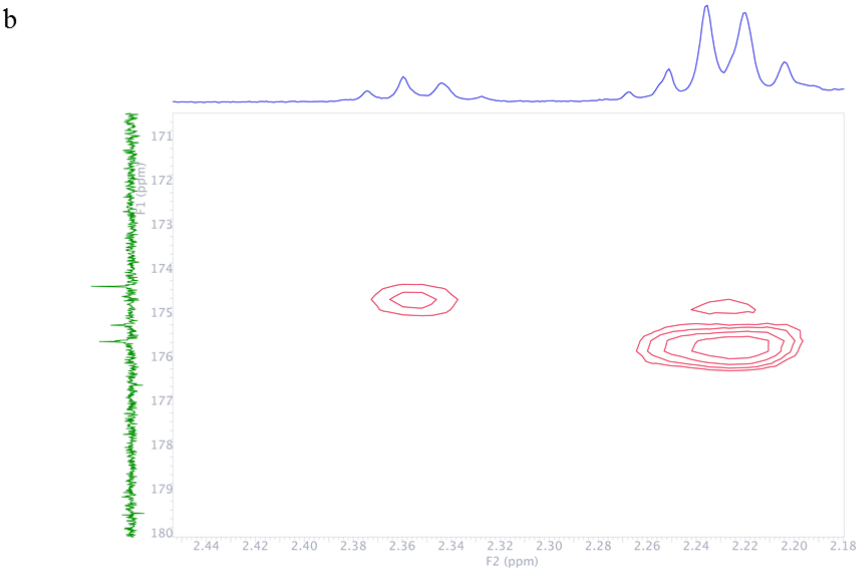

Figure 26. (a) gHMBC- NMR region (2.18-2.44 ppm) of the reaction with ethane in D_2O-SDS. (b) gHMBC-NMR of reaction without ethane in D_2O-SDS

Conclusions of Section 3

Methane and other C_2-C_4 gaseous alkanes have been functionalized at room temperature and in water as the reaction medium, in their reaction with ethyl diazoacetate in the presence of complex $Tp^{(CF3)2,Br}Ag(thf)$ (**3**) as catalyst and sodium dodecyl sulfate as surfactant.

The surfactant promotes the formation of micelles that concentrates in the apolar inner volume the catalyst and reactants. The lack of water functionalization supports this proposal.

The observance of regioselectivities identical to those previously determined in *sc*CO_2 as reaction medium also points toward the absence of any effect of the reaction system in the catalytic reaction.

EXPERIMENTAL

METHODS

6. Experimental methods: general procedures.

Preparations and manipulations of metal complexes were carried out under an oxygen free nitrogen atmosphere using conventional Schlenk techniques. The ethyl diazoacetate (EDA), the liquid alkanes and the surfactants TPGS-750-M, Triton-X-100 and sodium dodecyl sulphate were purchased from Aldrich or Alfa Aesar and employed without further purification, while the gaseous alkanes were purchased from Air Liquide. The pyrazole $pz^{(CF3)2,Br}$ and $TlBH_4$ were prepared according to literature procedures.[58,85] The silver complexes $Tp^{F27}Ag(thf)$ (**4**) and $Tp^{F39}Ag(thf)$ (**5**) and the rhodium complex $[Rh_2(CF_3COO)_4]_2$ (**6**) were prepared following already described protocols.[33,75] The supercritical experiments were carried out in a commercial THAR Technologies R100SYS supercritical plant or in Phenomenex empty 33 mL HPLC columns 21.2mm ID x 1in OD x 100 mm L connected to a HIP valve through 1/16" stainless steel tubes. NMR experiments were run in Agilent Technologies 400 MHz and 500 MHz spectrometers. Chemical shift values for ^1H and ^{13}C are reported as δ values (ppm) relative to internal $SiMe_4$. GC studies were performed using a Varian 450 chromatograph.

6.1 Experimental Methods for Section 1

*6.1.1 Synthesis of hydrotris(4-bromo-3,5-bis(trifluoromethyl)pyrazole-1-yl)borate thallium(I) ($TlTp^{(CF3)2,Br}$, **1**).*

1.41 g of 4-bromo-3,5-bis(trifluoromethyl)pyrazole (5 mmol) and 0.275 g of thallium borohydride (1.25 mmol) were place inside a glass pressure vessel. The mixture was heated with slow stirring under nitrogen at 140 °C for 1 h allowing the gases to leave the reactor. After that time, the temperature was raised to 170 °C and the reactor was closed. After 3 h at that temperature, the mixture was allowed to reach the room temperature and the residue was dissolved in $CHCl_3$. After filtration through a short pad of neutral alumina, the solution was evaporated affording complex **1** as a white solid. Purification upon

crystallization from $CHCl_3$ solutions at -30 ºC gave colorless crystals suitable for X-ray diffraction studies. Yield: 75 %.

$^{19}F\{^1H\}$NMR (470 MHz, $CDCl_3$, 20 ºC), δ (ppm): -57.13 (d, $J_{F\text{-}F}$ = 3.5 Hz), -60.03 (d, $J_{F\text{-}Tl}$ = 972.0 Hz); $^{13}C\{^1H\}$ NMR (125 MHz, $CDCl_3$, 20 ºC), δ (ppm): 143.0 (dq, *J* = 36.1 Hz, *J* = 18.1 Hz), 139.0 (q, *J* = 39.5 Hz), 120.7 (dq, *J* = 269.7 Hz, *J* = 11.5 Hz), 119.1 (q, *J* = 269.7 Hz), 95.0. $^{11}B\{^1H\}$ NMR (160 MHz, $CDCl_3$, 20 ºC), δ (ppm): -4.48. Anal. Calcd. for $C_{15}HBBr_3F_{18}N_6Tl$: C 16.96, H 0.09, N 7.91. Found: C 16.66, H 0.04, N 9.21.

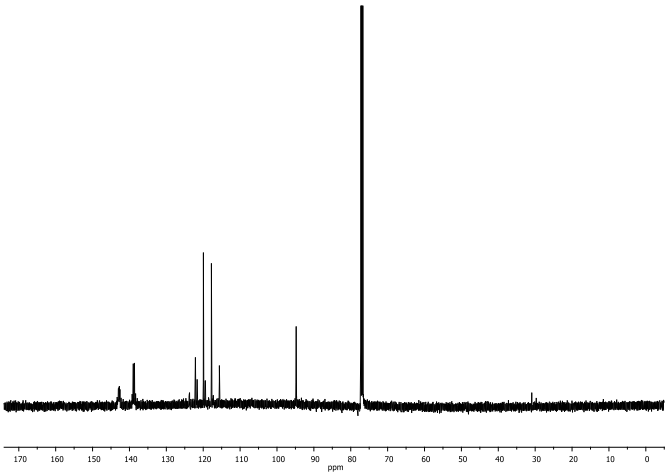

Figure E1. $^{13}C\{^1H\}$ NMR spectrum of complex **1**.

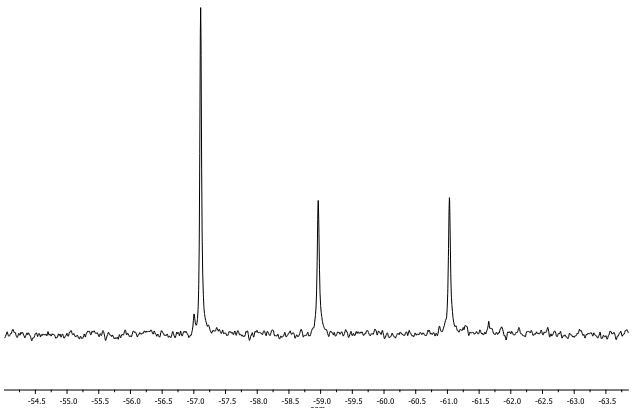

Figure E2. $^{19}F\{^1H\}$ NMR spectrum of complex **1**.

*6.1.2 Synthesis of hydrotris(4-bromo-3,5-bis(trifluoromethyl)pyrazole-1-yl)borate copper(I) acetonitrile ($Tp^{(CF3)2,Br}Cu(NCCH_3)$, **2**).*

A solution of 38 mg of CuI (0.2 mmol) in 5 mL of acetonitrile was mixed with another solution of 212 mg of $TlTp^{(CF3)2,Br}$ (0.2 mmol) in 5 mL of acetonitrile. The mixture was stirred at room temperature for 15 h before evaporating the volatiles. The residue was extracted with n-hexane (3x7 mL). The extracts were combined and the solvent removed under vacuum yielding **2** as a white solid which was crystallized from acetonitrile. Yield: 75%.

^{1}H NMR (500 MHz, $CDCl_3$, 20 ºC), δ (ppm): 2.17 (s, 3H). $^{19}F\{^{1}H\}$ NMR (470 MHz, $CDCl_3$, 20 ºC), δ (ppm): -56.41 (d, J = 4.5 Hz), -61.26 (s). $^{13}C\{^{1}H\}$ NMR (125 MHz, $CDCl_3$, 20 ºC), δ (ppm): 142.1 (q, J = 37.5 Hz), 137.8 (q, J = 40 Hz), 119.8 (q, J = 270.9 Hz), 119.1 (q, J =272.6 Hz), 114.1, 94.7, 2.47. $^{11}B\{^{1}H\}$ NMR (160 MHz, $CDCl_3$, 20 ºC), δ (ppm): -6.5. Anal. Calcd. for $C_{17}H_4BBr_3CuF_{18}N_7$: C 21.22, H 0.42, N 10.19. Found: C 20.92, H 0.32, N 11.56.

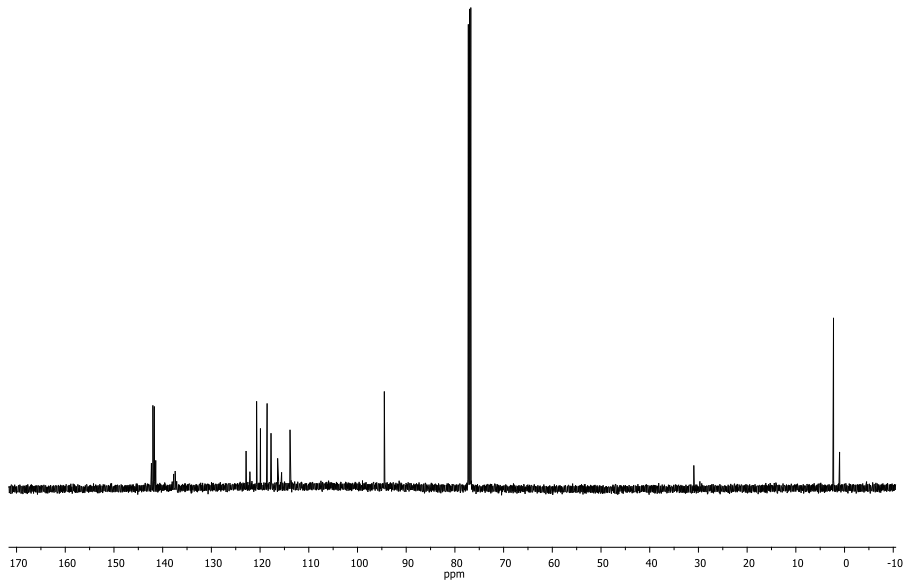

Figure E3. $^{13}C\{^{1}H\}$ NMR spectrum of complex **2**.

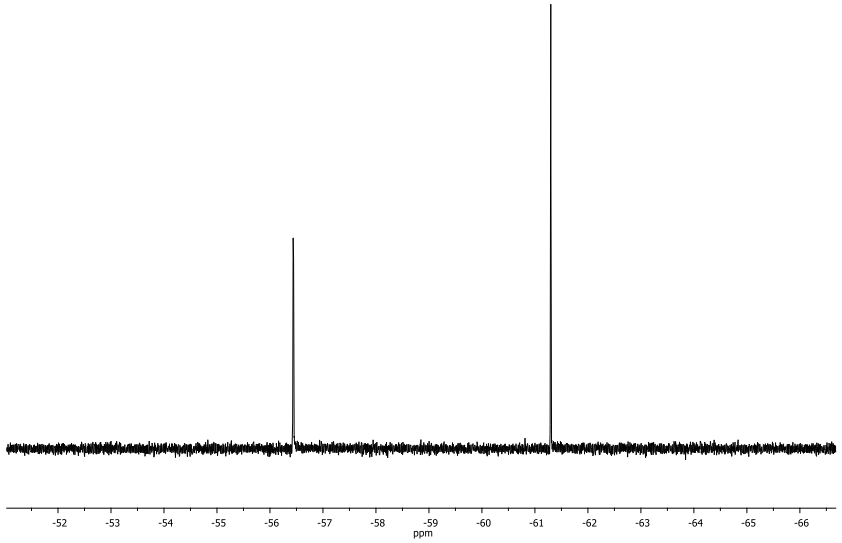

Figure E4. $^{19}F\{^{1}H\}$ NMR spectrum of complex **2**.

*6.1.3 Synthesis of tris(4-bromo-3,5-bis(trifluoromethyl)pyrazole-1-yl)borate silver(I) ($Tp^{(CF3)2,Br}Ag(thf)$, **3**).*

To a solution of 51 mg of AgOTf (0.2 mmol) in 5 mL of tetrahydrofuran was added a solution of 212 mg of $TlTp^{(CF3)2,Br}$ (0.2 mmol) in 5 mL of tetrahydrofuran. The mixture was stirred for 5 h previously to evaporation of volatiles. Extraction with n-hexane (3x7 mL), and removal of the solvent led to the isolation of a white solid of **3** that could be crystallized upon cooling their tetrahydrofuran solutions. Yield: 70%.

$^{19}F\{^{1}H\}$ NMR (470 MHz, $CDCl_3$, 20 ºC), δ (ppm): -56.81 (s), -62.22 (s); $^{13}C\{^{1}H\}$ NMR (125 MHz, $CDCl_3$, 20 ºC), δ (ppm): 143.0 (q, J = 36 Hz), 138.7 (q, J = 39.7 Hz), 119.9 (q, J = 270.5 Hz), 119.1 (q, J = 273.2 Hz), 94.4, 71.6, 25.8. $^{11}B\{^{1}H\}$ NMR (160 MHz, $CDCl_3$, 20 ºC), δ (ppm): -5.53. Anal. Calcd. For $C_{19}H_9AgBBr_3F_{18}N_6$: C 21.99, H 0.87, N 8.10. Found: C 21.64, H 0.42, N 8.51.

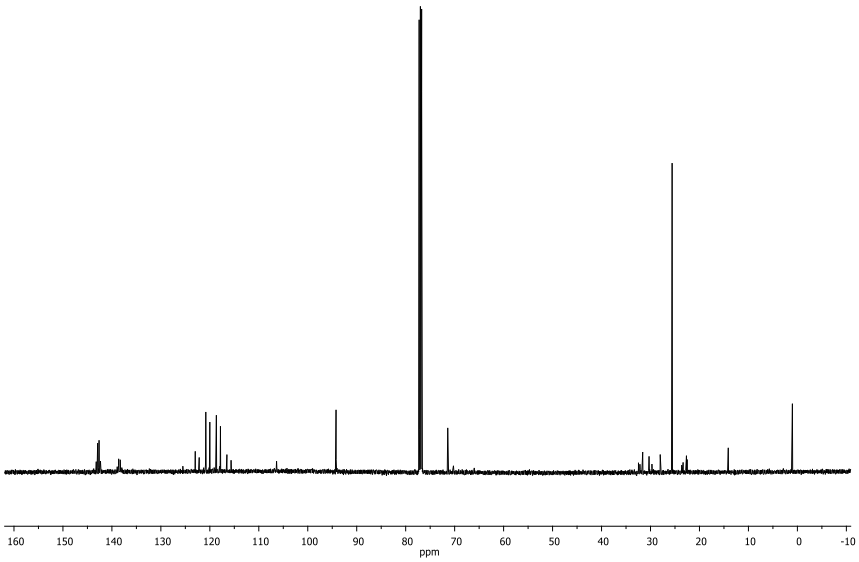

Figure E5. $^{13}C\{^{1}H\}$ NMR spectrum of complex **3**.

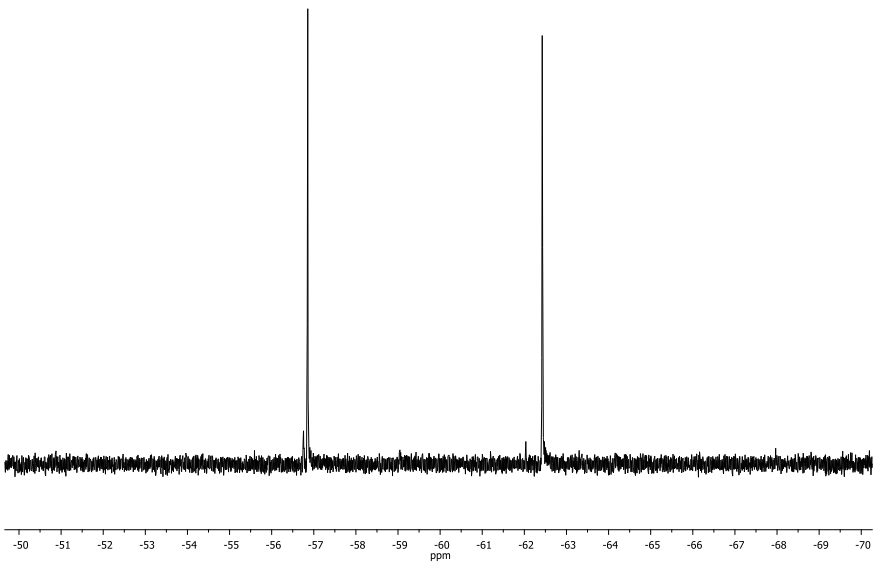

Figure E6. $^{19}F\{^{1}H\}$ NMR spectrum of complex **3**.

6.1.4 General catalytic procedures for alkane functionalization.

(a) Catalytic experiments under supercritical conditions with methane.

These reactions were performed in a 100 mL stainless steel reactor mechanically stirred by paddles. The corresponding complex (**2-3**, 0.005 mmol) was placed into a polypropylene tube, and both sides were closed with a permeable cap. A second polypropylene container was charged with ethyl diazoacetate (0.35 mmol). Both containers were fixed to the mixer axis of the reactor, that was closed and pressurized first with 160 atm of methane and then with carbon dioxide up to a total pressure of 250 atm at a constant temperature of 40 ºC. Through a sapphire window (Figure E7) the differences in the solubility of the reaction components could be observed. After 14 h of stirring at 40 ºC, the reaction was analyzed by gas chromatography. The gas mixture was directly injected into the GC column by opening the valve connecting the reactor and the GC. The exact amounts of the products were determined using calibration curves previously recorded with commercial samples.

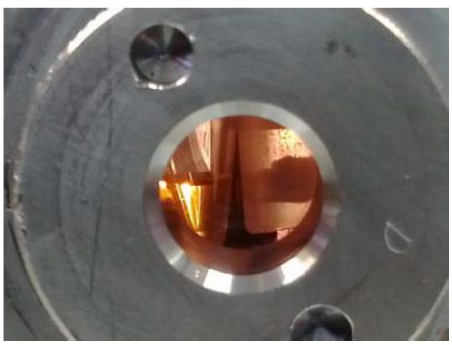

Figure E7. Inside the reactor: catalyst (right) and EDA (left) location, fixed to the stir axis.

(b) Catalytic experiments under supercritical conditions with C_nH_{2n+2} (n = 2-4).

In a high pressure reactor of 33 mL, the catalyst (0.005 mmol) was placed inside of a polypropylene container with permeable caps in both ends and 0.5 mmol of EDA in a second open container. For reactions with ethane the reactor was connected to an ethane bottle and pressurized to 30 atm. For reactions with propane, butane and isobutane, the reactor was cooled to 0ºC and connected to a pressurized bottle of the desired alkane for a period of time enough to charge 3 to 5 g of the alkane. The exact amount of alkane was determined by weight difference before and after pressurization. Then the reactor was placed in an ultrasonic bath thermostated at 40 ºC (Figure E8). After temperature stabilization the reactor was pressurized with CO_2 until a total pressure of 250 atm was reached. The reactor was sonicated for 4 hours before connecting it to the GC and the analysis of the reaction mixture. The exact amounts obtained of the different products were determined using calibration curves obtained with commercial samples.

Figure E8. The 33 mL reactors in the ultrasonic bath.

*(c) Reactions carried out using the neat alkanes as the reaction medium with complexes **2** and **3** as the catalysts.*

In a Schlenk flask 0.005 mmol of the complex **2** or **3** were dissolved in 5 mL of the corresponding alkane (pentane, hexane or 2-methylbutane). With the copper catalyst, a solution of EDA (57 µL in 5 mL of the alkane) was then added with the aid of a syringe pump during 8 h. In the silver case, the 57 µL of EDA were added in one portion and the mixture stirred for 3 h. The conversions and yields were determined by GC analysis using calibration curves. Experiments at room temperature or 40 ºC (oil bath) gave the same results.

(d) Catalytic experiments using liquid alkanes under CO_2 pressure.

Inside a 100 mL high pressure reactor, 0.005 mmol of catalyst was placed in a polypropylene container with permeable caps in both ends and 0.5 mmol of EDA in a second open container. The alkane was added (10 mL) and the reactor was filled with CO_2 up to 100 atm. The reaction was stirred for 8 h at either at room temperature or 40 ºC, the latter ensuring supercritical conditions, and then the system was depressurized before analysing the mixture by GC.

(e) Experiments under irradiation conditions.

With hexane as the substrate, the experiments were identical to those above, either in hexane as the solvent or in *sc*CO_2, but lacking of catalyst and using a UV lamp (340 nm) attached either to the Schlenk flask or to the high pressure reactor through the sapphire window.

(f) Analytical methods

The GC column was Varian Capillary Column CP-Sil5CB (50 mm x 0.32 mm x 1.2 µm), and methods was the following: initial column temperature, 40 ºC; final temperature, 200 ºC; ramp temperature, 15 ºC/min.

The quantification of the catalytic reactions was made using calibration curves for each product (Figure E9). These straight lines have been obtained by injecting into the gas chromatograph different solutions of commercial products, if available, previously quantified by NMR with an internal standard (biphenyl) or mixtures from catalytic reactions with the silver complex and quantified by NMR with internal standard

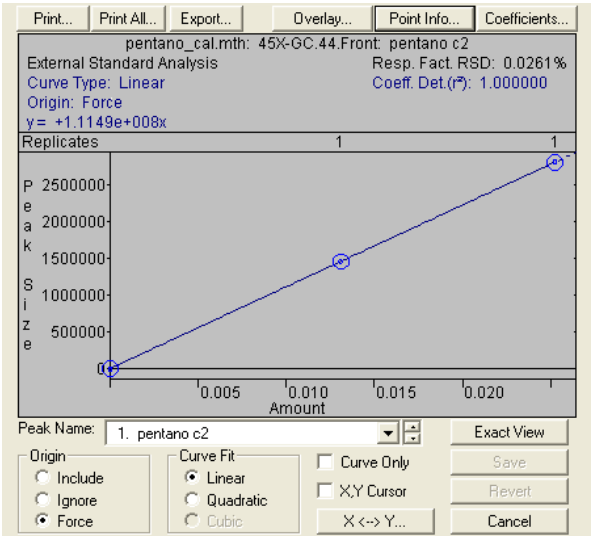

Figure E9. Calibration curve of the product derived from functionalization of C2-H in pentane.

*6.1.5 X-Ray structure analysis for **1**, **2** and **3**.*

These studies were carried out by Dr. Eleuterio Álvarez at the Instituto de Investigaciones Químicas (CSIC). Crystals of suitable size for X-ray diffraction analysis were coated with dry perfluoropolyether and mounted on glass fibers and fixed in a cold nitrogen stream (T = 100 K) to the goniometer head. Data collection was performed on a Bruker-Nonius X8Apex-II CCD diffractometer, using monochromatic radiation λ(Mo K_α) = 0.71073 Å, by means of ω and φ scans with a width of 0.50 degree. The data were reduced

(SAINT)[86] and corrected for absorption effects by the multi-scan method (SADABS).[87] The structures were solved by direct methods (SIR-2002)[88] and refined against all F^2 data by full-matrix least-squares techniques (SHELXTL-6.12)[89] minimizing $w[F_o^2\text{-}F_c^2]^2$. All the non-hydrogen atoms were refined anisotropically, while C-H hydrogen atoms were placed in geometrically calculated positions using a riding model.[90] CCDC-1037192 (**1**), 1037193 (**2**), and 1037194 (**3**) contain the supplementary crystallographic data for this paper. These data can also be obtained free of charge from The Cambridge Crystallographic Data centre via http//www.ccdc.cam.ac.uk/data_request/cif.

Table E1. Crystal data and structure refinement for **1**.

Empirical formula	$C_{15}HBBr_3F_{18}N_6Tl$	
Formula weight	1062.13	
Temperature	213(2) K	
Wavelength	0.71073 Å	
Crystal system	Triclinic	
Space group	$P\bar{1}$	
Unit cell dimensions	a = 9.4814(8) Å	α= 111.406(2)°.
	b = 10.7650(9) Å	β= 92.343(2)°.
	c = 13.9827(11) Å	γ = 99.301(2)°.
Volume	1303.49(19) Å3	
Z	2	
Density (calculated)	2.706 Mg/m3	
Absorption coefficient	10.944 mm-1	
F(000)	972	
Crystal size	0.40 x 0.40 x 0.30 mm3	
Theta range for data collection	1.57 to 25.25°.	
Index ranges	-11<=h<=11, -12<=k<=12, -16<=l<=16	
Reflections collected	20328	
Independent reflections	4681 [R(int) = 0.0365]	
Completeness to theta = 25.25°	99.2 %	
Absorption correction	Semi-empirical from equivalents	
Max. and min. transmission	0.1378 and 0.0969	
Refinement method	Full-matrix least-squares on F2	
Data / restraints / parameters	4681 / 0 / 397	
Goodness-of-fit on F2	1.032	
Final R indices [I>2sigma(I)]	R1 = 0.0420, wR2 = 0.1142	
R indices (all data)	R1 = 0.0451, wR2 = 0.1165	
Largest diff. peak and hole	2.923 and -2.702 e.Å^{-3}	

Table E2. Crystal data and structure refinement for **2**.

Empirical formula	$C_{17}H_4BBr_3CuF_{18}N_7$	
Formula weight	962.35	
Temperature	253(2) K	
Wavelength	0.71073 Å	
Crystal system	Monoclinic	
Space group	C 2/c	
Unit cell dimensions	a = 21.9569(12) Å	α= 90°.
	b = 16.6067(10) Å	β= 105.863(2)°.
	c = 17.0174(9) Å	γ = 90°.
Volume	5968.8(6) Å3	
Z	8	
Density (calculated)	2.142 Mg/m3	
Absorption coefficient	4.885 mm-1	
F(000)	3648	
Crystal size	0.50 x 0.40 x 0.30 mm3	
Theta range for data collection	1.82 to 25.25°.	
Index ranges	-26<=h<=26, -19<=k<=5, -20<=l<=20	
Reflections collected	27065	
Independent reflections 5	310 [R(int) = 0.0380]	
Completeness to theta = 25.25°	97.9 %	
Absorption correction	Semi-empirical from equivalents	
Max. and min. transmission	0.2309 and 0.1098	
Refinement method	Full-matrix least-squares on F2	
Data / restraints / parameters	5310 / 0 / 424	
Goodness-of-fit on F2	1.066	
Final R indices [I>2sigma(I)]	R1 = 0.0611, wR2 = 0.1705	
R indices (all data)	R1 = 0.0975, wR2 = 0.1895	
Largest diff. peak and hole	1.019 and -0.810 e.Å^{-3}	

Table E3. Crystal data and structure refinement for **3**.

Empirical formula	$C_{19}H_9AgBBr_3F_{18}N_6O$	
Formula weight	1037.73	
Temperature	173(2) K	
Wavelength	0.71073 Å	
Crystal system	Triclinic	
Space group	$P\bar{1}$	
Unit cell dimensions	a = 9.5396(11) Å	α= 100.867(3)°.
	b = 12.6988(15) Å	β= 94.371(3)°.
	c = 12.9452(16) Å	γ = 98.592(3)°.
Volume	1514.0(3) Å3	
Z	2	
Density (calculated)	2.276 Mg/m3	
Absorption coefficient	4.765 mm-1	
F(000)	984	
Crystal size	0.30 x 0.20 x 0.20 mm3	
Theta range for data collection	1.61 to 25.25°.	
Index ranges	-11<=h<=11, -15<=k<=14, -15<=l<=14	
Reflections collected	26014	
Independent reflections	5502 [R(int) = 0.0399]	
Completeness to theta = 25.25°	98.1 %	
Absorption correction	Semi-empirical from equivalents	
Max. and min. transmission	0.3892 and 0.3290	
Refinement method	Full-matrix least-squares on F2	
Data / restraints / parameters	5502 / 23 / 442	
Goodness-of-fit on F2	1.081	
Final R indices [I>2sigma(I)]	R1 = 0.0626, wR2 = 0.1352	
R indices (all data)	R1 = 0.0912, wR2 = 0.2075	
Largest diff. peak and hole	1.513 and -1.295 e.Å^{-3}	

6.2 Experimental Methods for Section 2.

6.2.1 Competition experiments between ethane and methane.

In a high pressure stainless-steel reaction vessel, ethyl diazoacetate (23 µL, 0.2 mmol) was placed in an open polypropylene container whereas the silver catalyst (7 mg for **3**, 11 mg for **4** or 14 mg for **5**, 0.01 mmol, 5 mol%) was introduced in a cylindrical polypropylene container equipped with filters in the upper and bottom side. The vessel was closed, connected to a pressurized cylinder of ethane and filled up to a pressure of 35 bar. Pressure was increased to 180 bar by introducing methane from a pressurized bottle. Exact amount of gases inside the vessel were determined by weight differences before and after each pressurization step. Finally, the reactor was heated to 40 ^{o}C and carbon dioxide was pumped inside until a total pressure of 250 bar. The vessel was thermostated at 40 ^{o}C and placed in a sonication bath during 4 hours. The gaseous mixture was directly injected in a modified gas chromatograph equipped with a pressure reduction device and a rheodyne valve. Products were quantified using calibration curves (see analytical procedures).

6.2.2 Competition experiments between ethane and other gaseous alkanes.

Following a procedure similar to above, EDA and catalyst were introduced into the vessel before connecting it to the appropriate gas cylinder during a period of five minutes while cooling in an ice-water bath. The reactor was then allowed to reach room temperature and connected to a pressurized bottle of ethane and filled up to a pressure of 35 bar. Amount of gases inside the reactor were determined by weight differences before and after each pressurization step. The vessel was heated to 40 ^{o}C and CO_2 was pumped inside up to a total pressure of 250 bar. The reaction was heated during 4 h in a sonication bath. The reactor was then cooled to -100 ^{o}C with a methanol-liquid nitrogen bath before depressurization was performed through two traps consecutively connected and cooled with liquid nitrogen. Once

depressurization was completed, the reactor was allowed to reach room temperature and the complete system was rinsed with dichloromethane. The resulting combined solutions were diluted to an exact volume in a volumetric flask. Products were analyzed by GC using calibration curves (see analytical procedures).

6.2.3. Competition experiments between ethane and liquid alkanes.

In a high pressure stainless-steel reaction vessel three polypropylene receptacles were introduced, two open ones containing ethyl diazoacetate (23 µL, 0.2 mmol) and 1 mL of the desired liquid alkane, and a third, closed with filters, with the silver catalyst (7 mg for **3**, 11 mg for **4** or 14 mg for **5**, 0.01 mmol, 5 mol%). The vessel was closed and pressurized with ethane up to 35 bar. Charge of gas was determined by weight differences before and after pressurization. The reactor was then heated to 40 ^{o}C and carbon dioxide was pumped inside until a total pressure of 250 bar. The vessel was sonicated at 40 ^{o}C for 4 h. Work-up was carried out identically to the previous experiment.

6.2.4. Competition experiments between cyclohexane and linear and branched alkanes.

For silver complexes, catalyst (7 mg for **3**, 11 mg for **4** or 14 mg for **5**, 0.01 mmol, 5 mol%) was introduced in an ampoule and deoxygenated under vaccum. The linear or branched alkane (5 mL) and the corresponding amount of cyclohexane to accomplish a 20:1 molar ratio alkane: cyclohexane were added. Finally, ethyl diazoacetate (23 µL, 0.2 mmol) was incorporated to the solution in one portion. The ampoule was then closed and the solution stirred at room temperature during 8 h. For rhodium complex **6**, a solution of ethyl diazoacetate (23 µL, 0.2 mmol) in 3 mL of dichloromethane was added during a period of 18 h over a solution of catalyst (6.6 mg, 0.01 mmol 5 mol%) in a mixture of dichloromethane (1 mL), alkane (5 mL) and the corresponding amount of cyclohexane to accomplish a 20:1 molar ratio alkane: cyclohexane.

For copper complex **2**, a mixture of alkane (7 mL) and the corresponding amount of cyclohexane to accomplish a 20:1 molar ratio alkane: cyclohexane was prepared and separated in two protions. Ethyl diazoacetate (23 µL, 0.2 mmol) was dissolved in 2 mL of this mixture and catalyst **2** (9.1 mg, 0.01 mmol, 5 mol%) was added to the rest. The solution of EDA was then added over the solution of the catalyst during a period of 18 h. The reaction mixture was transferred to a volumetric flask and diluted to an exact volume with dichloromethane. Products were quantified by GC analysis using calibration curves.

This same procedure has been applied to competition experiments between two cyclic alkanes, using 3 mL of each one.

6.2.5. Determination of relative C-H reactivity.

Two different sets of competition experiments were performed, namely: i) reactivity of gaseous alkanes was studied using ethane as reference in supercritical conditions, ii) reactivity of liquid alkanes was compared with that of cyclohexane in liquid mixtures of neat alkanes. Both sets were correlated using the competition between ethane and cyclohexane in supercritical carbon dioxide. Figure E10 shows the complete array of competition experiments and the equations employed to calculate the relative reactivity of the different C-H bonds referred to cyclohexane and to methane. Table E4 contains the complete data set for the three silver complexes $Tp^xAg(thf)$ (**3**-**5**) referred to methane. Table E5 contains the complete data set for the five metal complexes (**2**-**6**) referred to cyclohexane. The values of R_r displayed are an average of at least two independent experiments.

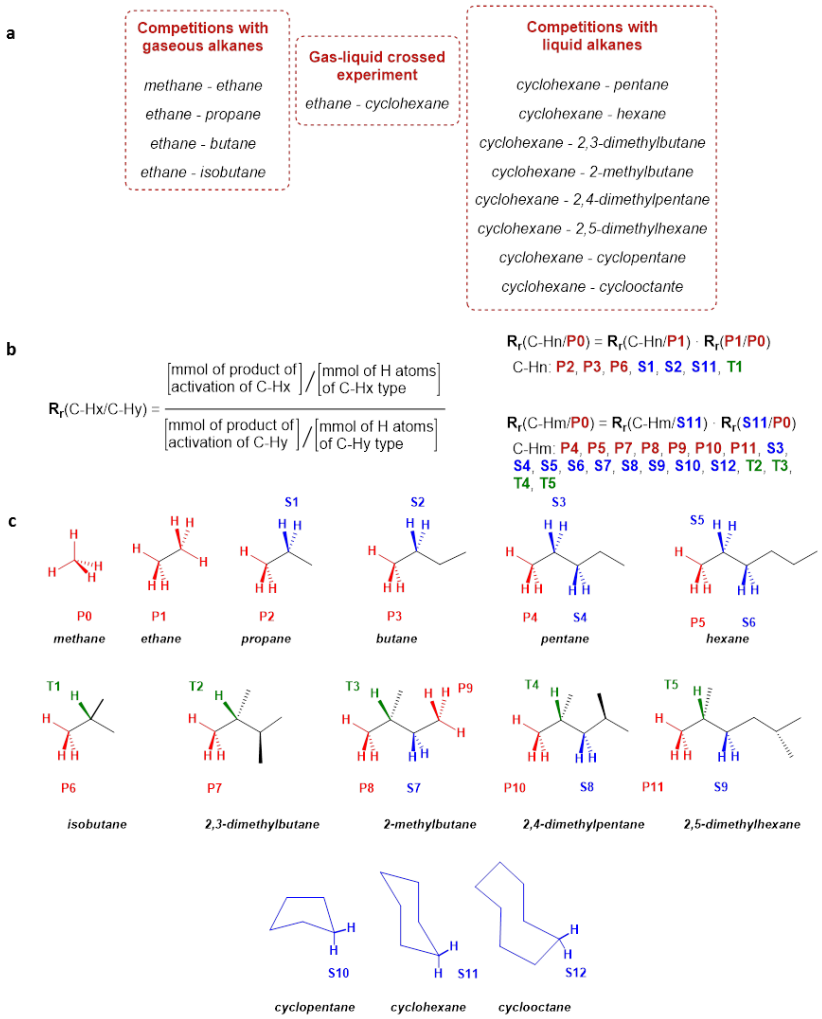

Figure E10. (a) Array of competition reactions performed. (b), Equations used to calculate the relative reactivity of the twenty-nine different C-H bonds referred to cyclohexane or to methane, correcting the number of H of the same type in each alkane. (c) The fourteen alkanes employed bearing twenty-nine different C-H bonds.

Table E4. Values of R_r and $\log(R_r)$ for the twenty-nine C-H bonds studied with the three silver complexes referred to methane. Absolute errors are indicated in brackets.

C-H Bond	3		4		5	
	R_r	$\log(R_r)$	R_r	$\log(R_r)$	R_r	$\log(R_r)$
P0	1	0	1	0	1	0
P1	24.5 (0.7)	1.39	22.4 (0.6)	1.35	28.4 (0.3)	1.45
P2	21.4 (0.6)	1.33	18.6(0.4)	1.27	26.2 (0.1)	1.42
P3	25.1 (0.7)	1.4	25.1 (0.3)	1.4	40.7 (21.4)	1.61
P4	42.7 (1.4)	1.63	47.9 (0.1)	1.68	50.6 (1.8)	1.70
P5	49.0 (2.3)	1.69	45.7 (3.3)	1.66	53.2 (2.2)	1.73
P6	11.5 (0.4)	1.06	13.2 (0.4)	1.12	10.1 (2.8)	1.01
P7	19.1 (0.9)	1.28	17.0 (0.1)	1.23	22.2 (0.2)	1.35
P8	20.4 (0.01)	1.31	22.4 (0.6)	1.35	22.3 (1.3)	1.35
P9	39.8 (0.02)	1.6	38.0 (0.9)	1.58	38.7 (2.1)	1.59
P10	15.5 (0.04)	1.19	14.5 (0.03)	1.16	16.1 (0.03)	1.21
P11	16.6 (0.1)	1.22	14.1 (0.2)	1.15	15.8 (0.09)	1.20
S1	70.8 (1.9)	1.85	66.1 (0.8)	1.82	91.3 (0.1)	1.96
S2	55.0 (1.5)	1.74	46.8 (0.3)	1.67	75 (39.0)	1.88
S3	79.4 (3.8)	1.9	79.4 (0.2)	1.9	87.3 (3.3)	1.94
S4	44.7 (2.1)	1.65	39.8 (0.3)	1.6	43.9 (4.4)	1.64

C-H Bond	3		4		5	
	R_r	$\log(R_r)$	R_r	$\log(R_r)$	R_r	$\log(R_r)$
S5	95.5 (4.4)	1.98	81.3 (3.0)	1.91	101.7 (0.04)	2.01
S6	40.7 (2.0)	1.61	32.4 (1.9)	1.51	40.1 (0.7)	1.60
S7	40.7 (0.8)	1.61	32.4 (0.9)	1.51	35.9 (2.0)	1.55
S8	1.9 (0.01)	0.28	1.8 (0.9)	0.26	1.5 (0.01)	0.17
S9	16.6 (0.05)	1.22	14.9 (0.2)	1.17	22.9 (0.1)	1.36
S10	100.0 (4.6)	2	112.2 (0.6)	2.05	126 (1.7)	2.10
S11	61.7 (1.7)	1.79	69.2 (0.3)	1.84	77.6 (0.2)	1.89
S12	85.1 (3.0)	1.93	95.6 (0.6)	1.98	113.3 (0.4)	2.05
T1	56.2 (1.3)	1.75	53.7 (0.9)	1.73	51.8 (14.0)	1.71
T2	29.5 (1.3)	1.47	22.9 (0.5)	1.36	37.6 (0.6)	1.58
T3	47.9 (0.03)	1.68	42.7 (1.3)	1.63	52.4 (3.1)	1.72
T4	5.5 (0.03)	0.74	3.7 (0.04)	0.57	5.5 (0.01)	0.74
T5	5.0 (0.1)	0.7	5.2 (0.1)	0.72	7.1 (0.04)	0.85

Table E5. Values of R_r and log(R_r) for the twenty-one C-H bonds studied with the five metal complexes (**2-6**) referred to cyclohexane. Absolute errors are indicated in brackets.

	3		4		5		6		2	
C-H Bond	**R_r**	**Log(R_r)**	**R_r**	**Log(R_r)**	**R_r**	**Log(R_r)**	**R_r**	**Log(R_r)**	**R_r**	**Log(R_r)**
P4	0.680 (0.009)	-0.17	0.706 (0.010)	-0.15	0.619 (0.023)	-0.21	0.135 (0.003)	-0.87	0.032 (0.001)	-1.5
P5	0.772 (0.056)	-0.11	0.667 (0.047)	-0.18	0.652 (0.028)	-0.19	0.138 (0.006)	-0.86	0.040 (0.001)	-1.4
P7	0.299 (0.012)	-0.52	0.238 (0.003)	-0.62	0.268 (0.002)	-0.57	0.060 (0.003)	-1.22	0.007 (0.0001)	-2.17
P8	0.331 (0.005)	-0.48	0.323 (0.012)	-0.49	0.291 (0.017)	-0.54	0.069 (0.007)	-1.16	0.015 (0.0007)	-1.83
P9	0.645 (0.010)	-0.19	0.549 (0.022)	-0.26	0.503 (0.028)	-0.3	0.158 (0.016)	-0.8	0.017 (0.0006)	-1.77
P10	0.251 (0.001)	-0.6	0.210 (0.008)	-0.68	0.207 (0.004)	-0.68	0.052 (0.001)	-1.29	0.001 (0.0003)	-2.92
P11	0.27 (0.001)	-0.57	0.203 (0.003)	-0.69	0.206 (0.001)	-0.69	0.044 (0.001)	-1.36	0.019 (0.0001)	-1.73
S3	1.275 (0.001)	0.11	1.151 (0.003)	0.06	1.070 (0.043)	0.03	1.059 (0.131)	0.02	0.613 (0.094)	-0.21
S4	0.725 (0.011)	-0.14	0.575 (0.004)	-0.24	0.610 (0.057)	-0.21	0.953 (0.23)	-0.02	0.13 (0.062)	-0.89
S5	1.509 (0.023)	0.18	1.19 (0.043)	0.08	1.191 (0.001)	0.08	1.205 (0.069)	0.08	0.778 (0.006)	-0.11
S6	0.663 (0.034)	-0.18	0.472 (0.027)	-0.33	0.479 (0.009)	-0.32	0.580 (0.034)	-0.24	0.183 (0.001)	-0.74
S7	0.660 (0.014)	-0.18	0.468 (0.040)	-0.33	0.466 (0.025)	-0.33	0.629 (0.063)	-0.2	0.117 (0.006)	-0.93
S8	0.031 (0.001)	-1.51	0.026 (0.014)	-1.58	0.019 (0.001)	-1.72	0.103 (0.004)	-0.99	0.332 (0.024)	-0.48
S9	0.272 (0.001)	-0.57	0.216 (0.003)	-0.67	0.295 (0.002)	-0.53	0.535 (0.009)	-0.27	0.530 (0.004)	-0.28
S10	1.621 (0.075)	0.21	1.621 (0.009)	0.21	1.620 (0.025)	0.21	1.213 (0.006)	0.08	1.201 (0.021)	0.08

	3		4		5		6		2	
C-H Bond	**R_r**	**Log(R_r)**	**R_r**	**Log(R_r)**	**R_r**	**Log(R_r)**	**R_r**	**Log(R_r)**	**R_r**	**Log(R_r)**
S11	1.000	0	1.000	0	1.000	0	1.000	0	1.000	0
S12	1.471 (0.044)	0.17	1.382 (0.009)	0.14	1.460 (0.005)	0.16	1.626 (0.006)	0.21	5.247 (0.026)	0.72
T2	0.489 (0.009)	-0.31	0.340 (0.004)	-0.47	0.484 (0.008)	-0.32	1.460 (0.011)	0.16	0.290 (0.003)	-0.54
T3	0.776 (0.020)	-0.11	0.617 (0.062)	-0.21	0.684 (0.040)	-0.16	2.250 (0.208)	0.35	1.088 (0.070)	0.04
T4	0.090 (0.090)	-1.05	0.054 (0.001)	-1.27	0.070 (0.001)	-1.15	0.170 (0.006)	-0.77	0.068 (0.001)	-1.17
T5	0.081 (0.002)	-1.09	0.076 (0.001)	-1.12	0.092 (0.001)	-1.04	0.106 (0.002)	-0.97	n.d.	n.d.

Additional competition experiments were run in order to ensure the accuracy of the results (Figure E11). Evaluation of the influence of the reaction medium was determined by performing competitions of cyclohexane and hexane using the neat alkanes or their *sc*CO_2 solutions as the reaction medium. Both experiments provided similar ratio of products. The similar relative reactivity of 2-methylbutane and cyclohexane observed in two different reactions performed in liquid mixtures of alkanes at 40 ºC and at room temperature reveals that temperature is not a determinant parameter.

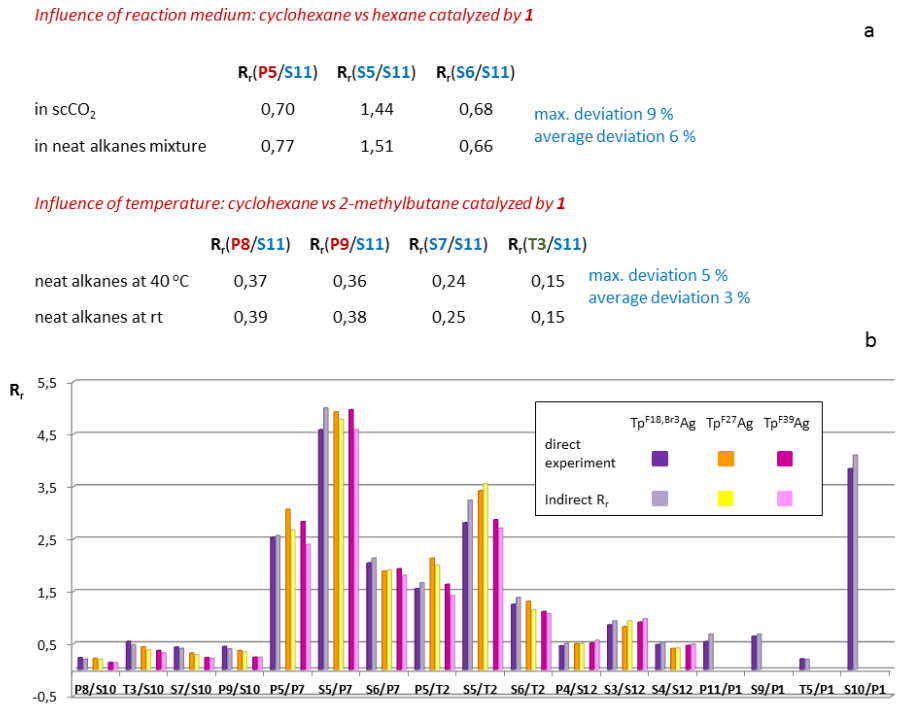

Figure E11. Additional competition experiments. (a) The influence of the reaction medium and the temperature on the relative reactivity. (b) Crossed-competitions for the three silver complexes. Dark bars indicate values obtained through direct experiments. Light bars display indirect R_r obtained as $R_r(C\text{-}H_x/C\text{-}H_y) = R_r(C\text{-}H_x/P0)/R_r(C\text{-}H_y/P0)$ from the data in Table E4.

Several crossed competition reactions were performed in order to verify the accuracy of the relative reactivity of the twenty-nine C-H bonds. For instance direct competitions between cyclopentane and 2-methylbutane, hexane and 2,3-dimethylbutane or pentane and cyclooctane were performed using the three silver complexes **3**–**5**. Relative reactivity of 2,5-dimethylhexane and ethane was specifically tested using $Tp^{(CF3)2,Br}Ag(thf)$ (**3**) as catalyst.

6.2.6 Characterization of products and analytical procedures.

All insertion products, except those derived from the functionalization of 2,4-dimethylpentane and 2,5-dimethylhexane, are commercially available. However, some of them were prepared in the laboratory. Calibration curves for the products derived from EDA insertion in C-H bonds P0, P1, P2, P3, P4, P5, P6, S1 S2, S3, S11 and T1 were built using commercial samples. Product derived from the insertion in C-H bond P9 was prepared through esterification of the commercial acid with ethanol under acidic conditions. Products from the insertion in C-H bonds P7, S10 and S12 were prepared through the reaction of the corresponding cycloalkane (5 mL) and EDA (0.5 mL, 4.7 mmol) catalyzed by complex **3** (166 mg, 0.24 mmol) followed by evaporation. Crude reaction mixtures were directly used for the building of the calibration curve. Products from the insertion in C-H bonds P8, P10, P11, S4, S5, S6, S7, S8, S9, T2, T3, T4 and T5 were prepared through reaction of the adequate couple of substituted ethyl acrylate and alkylmagnesiumhalide in the presence of copper(I) chloride followed by kugelrohr distillation. Purity of the products was determined through ^{1}H-NMR using biphenyl as standard prior to their use in the calibration curve. NMR spectra of all prepared products are shown in Figures E12-E28.

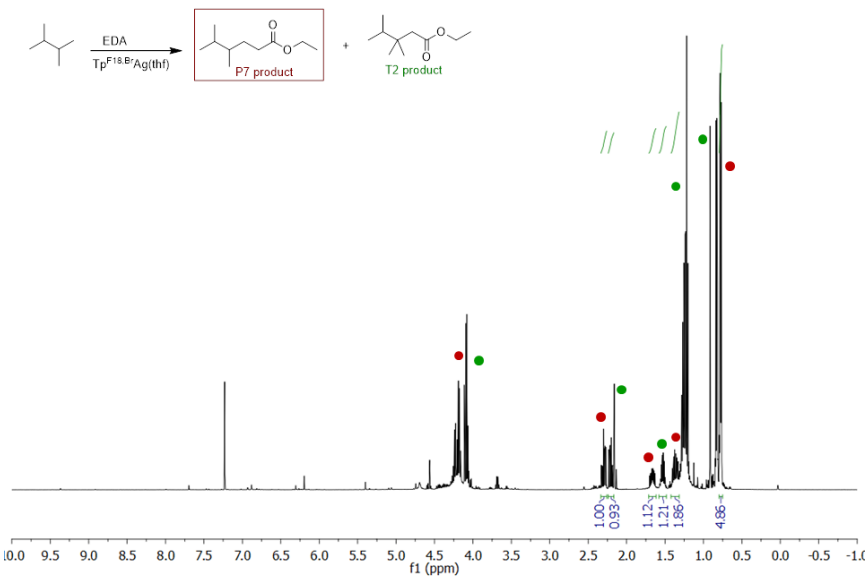

Figure E12. ^{1}H-NMR spectrum in $CDCl_3$ of product derived from insertion in P7.

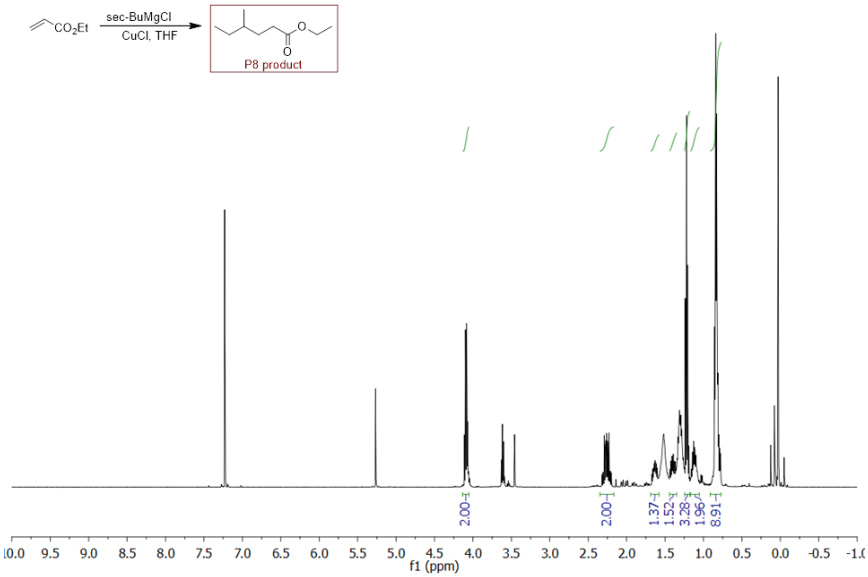

Figure E13. ^{1}H-NMR spectrum in $CDCl_3$ of product derived from insertion in P8.

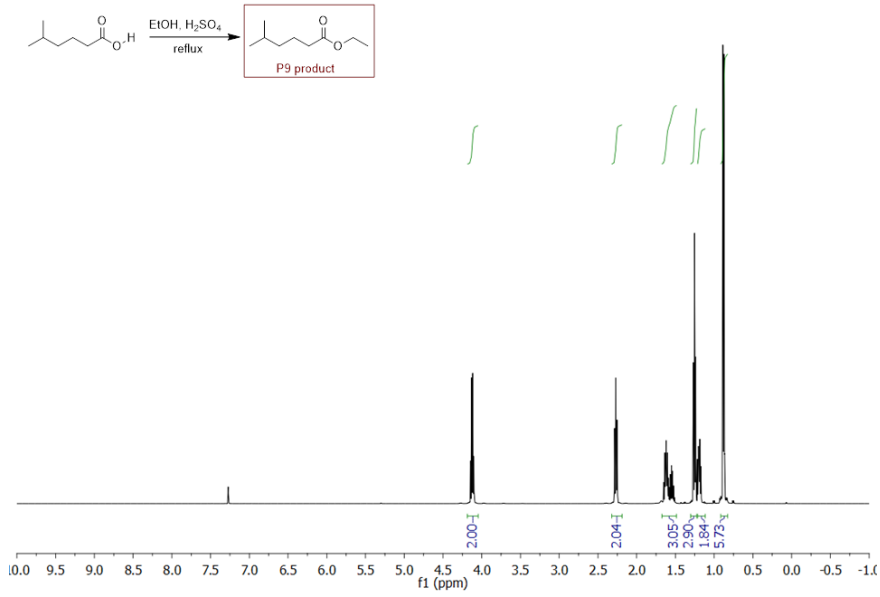

Figure E14. ^{1}H-NMR spectrum in $CDCl_3$ of product derived from insertion in P9.

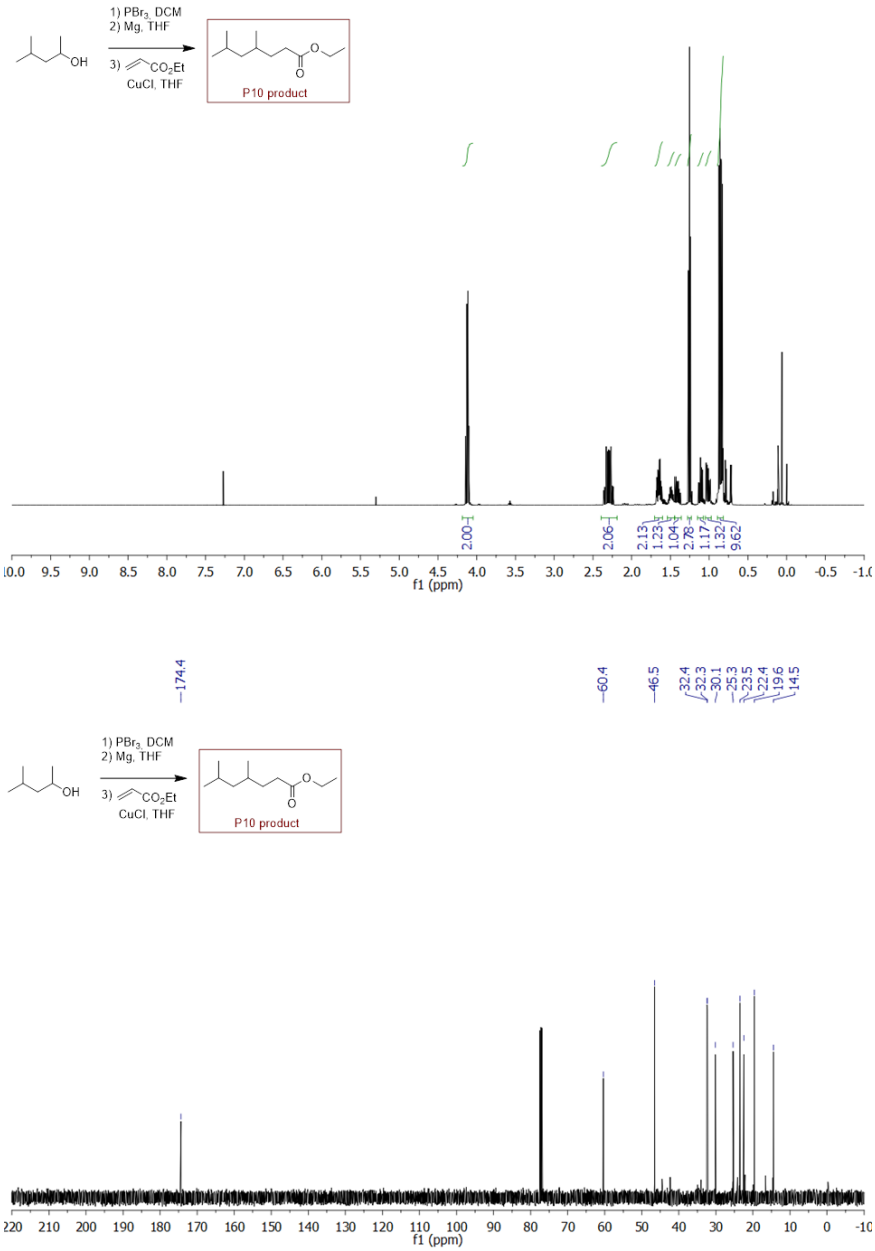

Figure E15. ^{1}H NMR and $^{13}C\{^{1}H\}$ NMR spectra in $CDCl_3$ of product derived from insertion in P10.

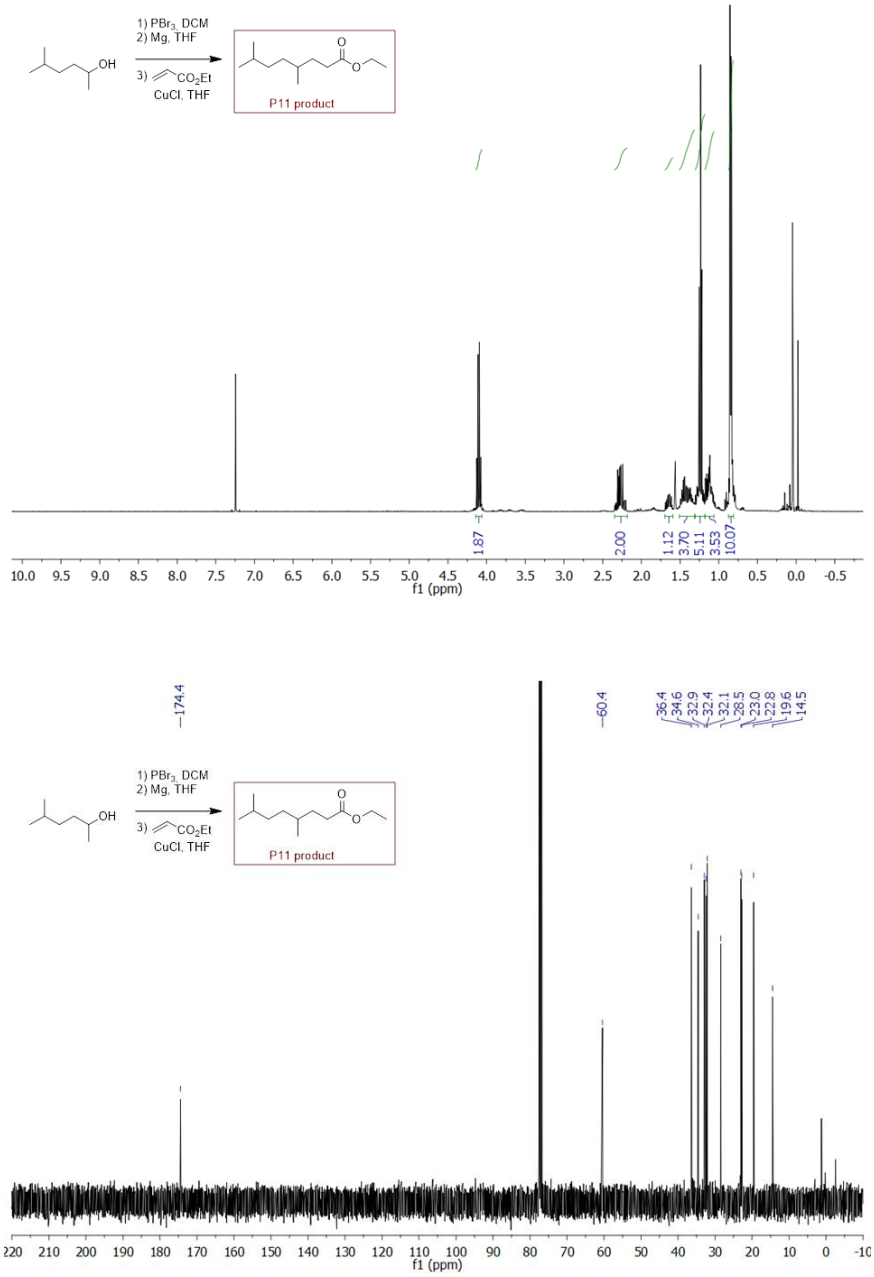

Figure E16. ^{1}H and $^{13}C\{^{1}H\}$ NMR spectra in $CDCl_3$ of product derived from insertion in P11.

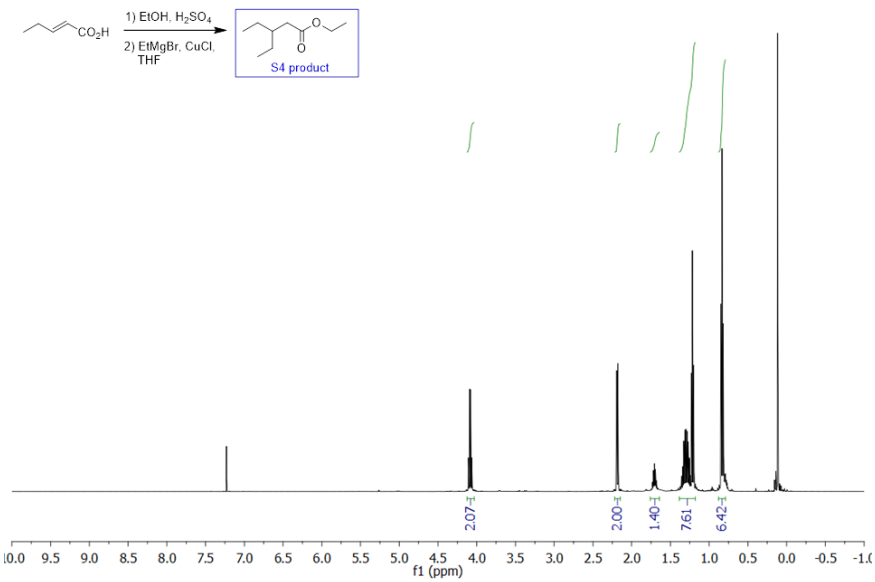

Figure E17. ^{1}H-NMR spectrum in $CDCl_3$ of product derived from insertion in S4.

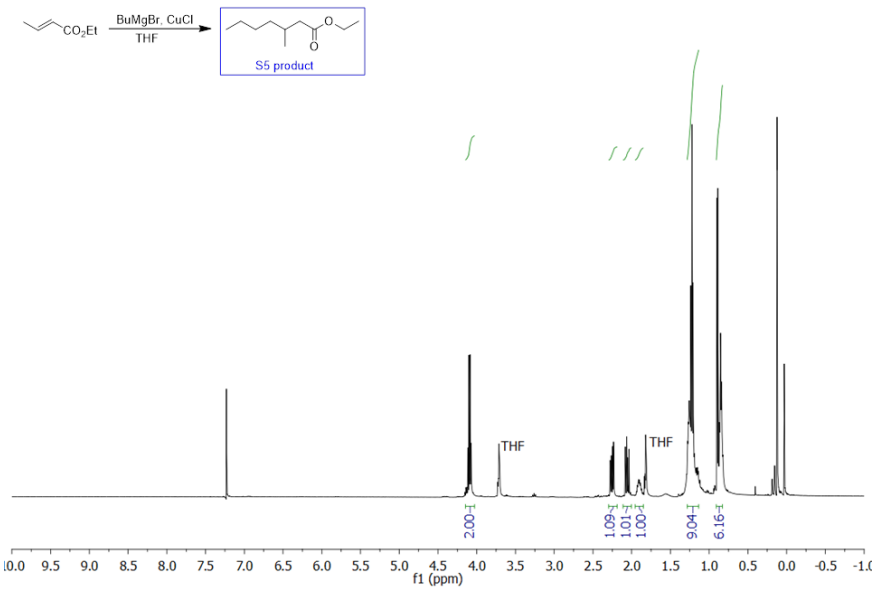

Figure E18. ^{1}H-NMR spectrum in $CDCl_3$ of product derived from insertion in S5.

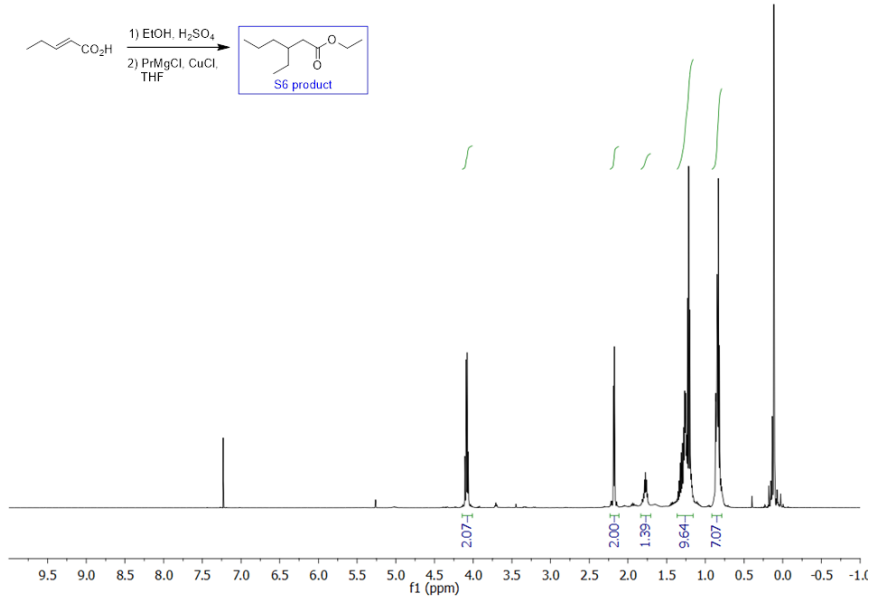

Figure E19. ^{1}H-NMR spectrum in $CDCl_3$ of product derived from insertion in S6.

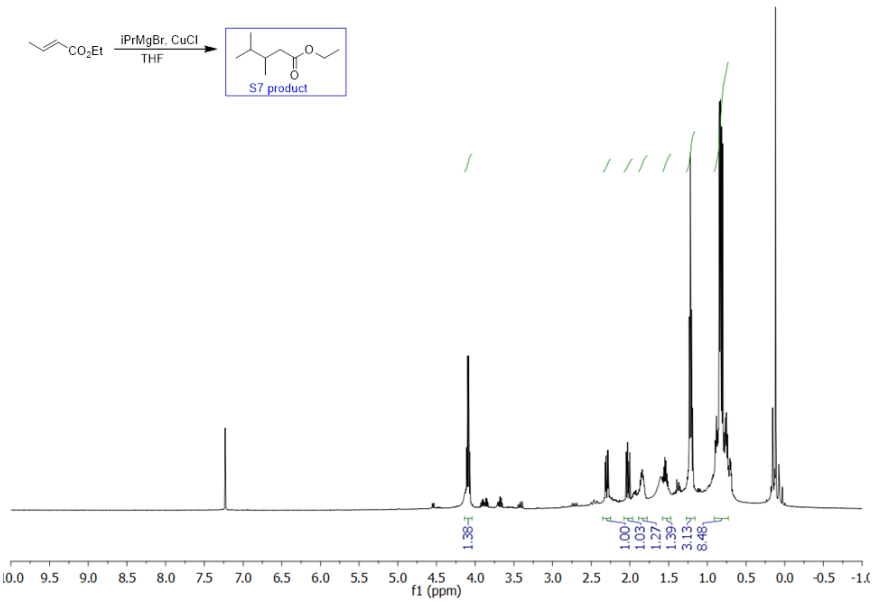

Figure E20. ^{1}H-NMR spectrum in $CDCl_3$ of product derived from insertion in S7.

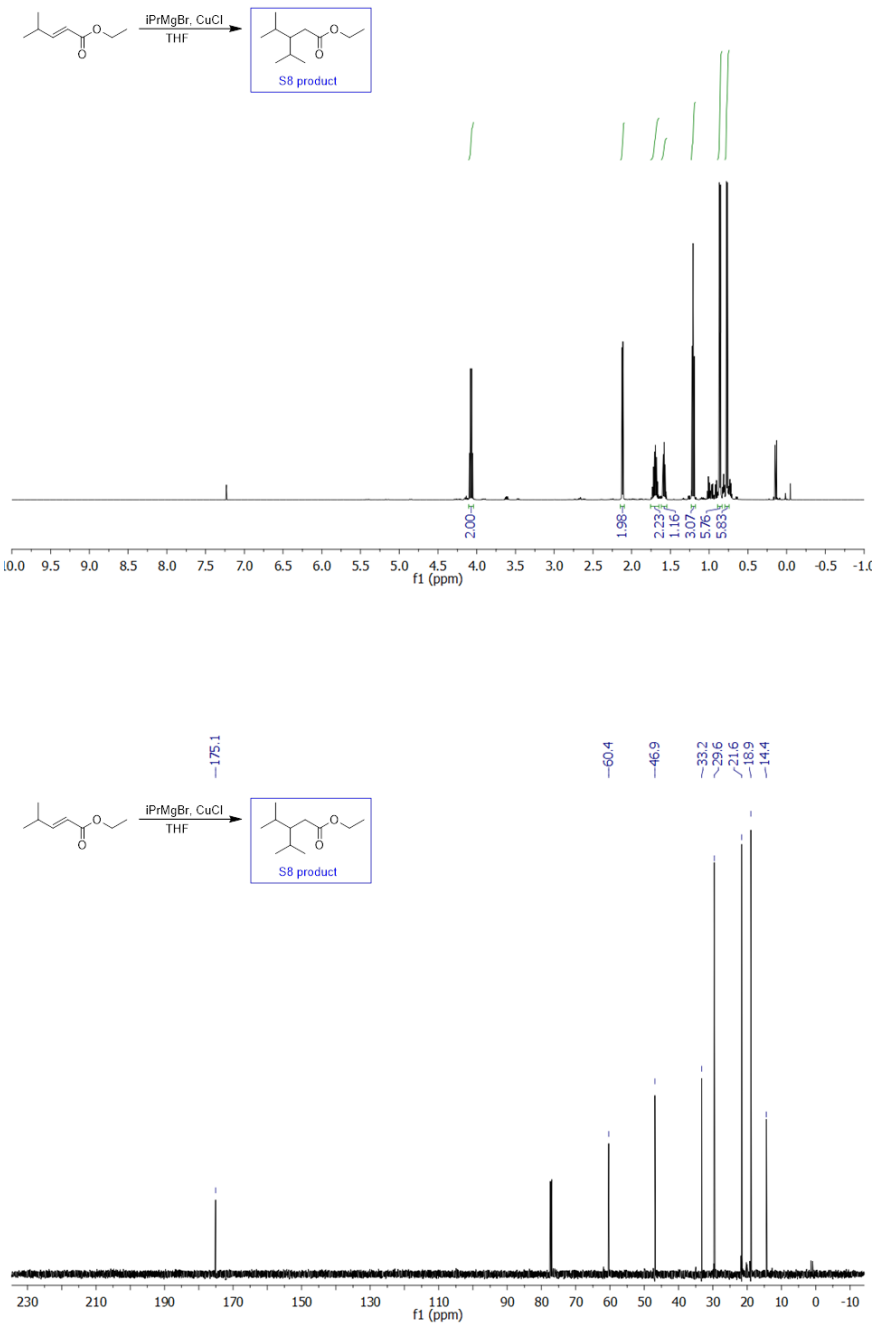

Figure E21. ^{1}H and $^{13}C\{^{1}H\}$ NMR spectra in $CDCl_3$ of product derived from insertion in S8.

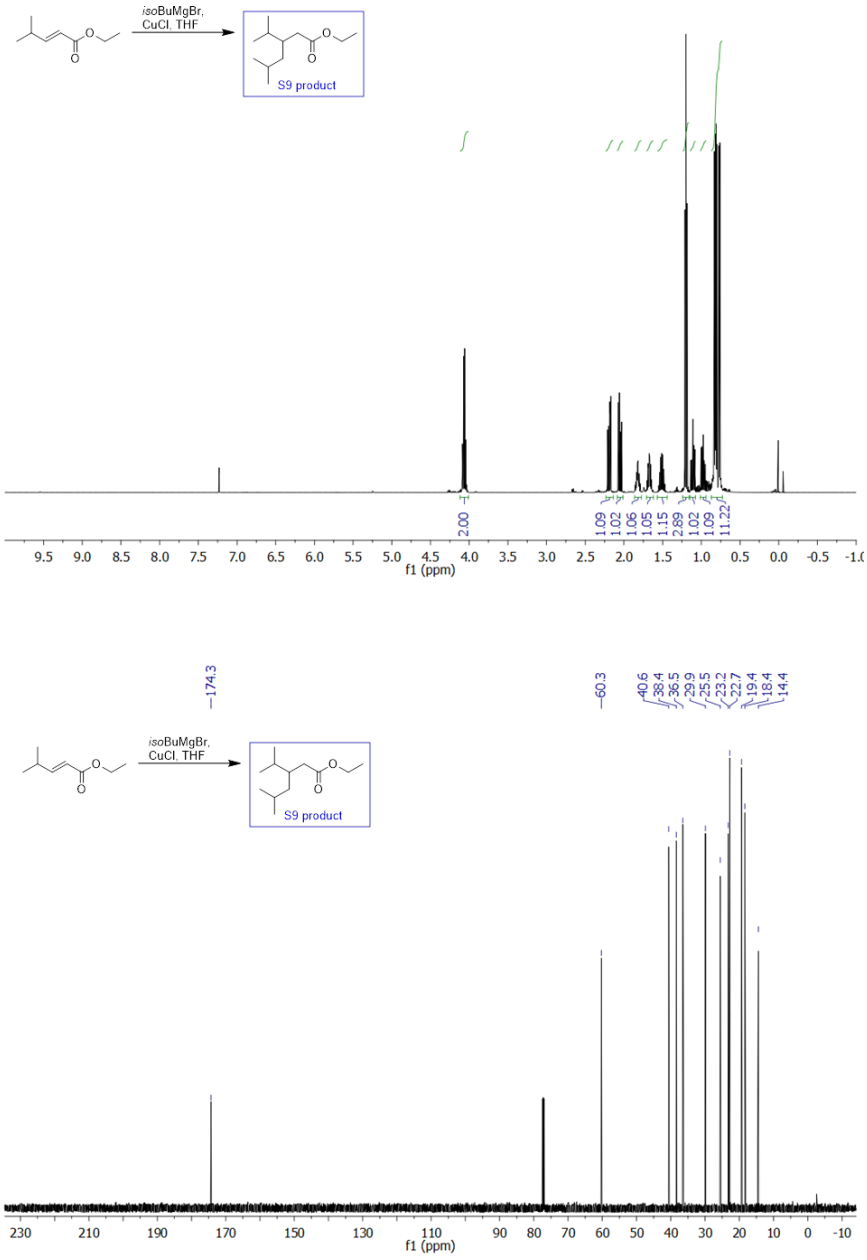

Figure E22. ^{1}H and $^{13}C\{^{1}H\}$ NMR spectra in $CDCl_3$ of product derived from insertion in S9.

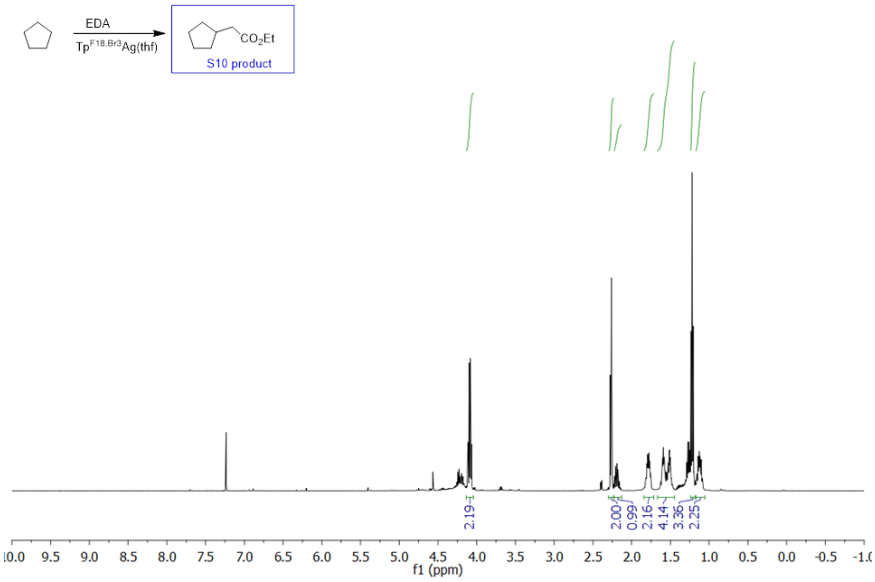

Figure E23. ^{1}H-NMR spectrum in $CDCl_3$ of product derived from insertion in S10.

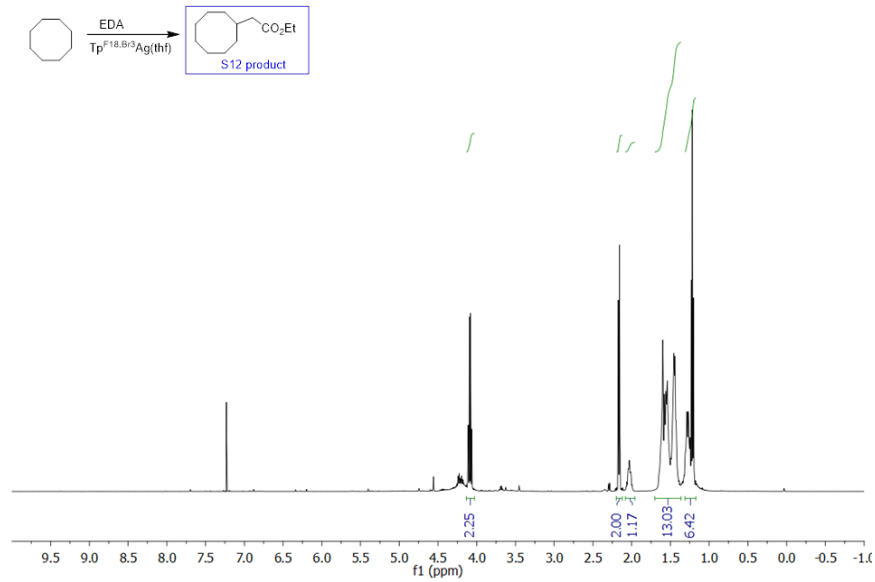

Figure E24. ^{1}H-NMR spectrum in $CDCl_3$ of product derived from insertion in S12.

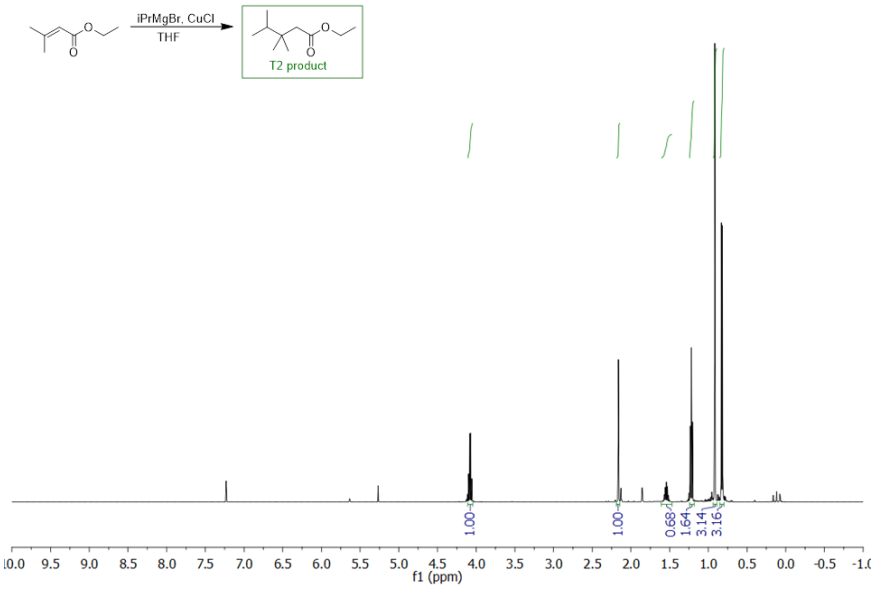

Figure E25. ^{1}H-NMR spectrum in $CDCl_3$ of product derived from insertion in T2.

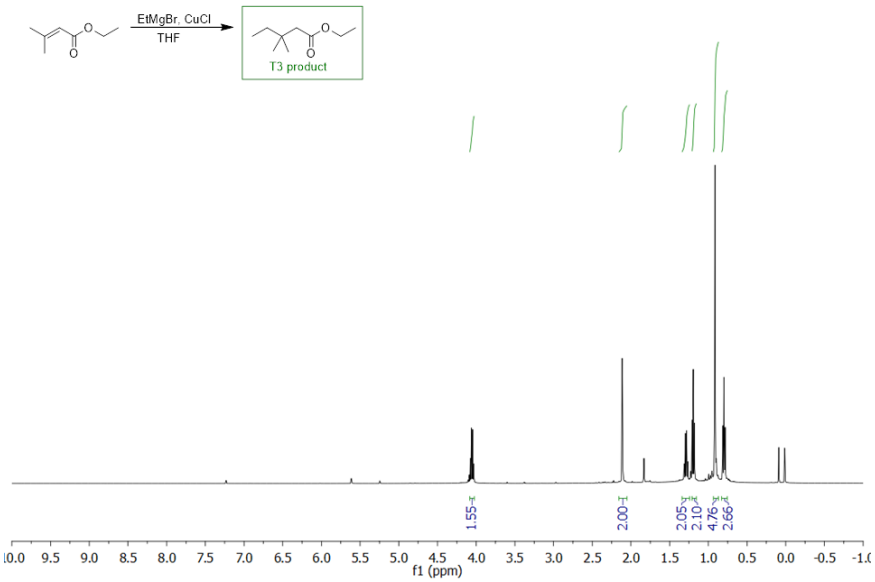

Figure E26. ^{1}H-NMR spectrum in $CDCl_3$ of product derived from insertion in T3.

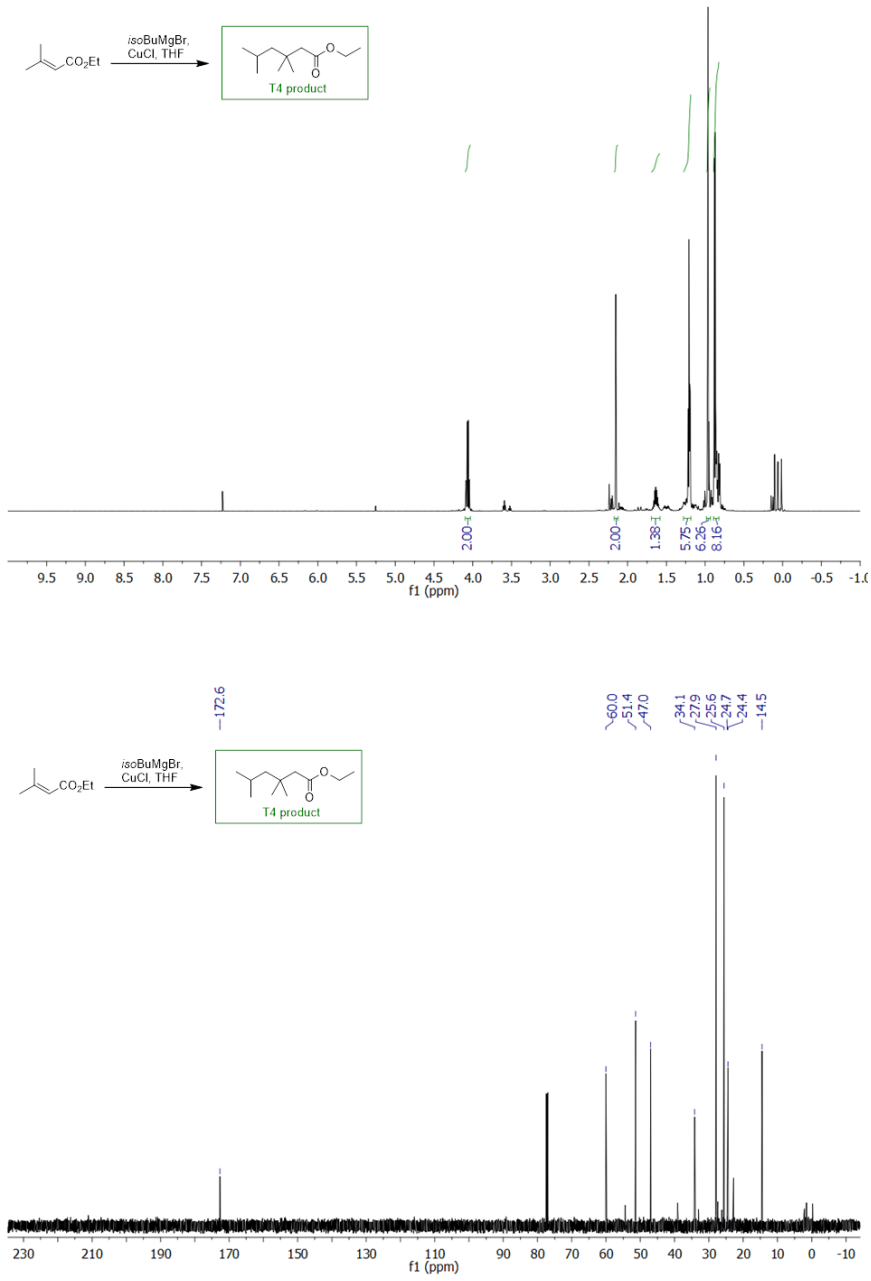

Figure E27. ^{1}H and $^{13}C\{^{1}H\}$ NMR spectra in $CDCl_3$ of product derived from insertion in T4.

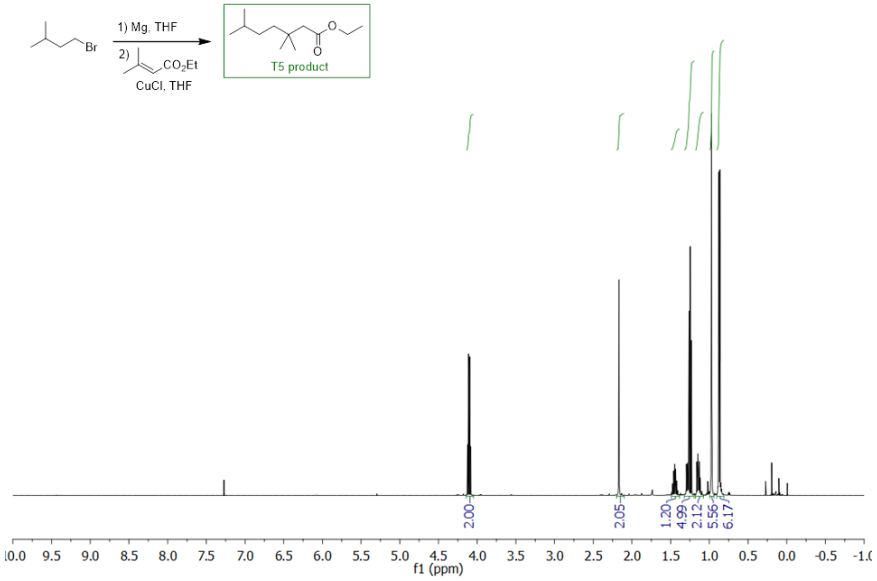

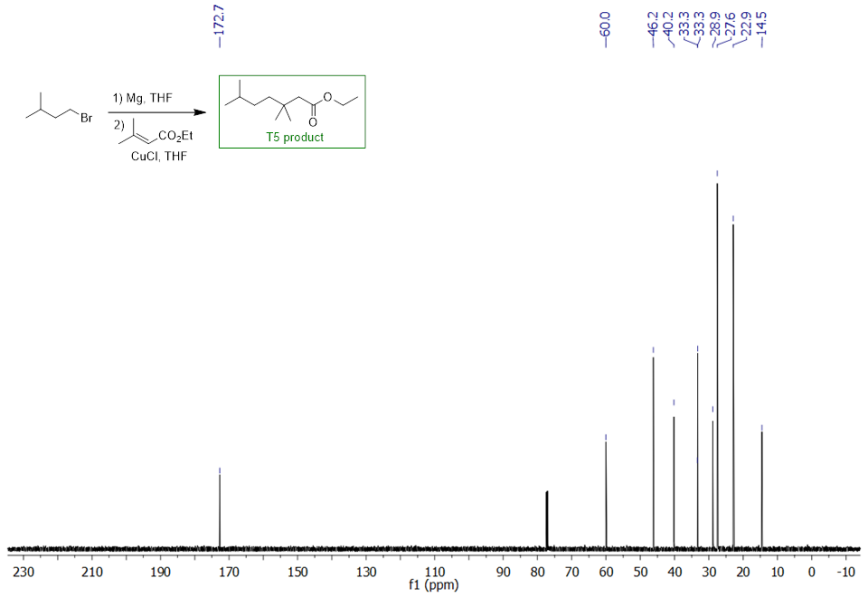

Figure E28. ^{1}H and $^{13}C\{^{1}H\}$ NMR spectra in $CDCl_3$ of product derived from insertion in T5.

Products were quantified by GC analysis either in a Varian GC 450 (column CP-Sil 5CB 50 m x 0,32 mm x 1,2 µm; T_{iny} 200 ºC, T_{det} 250 ºC, ϕ_{N2} 2.0 mL/min. Program: 40 ºC x 0,1 min 15 ºC/min 200 ºC x 7 min 20 ºC/min 270 ºC x 3,5 min) or in a gas chromatograph Agilent 7820A GC (column HP-5 30 m x 0,32 mm x 0,25 µm. T_{iny} 225 ºC, T_{det} 255 ºC, ϕ_{N2} 1.0 mL/min. Program: 40 ºC x 5 min 2 ºC/min 150 ºC 15 ºC/min 250 ºC x 5 min).

Examples of chromatograms and calibration curves employed for the analysis of the reaction crudes of competition experiments catalyzed by $Tp^{(CF3)2,Br}$ Ag(thf) (**3**) are shown in Figures E29-E41.

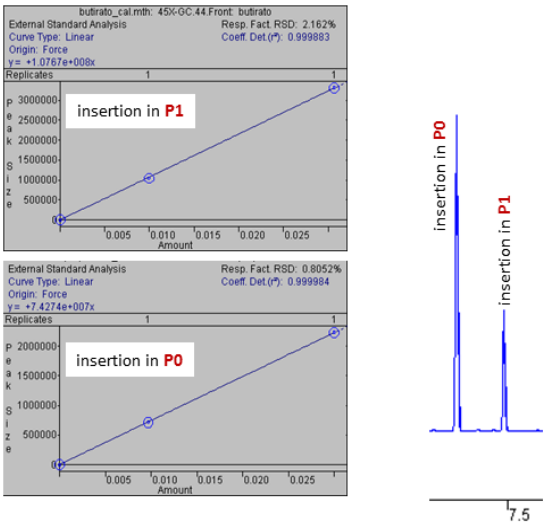

Figure E29. Competition experiment between methane and ethane.

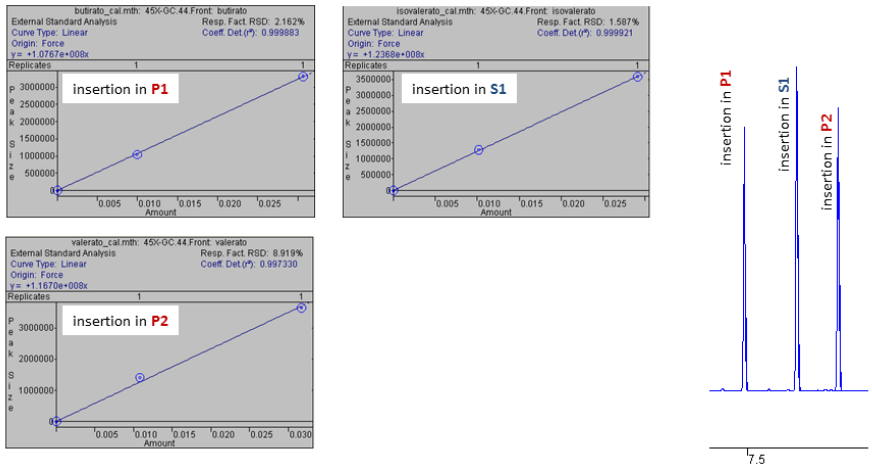

Figure E30. Competition experiment between ethane and propane.

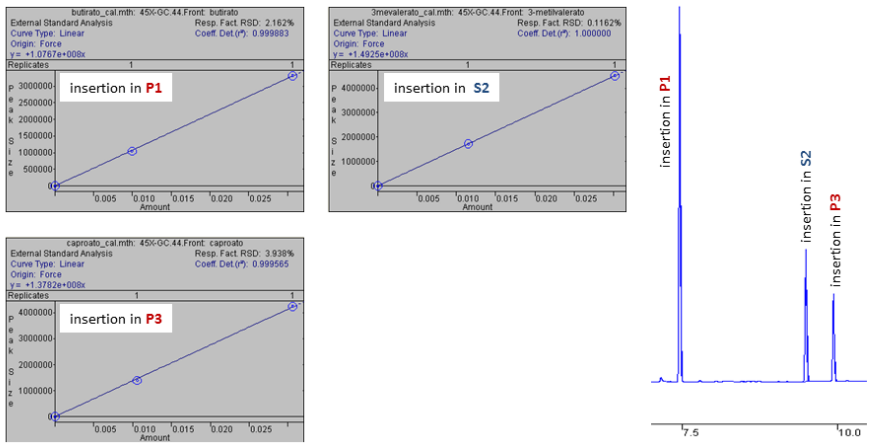

Figure E31. Competition experiment between ethane and butane.

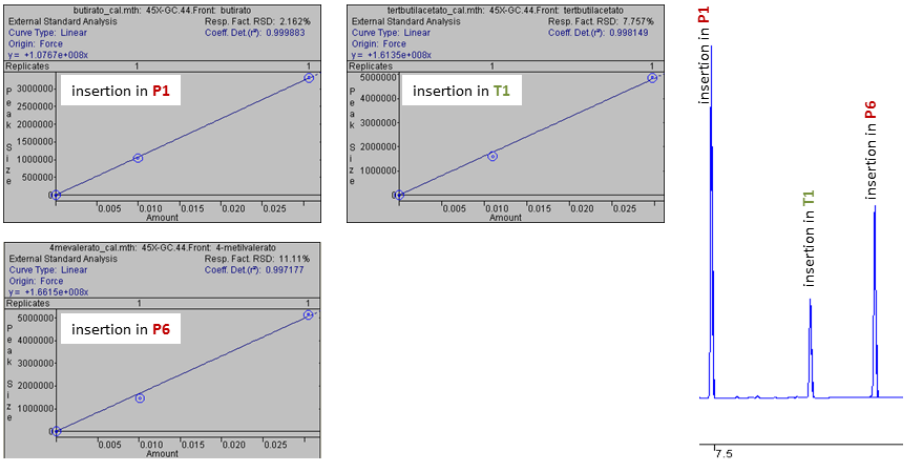

Figure E32. Competition experiment between ethane and isobutane.

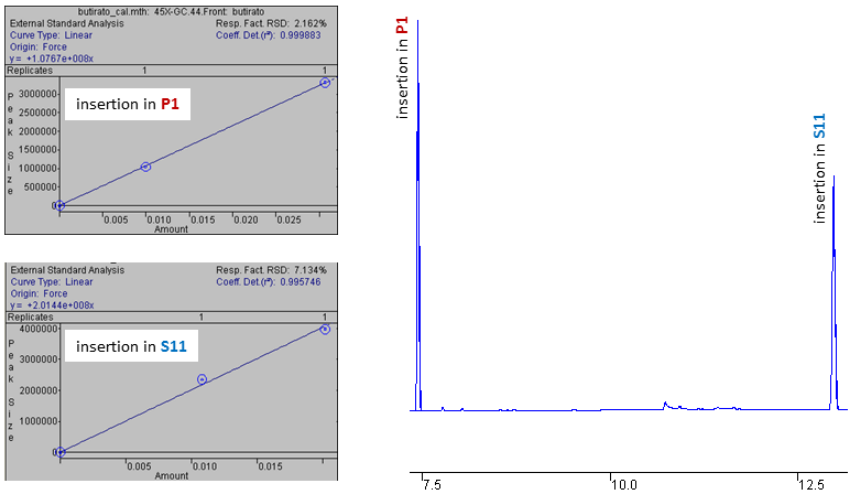

Figure E33. Competition experiment between ethane and cyclohexane.

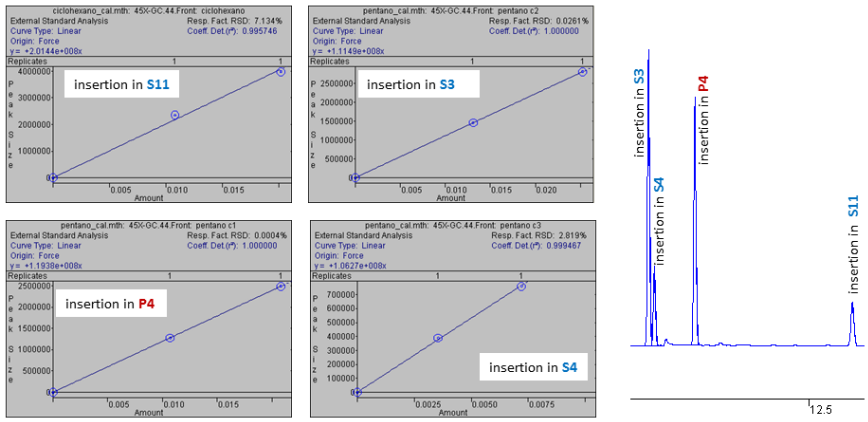

Figure E34. Competition experiment between pentane and cyclohexane.

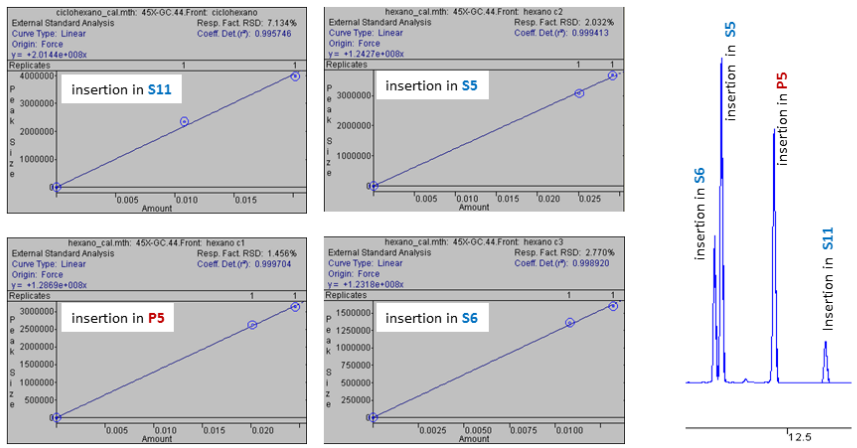

Figure E35. Competition experiment between hexane and cyclohexane.

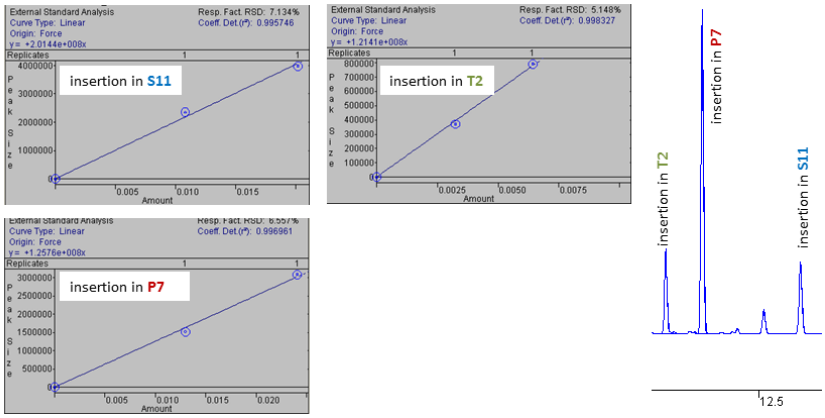

Figure E36. Competition experiment between 2,3-dimethylbutane and cyclohexane.

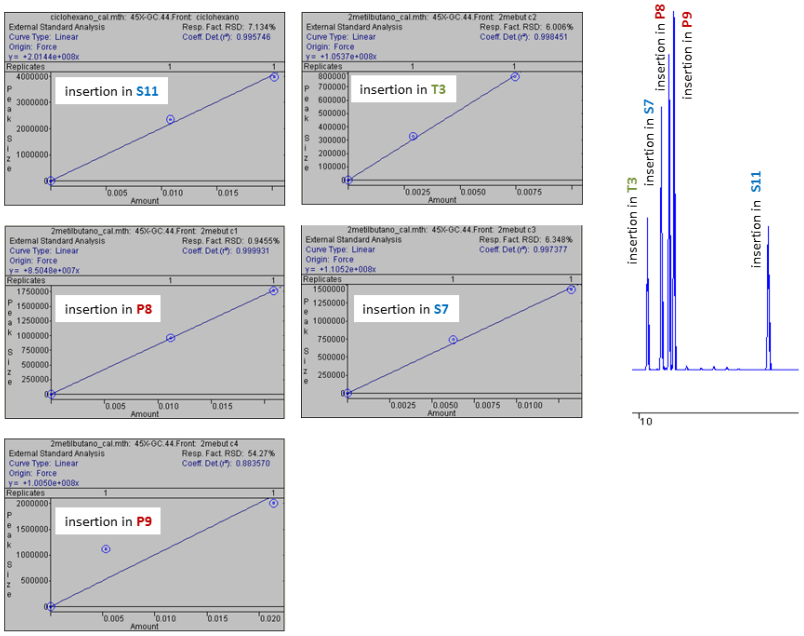

Figure E37. Competition experiment between 2-methylbutane and cyclohexane.

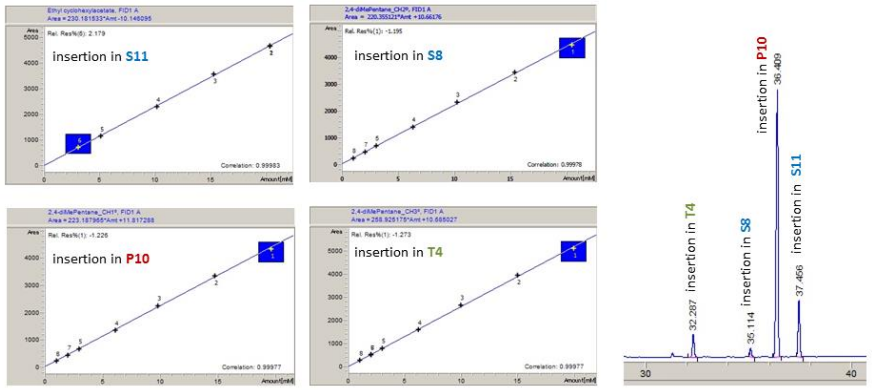

Figure E38. Competition experiment between 2,4-dimethylpentane and cyclohexane.

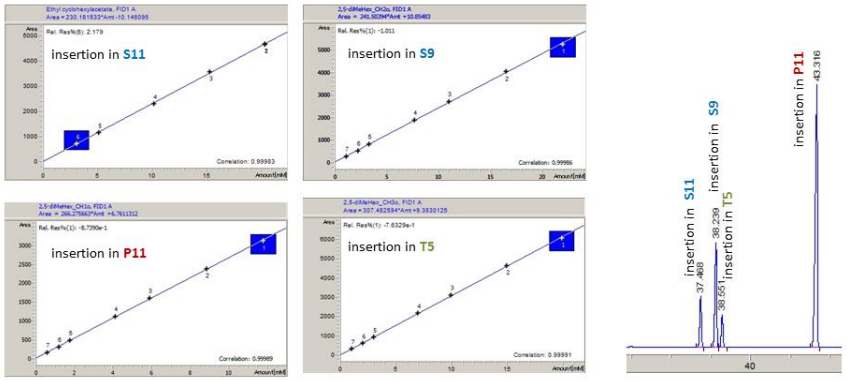

Figure E39. Competition experiment between 2,5-dimethylhexane and cyclohexane.

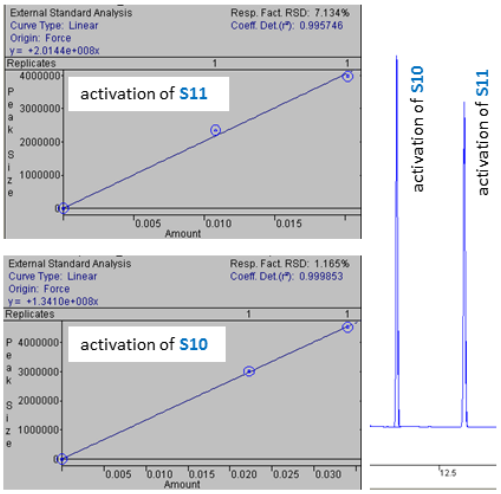

Figure E40. Competition experiment between cyclopentane and cyclohexane.

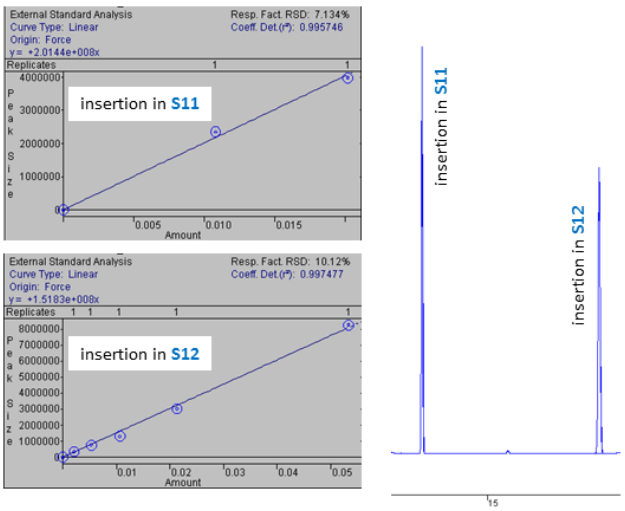

Figure E41. Competition experiment between cyclooctane and cyclohexane.

6.3 Experimental Methods for Section 3

Catalytic experiment for the reaction of methane and diazo compounds in water.

The experiment was carried out in a 100 mL high pressure reactor in which the catalyst (0.01 mmol) and diazocompound (0.25 mmol) were placed into a Teflon beaker inserted in the reactor. Then the surfactant solution (10% w/w, 20 mL) was added before and later the reactor charged with alkane. After 24 h of stirring the vessel was depressurized through two consecutively connected traps cooled with liquid nitrogen. Additionally, the depressurized reaction mixture was extracted with diethyl ether 3x10 mL. The organic phase and the collected material in the traps were mixed and diluted with more diethyl ether to an exact volume in volumetric flask. The final solution was analysed by GC using calibration curve.

The above procedure was also employed for the blank experiments without alkane and/or using D_2O as the solvent.

CONCLUSIONS

The new hydrotris((3,5-bis(trifluoromethyl)-4-bromo)-pyrazolyl)borate ligand ($Tp^{(CF3)2,Br}$) as its Tl, Cu and Ag complexes: $TlTp^{(CF3)2,Br}$ (**1**) $Tp^{(CF3)2,Br}Cu(NCMe)$ (**2**) and $Tp^{(CF3)2,Br}Ag(thf)$ (**3**) have been prepared and fully characterized. Complexes **2** and **3** catalyze the reaction of methane and gaseous alkanes with ethyl diazoacetate ($N_2=CHCO_2Et$) leading to carbene-insertion derivatives. In the case of **2**, this is the first example of an homogeneous copper-based catalyst for methane functionalization.

A novel *supercritical effect* has been found for **2** as the catalysts that enhances the regioselectivity of the primary sites toward carbene transfer reactions. This effect seems a consequence of the interaction of the catalyst fluorine atoms with the molecules of carbon dioxide in a supercritical phase.

The relative reactivity (R_r) of a series of fourteen alkanes (C_nH_{2n+2}, n = 1-8) and twenty-nine different carbon-hydrogen bonds has been determined upon performing competition experiments acting as (weak) nucleophiles in their reaction with *in situ* generated silver-carbene complexes as the (strong) electrophile both in *sc*CO_2 and/or neat alkanes as the reaction media has been measured.

The experimental data of the relative reactivity have served as the basis for a model that, with a set of simple rules derived from a statistical analysis, has led to a highly accurate fitting of the calculated values with respect to the experimental data, not only for silver but also for rhodium- and copper-based catalysts.

The first micellar catalytic system that operates in water at room temperature for the functionalization of methane and other C_2-C_4 gaseous alkanes has been developed, using sodium dodecyl sulphate as the surfactant, with **3** as the catalyst and EDA as the carbene precursor.

REFERENCES

(1) Pérez, P. J. *Alkane C–H Activation by Single-Site Metal Catalysis*; Springer: Dordrecht, 2012.

(2) (a) Shilov, A. E. *Activation and catalytic reactions of saturated hydrocarbons in the presence of metal complexes*, Klumer.; Dordrecht, 2000. (b) Shilov, A. E.; Shul'pin, G. B. *Chem. Rev.* **1997**, *97*, 2879–2932.

(3) Goldman, A. S.; Goldberg, K. I. *Activation and Functionalization of C—H Bonds*; American Chemical Society: Washington, 2004; The ACS Symposium Series 885.

(4) Arpe, H. J. *Industrial Organic Chemistry*, 5th ed.; Wiley-VCH, Ed.; Weinheim, Germany, 2010

(5) (a) Bergman, R. G. *Nature* **2007**, *446*, 391–393. (b) Labinger, J. A.; Bercaw, J. E. *Nature* **2002**, *417*, 507–514.

(6) Hartwig, J. F. *Organotransition Metal Chemestry: From Bonding to Catalysis*; University Science books, 2009.

(7) Luo, Y.-R. *Comprehensive Handbook of Chemical Bond Energies*, CRC Press, Boca Ratón, 2007.

(8) Caballero, A., Pérez, P. J. *Chem. Soc. Rev.* **2013**, *42*, 8809-8820.

(9) Gunsalus, N. J.; Koppaka, A.; Park, S. H., Bishof, S. M.; Hashigushi, B. G.; Periana, R. A. *Chem. Rev.* **2017**, *117*, 8521-8573.

(10) Schwach, P.; Pan, X.; Bao, X. *Chem. Rev.* **2017**, *117*, 8497-8520.

(11) *Chem. Rev*. **2017**, *117*, issue 13.

(12) Sun, M.; Zhang, J.; Putaj, P.; Caps, V.; Lefebvre, F.; Pelletier, J.; Basset, J.-M. *Chem. Rev.* **2014**, *114*, 981-1019.

(13) (a) Gol'dshleger, N. F.; Tyabin, M. B.; Shilov, A. E.; Shteinman, A. A. *Zhurnal Fizicheskoi Khimii* **1969**, *43*, 2174-2175. (b) Gol'dshleger, N. F.; Es'kova, V. V.; Shilov, A. E.; Shteinman, A. A. *Zhurnal Fizicheskoi Khimii* **1972**, *46*, 1353-1354.

(14) Periana, R. A.; Taube, D. J.; Evitt, E. R.; Loffler, D. G.; Wentrcek, P. R.; Voss, G.; Masuda, T. *Science* **1993**, *259*, 340−343.

(15) Sen, A.; Benvenuto, M. A.; Lin, M.; Hutson, A. C.; Basickes, N. *J. Am. Chem. Soc.* **1994**, *116*, 998–1003.

(16) Periana, R. A.; Taube, D. J.; Gamble, S.; Taube, H.; Satoh, T.; Fujii, H. *Science* **1998**, *280*, 560−564.

(17) Jones, C.; Taube, D.; Ziatdinov, V. R.; Periana, R. A.; Nielsen, R. J.; Oxgaard, J.; Goddard, W. A., III. *Angew. Chem., Int. Ed.* **2004**, 43, 4626−4629.

(18) Gretz, E.; Oliver, T. F.; Sen, A. *J. Am. Chem. Soc.* **1987**, *109*, 8109−8111.

(19) Muehlhofer, M.; Strassner, T.; Herrmann, W. A. *Angew. Chem., Int. Ed.* **2002**, *41*, 1745−1747.

(20) Periana, R. A.; Mironov, O.; Taube, D.; Bhalla, G.; Jones, C. J. *Science* **2003**, *301*, 814−818.

(21) Reis, P. M.; da Silva, J. A. L.; Palabra, A. F.; Frausto da Silva, J. J. R.; Kitamura, T.; Fujiwara, Y.; Pombeiro, A. J. L. *Angew. Chem., Int. Ed.* **2003**, *42*, 821-823.

(22) Sun, M.; Abou-Hamad, E.; Rossini, A. J.; Zhang, J.; Lesage, A.; Zhu, H.; Pelletier, J.; Emsley, L.; Caps, V.; Basset, J.-M. *J. Am. Chem. Soc.* **2013**, *135*, 804-810.

(23) Lin, M.; Sen, A. *Nature* **1994**, *368*, 613−615.

(24) Hristov, I. H.; Ziegler, T. *Organometallics* **2003**, *22*, 3513−3525.

(25) (a) Sadow, A. D.; Tilley, T. D. *Angew. Chem., Int. Ed.* **2003**, *42*, 803−805. (b) Sadow, A. D.; Tilley, T. D. *J. Am. Chem. Soc.* **2005**, *127*, 643−656.

(26) Sadow, A. D.; Tilley, T. D. *J. Am. Chem. Soc.* **2003**, *125*, 7971−7977.

(27) Smith, K. T.; Berritt, S.; González-Moreiras, M.; Ahn, S.; Smith, M. R., III; Baik, M.-H.; Mindiola, D. J. *Science* **2016**, *351*, 1424−1427.

(28) Cook, A. K.; Schimler, S. D.; Matzger, A. J.; Sanford, M. S. *Science* **2016**, *351*, 1421−1424.

(29) (a) Díaz-Requejo, M. M.; Belderraín, T. R.; Nicasio, M. C.; Pérez, P. J. *Dalton Trans.* **2006**, 5559-5566 (b) Caballero, A.; Díaz-Requejo, M. M.; Fructos, M. R.; Olmos, A.; Urbano, J.; Pérez, P. J. *Dalton Trans.* **2015**, *44*, 20295–20307. (c) Doyle, M. P.; McKervey, M. A.; Ye, T. *Modern Catalytic Methods for Organic Synthesis with Diazo Compounds*; New York, 1998.

(30) (a) Nakamura, E.; Yoshikai, N.; Yamanaka, M. *J. Am. Chem. Soc.* **2002**, *124*, 7181-7192. (b) Braga, A. A. C.; Maseras, F.; Urbano, J.; Caballero, A.; Díaz-Requejo, M. M.; Pérez, P. J. *Organometallics* **2006**, *25*, 5292–5300.

(31) Wax, M. J.; Stryker, J. M.; Buchanan, J. M.; Kovac, C. A.; Bergman, R. G. *J. Am. Chem. Soc.* **1984**, *106*, 1121-1122.

(32) Despagnet-Ayoub, E.; Jacob, K.; Vendier, L.; Etienne, M.; Álvarez, E.; Caballero, A.; Díaz-Requejo, M. M.; Pérez, P. J. *Organometallics* **2008**, *27*, 4779-4787.

(33) Fuentes, M. A.; Muñoz, B. K.; Jacob, K.; Vendier, L.; Caballero, A.; Etienne, M.; Pérez, P. J. *Chem. Eur. J.* **2013**, *19*, 1327–1334.

(34) Caballero, A.; Despagnet-Ayoub, E.; Díaz-Requejo, M. M.; Díaz-Rodríguez, A.; González-Núñez, M. E.; Mello, R.; Muñoz, B. K.; Solo Ojo, W.; Asensio, G.; Etienne, M.; Pérez, P. J. *Science* **2011**, *332*, 835-838.

(35) (a) Olah, G. A.; Klopman, G.; Schlosberg, R. H. *J. Am. Chem. Soc.* **1969**, *91*, 3261–3268. (b) Olah, G. A.; Mo, Y. K.; Olah, J. A. *J. Am. Chem. Soc.* **1973**, *95*, 4939–4951. (c) Olah, G. A. *Angew. Chem. Int. Ed. Engl.* **1973**, *12*, 173–212. (d) Olah, G. A; Ramaiah, P.; Prakash, G. K. *Proc. Natl. Acad. Sci.* **1997**, *94*, 11783–11785.

(36) (a) Olah, G. A.; Malhotra, R.; Narang, S. C. *Nitration. Methods and mechanisms*; VCH: New York, 1989. (b) Olah, G. A.; Prakash, G. K. S.; Sommer, J. *Superacids*; John Wiley & Sons: New York, 1985.

(37) (a) Jain, T.; Jain, V.; Pandey, R.; Daharwal, S. J.; Shukla, S. S.; Vyas, A. *Res. J. Pharm. Technol.* **2009**, *2*, 65-71. (b) Filardo, G.; Galia, A.; Giacona, A. *Carbon Dioxide Recovery and Utilization*; Springer: Dordrecht, 2003. (c) McHugh, M.; Krukonis, V. J. *Supercritical Fluid Extraction*; Boston, 1994.

(38) (a) Zhang, X.; Heinonen, S.; Levänen, E. *RSC Adv.* **2014**, *4*, 61137–61152. (b) Ichikawa, S.; Seki, T.; Ikariya, T. *Adv. Synth. Catal.* **2014**, *356*, 2643–2652. (c) Han, X.; Poliakoff, M. *Chem. Soc. Rev.* **2012**, *41*, 1428-1436. (d) Jessop, P. G. *J. Supercrit. Fluids* **2006**, *38*, 211–231.

(39) http://corinto.pucp.edu.pe/quimicageneral/contenido/56-cambios-de-estado-diagramas-de-calentamiento-diagramas-de-fase.html

(40) Beckman, E. J. *J. Supercrit. Fluids* **2004**, *28*, 121–191.

(41) Huang, Z.; Sun, G. B.; Chiew, Y. C.; Kawi, S. *Powder Technol.* **2005**, *160*, 127–134.

(42) (a) Jain, T.; Jain, V.; Pandey, R.; Daharwal, S. J.; Shukla, S. S.; Vyas, A. *Res. J. Pharm. Technol.* **2009**, *2*, 65-71. (b) Filardo, G.; Galia, A.; Giacona, A. *Carbon Dioxide Recovery and Utilization*; Springer: Dordrecht, 2003.

(43) Olmos, A.; Asensio, G.; Pérez, P. J. *ACS Catal.* **2016**, *6*, 4265–4280.

(44) Burguete, M. I.; García-Verdugo, E.; Luis, S. V. *Beilstein J. Org. Chem.* **2011**, *7*, 1347–1359.

(45) (a) Peach, J.; Eastoe, J. *Beilstein J. Org. Chem.* **2014**, *10*, 1878–1895. (b) Horváth, I. T. *Acc Chem. Res* **1998**, *31*, 641–650.

(46) (a) Anastas, P. T.; Kirchhoff, M. M. *Acc. Chem. Res.* **2002**, *35*, 686–694. (b) Anastas, P. T.; Warner, J. C. *Green Chemistry: Theory and Practice*; Oxfird University Press Ed.; New York, 1998.

(47) (a) La Sorella, G.; Strukil, G.; Scarso, A. *Green Chem.* **2015**, *17*, 644–683. (b) Sheldon, R. A. *Green Chem.* **2007**, *9*, 1273-1283.

(48) Sheldon, R. A. *Green Chem.* **2005**, *7*, 267-278.

(49) (a) Lindström, U. M.; Andersson, F. *Angew. Chem. Int. Ed.* **2006**, *45*, 548–551. (b) Adams, D.; Dyson, P.; Tavener, S. *Chemistry in Alternative Reaction Media*; John Wiley & Sons, 2004.

(50) Sorrenti, A.; Illa, O.; Ortuño, R. M. *Chem. Soc. Rev.* **2013**, *42*, 8200-8219.

(51) Varszegi, C.; Ernst, M.; Van Laar, F.; Sels, B. F.; Schwab, E.; De Vos, D. E. *Angew. Chem. Int. Ed.* **2008**, *47*, 1477–1480.

(52) Szabó, F.; Pethő, B.; Gonda, Z.; Novák, Z. *RSC Adv.* **2013**, *3*, 4903-4908.

(53) Inamoto, K.; Nozawa, K.; Yonemoto, M.; Kondo, Y. *Chem. Commun.* **2011**, *47*, 11775-11777.

(54) Rosati, F.; Oelerich, J.; Roelfes, G. *Chem. Commun.* **2010**, *46*, 7804-7806.

(55) Mao, S.-L.; Sun, Y.; Yu, G.-A.; Zhao, C.; Han, Z.-J.; Yuan, J.; Zhu, X.; Yang, Q.; Liu, S.-H. *Org. Biomol. Chem.* **2012**, *10*, 9410-9417.

(56) Fuentes, M. A.; Olmos, A.; Muñoz, B. K.; Jacob, K.; González-Núñez, M. E.; Mello, R.; Asensio, G.; Caballero, A.; Etienne, M.; Pérez, P. J. *Chem. Eur. J.* **2014**, *20*, 11013–11018.

(57) Urbano, J.; Izarra, R.; Gómez-Ariza, J. L.; Trofimenko, S.; Díaz-Requejo, M. M.; Pérez, P. J. *Chem. Commun.* **2006**, 1000–1002.

(58) Maspero, A.; Giovenzana, G. B.; Monticelli, D.; Tagliapietra, S.; Palmisano, G.; Penoni, A. *J. Fluor. Chem.* **2012**, *139*, 53–57.

(59) (a) Trofimenko, S. *Scorpionates: Polypyrazolylborate Ligands and Their Coordination Chemistry*; Imperial College Press, Ed.; London, 1999. (b) Pettinari, C. *Scorpionates II: Chelating Borate Ligands*; London, 2008.

(60) Muñoz-Molina, J. M.; Sameera, W. M. C.; Álvarez, E.; Maseras, F.; Belderrain, T. R.; Pérez, P. J. *Inorg. Chem.* **2011**, *50*, 2458–2467.

(61) Dias, R.; Jin, W. *J. Am. Chem. Soc.* **1995**, 117, 11381–11382.

(62) Hurlburt, P. K.; Rack, J. J.; Luck, J. S.; Dec, S. F.; Webb, J. D.; Anderson, O. P.; Strauss, S. H. *J. Am. Chem. Soc.* **1994**, *116*, 10003–10014.

(63) (a) Rivilla, I.; Sameera, W. M. C.; Alvarez, E.; Díaz-Requejo, M. M.; Maseras, F.; Pérez, P. J. *Dalton Trans.* **2013**, *42*, 4132–4138. (b) Braga, A. A. C.; Caballero, A.; Urbano, J.; Diaz-Requejo, M. M.; Pérez, P. J.; Maseras, F. *ChemCatChem* **2011**, *3*, 1646–1652.

(64) Caballero, A.; Díaz-Requejo, M. M.; Trofimenko, S.; Belderraín, T. R.; Pérez, P. J. *Eur. J. Inorg. Chem.* **2007**, No. 18, 2848–2852.

(65) Pereira, A.; Champouret, Y.; Martín, C.; Álvarez, E.; Etienne, M.; Belderraín, T. R.; Pérez, P. J. *Chem. Eur. J.* **2015**, *21*, 9769–9775.

(66) Flores, J. A.; Komine, N.; Pal, K.; Pinter, B.; Pink, M.; Chen, C. H.; Caulton, K. G.; Mindiola, D. J. *ACS Catal.* **2012**, *2*, 2066–2078.

(67) Urbano, J.; Belderraín, T. R.; Nicasio, M. C.; Trofimenko, S.; Díaz-Requejo, M. M.; Pérez, P. J. *Organometallics* **2005**, *24*, 1528-1532.

(68) (a) Dias, H. V. R.; Browning, R. G.; Richey, S. A.; Lovely, C. J. *Organometallics* **2004**, *23*, 1200–1202. (b) Dias, H. V. R.; Browning, R. G.; Richey, A.; Lovely, C. J. *Organometallics* **2005**, *24*, 5784.

(69) Demonceau, A.; Noels, A. F.; Costa, J. L.; Hubert, A. J. *J. Mol. Catal.* **1990**, *58*, 21–26.

(70) Caballero, A.; Pérez, P. J. *J. Organomet. Chem.* **2015**, *793*, 108–113.

(71) (a) Tsukahara, T.; Kachi, Y.; Kayaki, Y.; Ikariya, T.; Ikeda, Y. *J. Phys. Chem. B* **2008**, *112*, 16445–16454. (b) Raveendran, P.; Wallen, S. L. *J. Phys. Chem. B* **2003**, *107*, 1473–1477.

(72) Caballero, A.; Díaz-Requejo, M. M.; Belderrain, T. R.; Nicasio, M. C.; Trofimenko, S.; Pérez, P. J. *J. Am. Chem. Soc.* **2003**, *125*, 1446–1447.

(73) Song, H. L. *Bull. Korean Chem. Soc.* **2008**, *29*, 1409–1411.

(74) Mayr, H.; Ofial, A. R. *Acc. Chem. Res.* **2016**, *49*, 952–965.

(75) Pirrung, M. C.; Morehead, A. T. *J. Am. Chem. Soc.* **1994**, *116*, 8991-9000.

(76) Bohr, N. *Philosophical Magazine* **1913**, *26***,** 1–24.

(77) Pauling, L. *J. Am. Chem. Soc.* **1932**, *54*, 3570-3582.

(78) Elvidge, C. D.; Erwin, E. H.; Baugh, K. E.; Tuttle, B. T.; Howard, A. T.; Pack, D. W.; Milesi, C. *Oil Gas J.* **2007**, *105*, 50−58.

(79) Zimmermann, T.; Soorholtz, M.; Bilke, M.; Schüth, F. *J. Am. Chem. Soc.*, **2016**, *138*, 12395–12400.

(80) Sirajuddin, S.; Rosenzweig, A. C. *Biochemistry* **2015**, *54*, 2283−2294.

(81) (a) Lipshutz, B. H.; Ghorai, S. *Aldrichimica Acta* **2012**, *45*, 3-16. (b) Lipshutz, B. H.; Ghorai, S. *Aldrichimica Acta* **2008**, *41*, 59-72.

(82) Álvarez, M.; Gava, R.; Rodríguez, M. R.; Rull, S. G.; Pérez, P. J. *ACS Catal.*, **2017**, *7*, 3707–3711.

(83) Morilla, M. E.; Molina, M. J.; Díaz-Requejo, M. M.; Belderrain, T. R.; Nicasio, M. C.; Trofimenko, S.; Pérez, P. J. *Organometallics*, **2003**, *22*, 2914–2918.

(84) (a) H. L. Clever and C. L. Young, Eds., *IUPAC Solubility Data Series, Vol. 27/28, Methane*, Pergamon Press, Oxford, England, 1987 (b) W. Hayduk, Ed., *IUPAC Solubility Data Series, Vol. 9, Ethane*, Pergamon Press, Oxford, England, 1982.

(85) Kitamura, M.; Takenata, Y.; Okuno, T.; Holl, R.; Wünsch, B.; *Eur. J. Inorg. Chem.* **2008**, 1188-1192.

(86) Bruker (**2007**). *APEX2*. Bruker AXS Inc., Madison, Wisconsin, USA.

(87) Bruker (**2001**). *APEX2*. Bruker AXS Inc., Madison, Wisconsin, USA.

(88) Burla, M.; Camalli, M.; Carrozzini, B.; Cascarano, G. L.; Giacovazzo, C.; Poliori, G.; Spagna, R.; SIR2002: the program; *J. Appl. Cryst.* **2003**, *36*, 1103–1103.

(89) Sheldrick, G. M. *Acta Crystallogr., Sect. A: Found. Crystallogr*., **2008**, *64*, 112-122

(90) Spek, A. L. *J. Appl. Crystallogr*., **2003**, *36*, 7-13.